The Anodic Dissolution of Covellite in Acidic, Chloride Solutions

by

P. Basson

B.Sc., University of Stellenbosch, 1993

B. Eng. (Chemical), University of Pretoria, 1996

Submitted to the University of Cape Town in fulfilment of the requirements for the degree of Masters of Science in Engineering

September 2010

ABSTRACT

An electrochemical study was conducted on a stationary, synthetically produced, covellite electrode in acidic, chloride solutions at ambient conditions to investigate the dissolution behaviour of the mineral over a surface potential range from the open circuit potential (OCP) to about 0.62 V (vs. SHE).

The electrode was mounted in an apparatus, which was designed to resemble leaching of the mineral under conditions applicable to heap leaching of whole ores, where the mineral occurs in cracks or pores in the gangue matrix or is covered (or partially covered) by reaction products.

Experimental rates of anodic dissolution of the mineral ranged from 7.00×10^{-13} mol Cu $cm^{-2}.s^{-1}$ at 0.560 V (vs. SHE) to 1.69×10^{-12} mol Cu $cm^{-2}.s^{-1}$ at 0.620 V (vs. SHE) in a 0.2 M HCl solution at 25°C. Corresponding dissolution rates for a 0.2 M HCl + 0.5 g/L Cu (as $CuSO_4$) solution were between 2 to 3 times lower. In addition, the rate of anodic dissolution of the mineral was found to show a half order rate-dependency on the cupric-to-cuprous ion ratio at the mineral surface over this potential range.

It was demonstrated by measurement of the solution potential close to the mineral surface (capillary solution potential) that cupric ions can oxidize covellite in acidic, chloride solutions by means of the Cu(II) / Cu(I) couple.

The mixed potential showed a 0.051 $V.decade^{-1}$ dependency on the cupric-to-cuprous ion ratio at the mineral surface and Tafel slope values of 0.100 $V.decade^{-1}$ to 0.107 $V.decade^{-1}$ were obtained confirming that the mineral dissolves by a direct oxidative mechanism with the anodic dissolution of the mineral, according to a one-electron process, as the rate-determining step.

A reaction mechanism has been proposed where cupric ions act as the primary oxidant (electron acceptor) at the mineral surface. These ions can then be regenerated by the oxidation of cuprous to cupric ions in the presence of dissolved oxygen and protons. Elemental sulphur is formed directly on the mineral surface as a result of the anodic dissolution of the mineral.

Chloride ions and copper ions were found to show a marked influence on the measured current density with an increase in current density with increased chloride concentration and an unexpected decrease in current density, especially at high chloride concentration, with increased copper concentration. However, the positive effect of increased chloride concentration on the measured current density only pertained to the initial stages of leaching and similar rates of mineral dissolution were achieved at high (2 M Cl^-) and low chloride concentration (0.2 M Cl^-) over prolonged periods. This might have been as a result of the increase in copper concentration with time by leaching of the mineral.

Capillary potential measurements showed that the solution potential close to the mineral surface decreased with increased capillary length. This could effect a decrease in the mixed potential and thereby also a decrease in the rate of leaching of the mineral.

ACKNOWLEDGEMENTS

During 2003 a research centre of a large, international mining company was tasked to develop a suitable technology for the heap leaching of low-grade, chalcopyrite-bearing, whole ores for its mining assets. An ambitious program was undertaken by an international project group, which included colleagues from Australia, Chile, South Africa and the United States of America. This effort culminated into the development of two technologies, namely a high-temperature, bioleaching and a low-temperature, chloride leaching technology. I was privileged to be part of that team for which I am forever grateful.

My involvement mainly focused around the fundamentals of the chloride leaching technology, which over time extended to also include the present study. For this purpose, I had the opportunity to spend some time at the laboratories of Murdoch University in Perth, Australia. Here I worked under the auspicious of Prof. M.J. Nicol, which has been one of the most memorable experiences of my career to date. Prof. Nicol, many thanks to you, your staff as well as your family, who made my stay in Perth, feel like home. I am also very appreciative of all the countless hours of discussions, sharing of ideas, knowledge and teachings.

Thanks also to my supervisor, Dr J. Petersen, of the Department of Chemical Engineering, University of Cape Town, for his advice, mentoring and patience.

I gratefully acknowledge the interest of various ex-colleagues, who encouraged me on the way. Thank you: Debbie Miller, Elmar Muller, John Batty, Marthie Kotzé and Dr D.W. Dew. Of the latter, I would like to say that I had the privilege to know Dave as a colleague, manager, client and friend, whose generosity and wisdom nurtured a keen interest in science. To me, Dave and Prof. Mike are men who plant trees for others to sit under.

To my friends and special girl, Ciska, thanks for your moral support and understanding.

Special thanks also to my dearest parents, Dr W.P. and Mrs K.H.M. Basson, for their support and whose unconditional love is an anchor in life.

Above all, thank All Mighty God.

TABLE OF CONTENTS

Chapters

Chapters

LIST OF FIGURES

List of Tables

CHAPTER 1

INTRODUCTION

1.1 Background

Chalcopyrite ($CuFeS_2$) is one of the most abundant and widely distributed copper sulphide minerals in the world, which makes it an important source of copper production [1]. However, the mineral is notorious among the copper sulphide minerals for its refractoriness to leach, especially in acidic, ferric chloride and ferric sulphate solutions, at low temperature. In both systems, this is characterized by the mineral's slow leaching kinetics, which level off with time [2]. Many investigators have attributed this levelling-off in the kinetics to a process of passivation, but great uncertainty still remains about what this exactly entails [3,4,5,6].

Chemical [7,8,9] and electrochemical [3,10,11] methods have shown that the oxidative dissolution of chalcopyrite is a potential-dependent process and that the onset of passivation occurs at a mineral surface potential (mixed potential) in excess of about 0.6 V (vs. SHE) [3,10,11,12,13,14,19,46,47,48]. Electrochemical studies have also shown that under normal ferric leaching conditions, such as bioleaching and atmospheric leaching in chloride and sulphate systems, the mixed potential is normally fixed in the so-called passive region of the oxidative process, even at corresponding high solution potentials, e.g. 0.8 V (vs. SHE) to 0.9 V (vs. SHE), as measured against an inert platinum electrode [10]. In this region, the mineral is subjected to the process of passivation, which is typified by the levelling-off in the leaching kinetics.

The above defines then the fundamental problem of oxidative dissolution of chalcopyrite by leaching in such systems at low temperature [12,13].

In the context of heap leaching of low-grade, chalcopyrite-bearing ores, bioleaching at elevated temperatures could be attempted in order to alleviate the problem of mineral passivation. For this purpose, the bioheap could be operated in such a way that the heap temperature is aimed to progress sequentially from mesophilic (ambient to 45°C), through moderately thermophilic (45°C to 60°C) to thermophilic levels (60°C to 80°C) [15], and maintained there for some time [16], in order to achieve improved rates and extents of chalcopyrite dissolution.

However, the success of such a strategy will depend, amongst other things, to a large extent on sufficient levels of available sulphide sulphur (S^{2-}) present in the ore, as well as the successful oxidation thereof in relatively fast, heat-generating (exothermic) reactions.

Pyrite (FeS_2) is an example of an appropriate sulphide mineral that could fulfil this role [15], and of which the occurrence is commonly associated with that of chalcopyrite [28,29,30,99]. For example, consider the overall reaction equation,

$$4FeS_2 + 15O_{2\,(aq)} + 2H_2O \rightarrow 2Fe_2(SO_4)_3 + 2H_2SO_4 \qquad (1.1)$$

which represents the microbial-assisted oxidation of the mineral in acidic, iron sulphate solutions [83]. The stoichiometry of the above reaction predicts a heat of reaction of -11.2 $MJ.kg^{-1}$ FeS_2 at 25°C [114]. Therefore, a substantial amount of heat could be generated, especially so at increased levels of pyrite present in the ore.

However, in order to achieve the required rate of heat generation to affect elevated heap temperatures, it will be advantageous to operate under conditions of high overpotentials (at the mineral surface) in order to ensure suitably fast kinetics of oxidation of pyrite [20,21,22,23,24].

On the other hand, in the case where pyrite concentrations are too low to generate the required heap temperatures, which are deemed suitable for moderate thermophile or thermophile bioleaching of chalcopyrite, a chemical leach could be considered instead.

The latter option may also be more suitable where the ore contains substantial amounts of acid-soluble, chloride-bearing minerals such as atacamite ($Cu_2Cl(OH)_3$) or even potassium- and sodium-bearing chlorides, because the introduction and accumulation of chloride ions in the leach solution may very well rule out the use of bioleaching.

One such technology, which was recently developed, entails the leaching of chalcopyrite under conditions of low-potential in acidic, chloride solutions at ambient temperature [12,13]. In this process, mineral dissolution without passivation is achieved within a potential range of 0.550 V (vs. SHE) to 0.600 V (vs. SHE), in the presence of chloride ions, dissolved oxygen and protons.

However, since copper sulphide minerals such as bornite (Cu_5FeS_4), chalcocite (Cu_2S) and covellite (CuS) are often associated with chalcopyrite [28,29,30], the leaching behaviour of these copper sulphide minerals also need to be taken into consideration in the evaluation of such a leaching process.

To date, it has been demonstrated that pyrite remains inert under the reigning conditions of the above technology, which has the advantage that less iron is introduced into the pregnant leach solution (PLS) for down-stream purification.

Also, that bornite, chalcocite and covellite could indeed be leached successfully from low-grade, copper-bearing whole ores by application of the above technology [25,26,60].

However, there is a requirement to study the leaching behaviour of covellite on a fundamental level, because the leaching conditions which are optimum for chalcopyrite may not always be conducive for successful covellite leaching. For example, it has been demonstrated that in low-potential leaching of chalcopyrite, a "covellite-like" intermediate can form under certain conditions, which in fact passivates the mineral's surface and prevents further leaching of chalcopyrite. By illustration, Figure 1.1 shows an optical microscopy photograph what appears to be a "covellite-like", intermediate product formed on the surface of a chalcopyrite electrode under conditions of low potential and no dissolved oxygen [14,17,19].

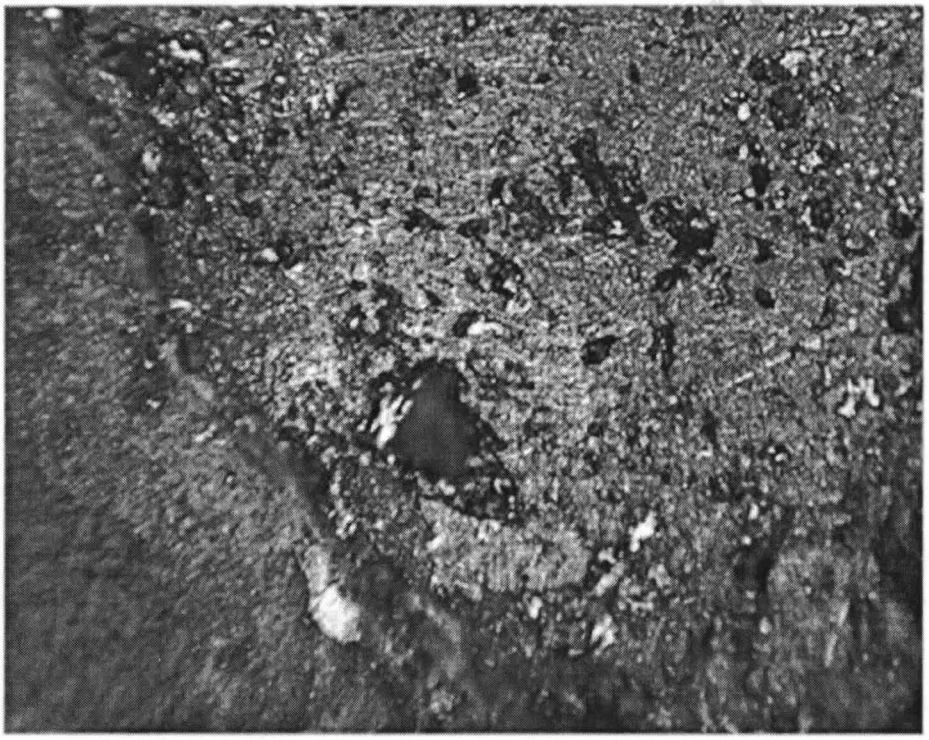

Figure 1.1 : Intermediate Product (Blue / Purple) on Chalcopyrite Surface (Gold)

Therefore, in order to establish an operating regime that is conducive for both chalcopyrite and covellite leaching, it is proposed that a fundamental study be undertaken to investigate the anodic dissolution of covellite in low-potential,

chloride solutions at ambient temperature. The information obtained from such a study may aid in the understanding of the leaching behaviour of covellite in such systems and may also provide insight with respect to process selection and the application of conditions necessary for maximum copper recovery.

1.2 Objectives

The objectives of this study are:

- To investigate the anodic processes involved in the dissolution of covellite in acidic, chloride solutions, especially within the potential range of 0.55 V (vs. SHE) to 0.62 V (vs. SHE) at low temperature (25°C);
- To investigate the possibility of active-passive behaviour within the applied potential range;
- To investigate the effect of potential on the rate of dissolution of covellite;
- To investigate the effect of parameters such as acidity (pH), chloride ion concentration, copper ion concentration and sulphate concentration on the rate of dissolution of covellite;
- To elucidate the role of the said parameters in the anodic processes involved, and
- To investigate the effect of pore length on the mineral's surface potential.

1.3 Approach

In order to make this study and its results more relevant to heap leaching of whole ore material, the electrochemical techniques were applied to a stationary, covellite electrode. Also, the electrode was studied in an apparatus, which would, to some measure, simulate the anodic dissolution behaviour of covellite positioned in a solution-filled pore of a larger whole ore particle.

In general, electrochemical techniques can be very useful in mechanistic or screening tests pertaining to the leaching of copper sulphide minerals. However, care has to be taken that the applied potential range is applicable to that induced during the conventional leaching process. Also, purity of the mineral electrode used, is also very important, because impurities oxidizing at applied potentials will cause bias towards the measured anodic (or cathodic) currents.

Furthermore, it should also be remembered that these techniques are conducted over relatively short periods of time, which may again introduce bias towards the rate of leaching in view of active-passive behaviour of the mineral electrode. Therefore, it is essential to conduct these in conjunction with longer-duration, conventional, leaching experiments. In this way, the electrochemical results could become even more useful. For this reason, published results of conventional, leaching tests have been included to compliment the electrochemical findings.

The selection of an appropriate electrode sample is very important to better relate the findings to operational applications. Unfortunately, a pure, natural sample of covellite could not be sourced for this study and an available, synthetic sample was used instead.

CHAPTER 2

LITERATURE REVIEW

2.1 Covellite

The copper sulphide mineral originally known as *Kupferglas* (Freiesleben) was later named indigo copper by Hoffmann and Breithaupt [27]. Later, it was named covelline or covellite by Beudant (1832) after the Italian mineralogist, Covelli (1790 - 1829), who discovered the Vesuvian specimen and determined its composition [27,28,29]. Chapman also referred to the mineral as *breithauptite* [27]; however, today, the mineral is commonly known as covellite.

Covellite (CuS) is not abundant, but is found as a supergene mineral, usually as a coating, in the sulphide enrichment zones of most copper-bearing, ore deposits [28,32]. It is often found in small, hydrothermal veins [30] associated with pyrite (FeS_2) [29] and other copper sulphide minerals [28,29,30] such as bornite (Cu_5FeS_4), chalcocite (Cu_2S), chalcopyrite ($CuFeS_2$) and enargite (Cu_3AsS_4), from which it can be derived by means of alteration [28,32].

The mineral has been found at Bor (Serbia), Leogang (Austria) and in large, iridescent crystals from the Calabona mine at Alghero (Sardinia). Other occurrences, amongst others, include: Butte, Montana (USA), Summittville, Colorado (USA), La Sal district, Utah (USA), Kennecott, Alaska (USA), Chile, Bolivia, Namibia, Italy, Germany and Romania [28,29,30].

Covellite has a chemical composition of 66.48% copper and 33.52% sulphide sulphur and its chemical properties include: it is soluble in hydrochloric acid (HCl) and hot nitric acid (HNO_3), fusible and burns with a blue flame releasing sulphur dioxide (SO_2) [28,29].

Physical properties include: a hardness of 1.5 - 2 Mohs, a specific gravity (SG) of 4.6 - 4.76, a metallic lustre, an indigo-blue or blue-violet colour (iridescent), a lead-gray to black (dark-blue when rubbed) streak, an opaque transparency and a dull to resinous lustre [28,29,30]. An example of the mineral is shown in Figure 2.1.

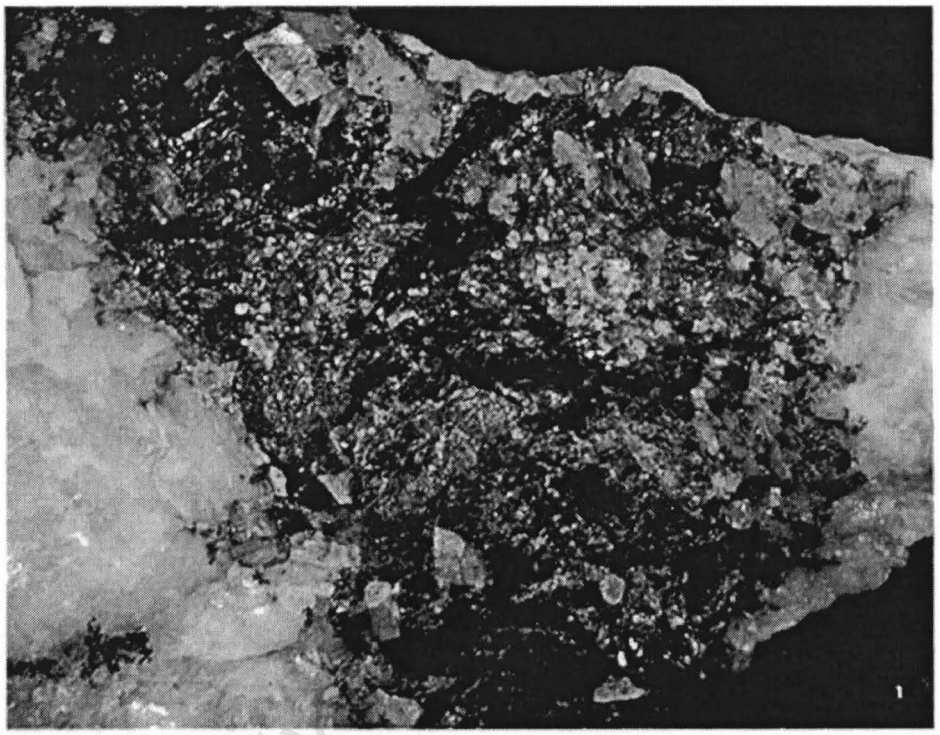

Figure 2.1 : A Granular Aggregate from the Oxidation Zone of Ore Veins from Železník, Czechoslovakia [29]

Covellite has a hexagonal crystal system with perfect cleavage on {0001} yielding flexible plates [28,29] and an ionic structure of $(Cu^{+})_2S_2^{2-}$ [31]. The mineral also shows good electrical conductivity [29] (metallic-type conductor [31]) with a resistivity of 7×10^{-7} to $8 \times 10^{-5}\ \Omega$ [31].

2.2 Thermodynamics

Pourbaix Diagrams

Pourbaix or potential vs. pH diagrams are graphical representations of thermodynamic data as a function of electrochemical potential (potential, y-axis) and acidity (pH, x-axis) [33]. These diagrams can be very useful in determining appropriate solution regimes, with regard to oxidation-reduction potential and pH for, amongst others, the leaching of copper mineral sulphides. In addition, if used correctly, these can aid in establishing whether a particular reaction is thermodynamically feasible or not, aid in the prediction of intermediate reaction products from dissolving minerals, as well as the identification of the major species in equilibrium at a particular potential and pH [33,34].

However, it is important to realize that the thermodynamics, as presented by these diagrams, do not specify the rate at which a specific process occurs. Neither do they identify mechanistic features of a process. These quantities can only be determined by experimental, kinetic studies [33].

Figures 2.2.1 and 2.2.2 show the Pourbaix diagrams for the copper-sulphur-water system at 25°C, in the absence and presence of chloride ions [36]. These have been constructed by ignoring sulphate. The reason for this is that conventional Pourbaix diagrams would predict, depending on pH, sulphate or bisulphate as the product of oxidation of the sulphide species, because of the greater thermodynamic stability of the former [34,35]. However, it is well-known that in practise, the chemical leaching of covellite in both acidic, chloride and sulphate solutions render almost complete yields of elemental sulphur (see 2.4.1 Chemistry of Reaction). Furthermore, the conventional diagram correctly predicts that the oxidation of chalcocite at pH 2, for example, will produce covellite, but then also predicts the latter to form chalcocite at even higher potentials (Figure 2.2.3) [35]. This is also not found in practise.

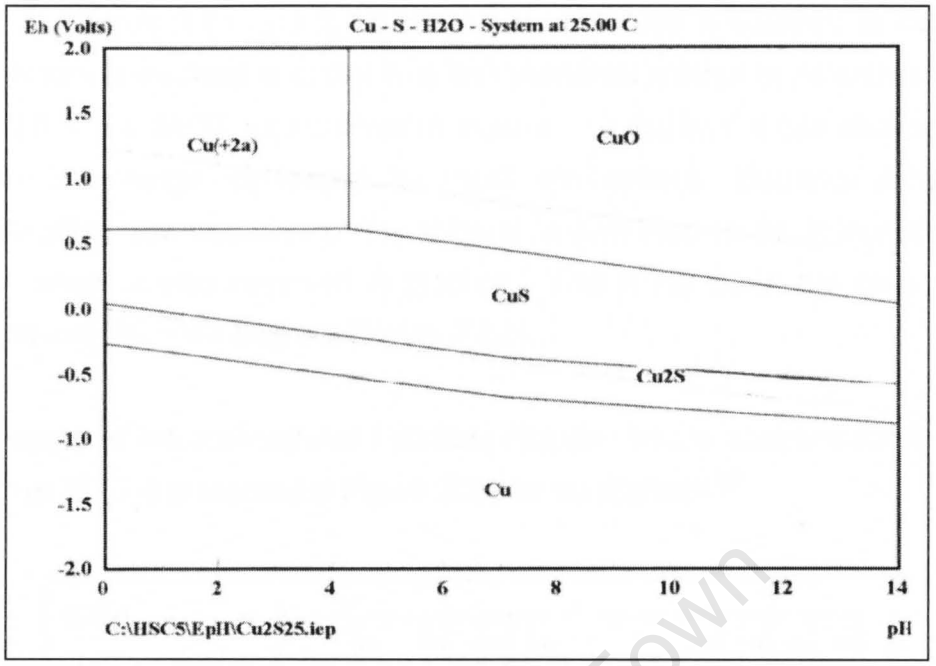

Figure 2.2.1 : Copper-Sulphur-Water System with Soluble Species at 0.1 M Activity (In the Absence of Chloride Ions) by Nicol [36]

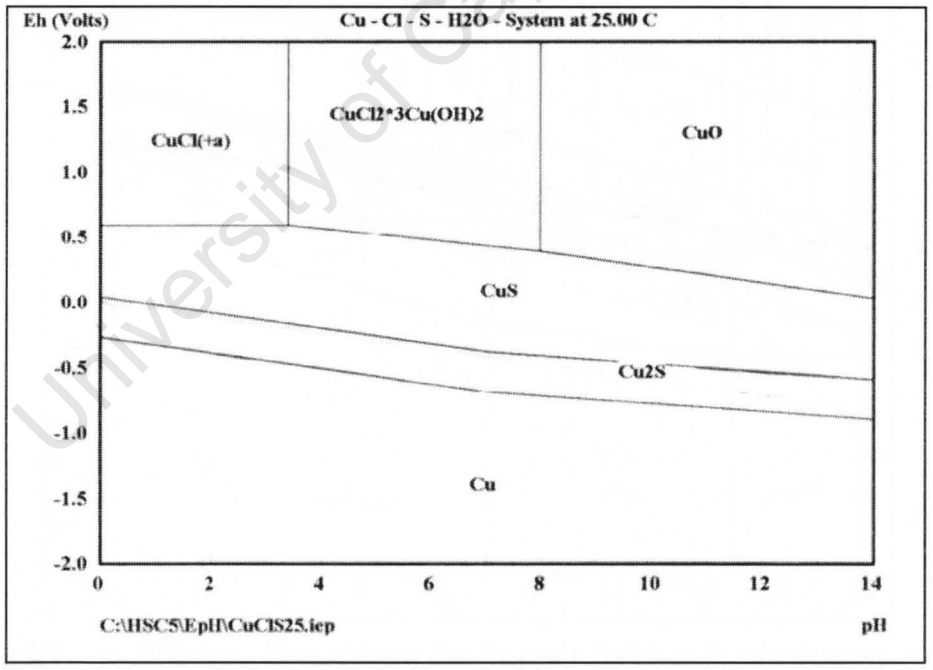

Figure 2.2.2 : Copper-Sulphur-Water System with Soluble Species at 0.1 M Activity (In the Presence of Chloride Ions at 1 M Activity) by Nicol [36]

At pH 2, Figures 2.2.1 and 2.2.2 show that chalcocite is oxidized to covellite, which in turn is oxidized to cupric ions and elemental sulphur at potentials above about 0.6 V (vs. SHE), as observed in practise. In addition, it can also be seen that in the range pertaining to most atmospheric leaching processes (pH 0 to pH2), the oxidation of the mineral is predicted to be independent of acidity, which is also observed in practise. This is not so in the case of the conventional Pourbaix diagram (Figure 2.2.3).

An example of the conventional Pourbaix diagram for the copper-sulphur-water system at 25°C is presented in Figure 2.2.3 for comparison [35].

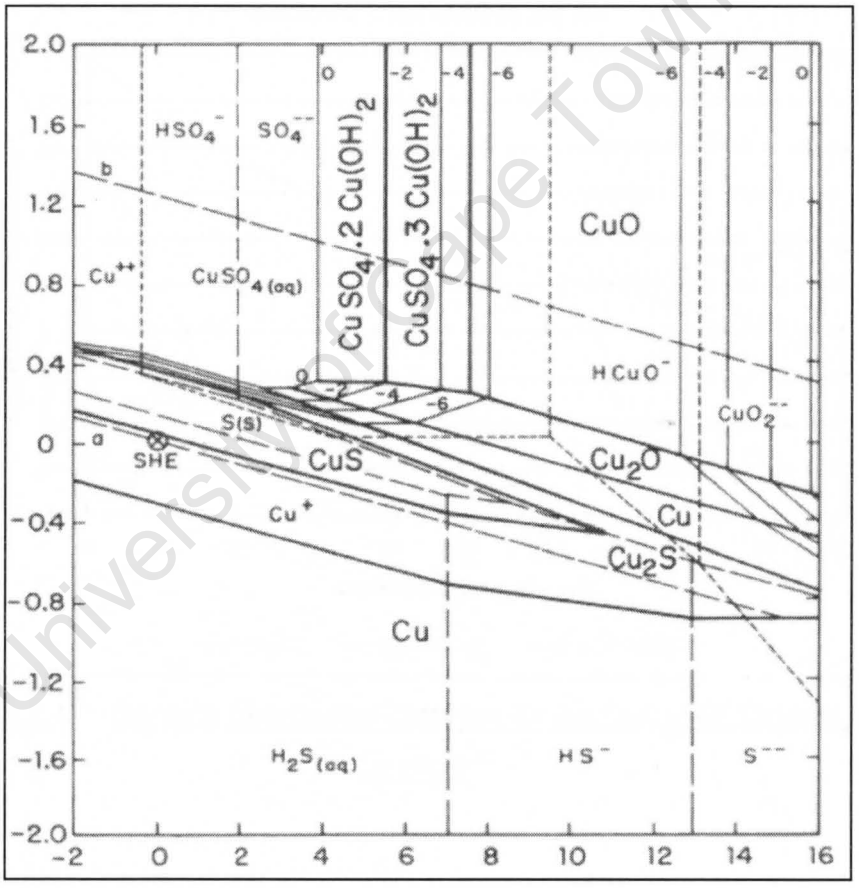

Figure 2.2.3 : Pourbaix Diagram for the Copper-Sulphur-Water System for Unit Activities of the Sulphur Ligands [35]

Chloride Complexation of Copper Species

In contrast to the sulphate system where copper is present as cupric ions only, both cupric and cuprous ions can exist in the chloride system as chloro-complexes [33,38,44].

Figures 2.2.4 and 2.2.5 show species distribution diagrams for the cuprous / chloride and cupric / chloride systems, which were generated from thermodynamic data of the NIST database [40].

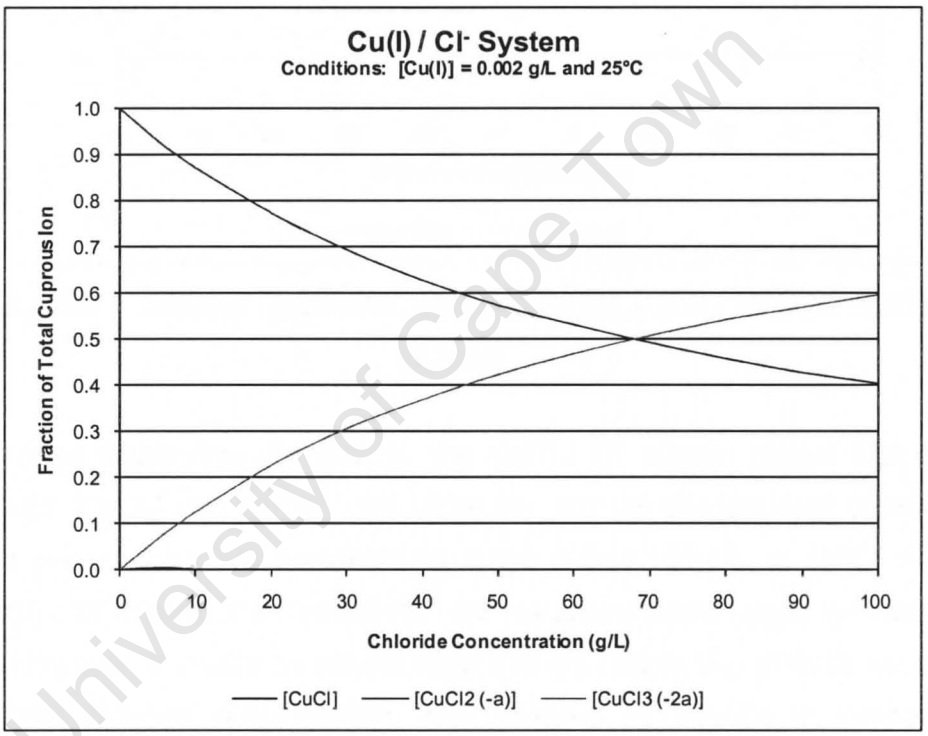

Figure 2.2.4 : Species Distribution Diagram for the Cu(I) / Cl^- System at 25°C by Nicol [41]

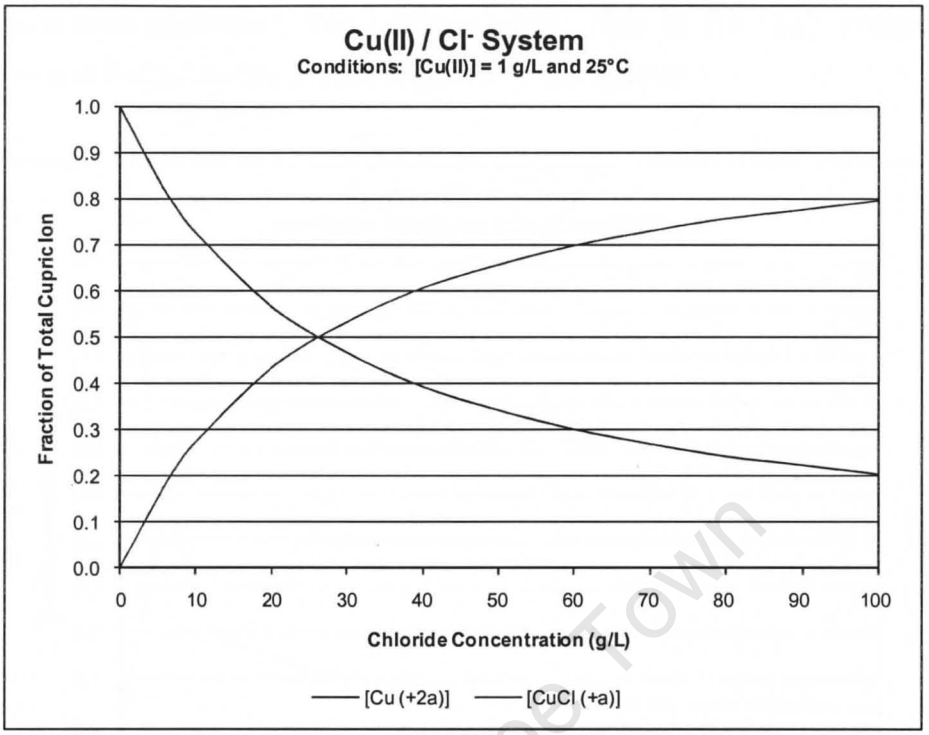

Figure 2.2.5 : Species Distribution Diagram for the Cu(II) / Cl^- System at 25°C by Nicol [41]

The species distribution diagram for the Cu(I) / Cl^- system shows that among Cu^+, CuCl, $CuCl_2^-$ and $CuCl_3^{2-}$, the latter two are the predominant cuprous ion species over the chloride concentration range of 0 to 100 g/L, at 25°C. And, for the Cu(II) / Cl^- system, Cu^{2+} and $CuCl^+$ are the predominant cupric ion species at 25°C. However, it should be emphasized that the distribution of such species is, apart from chloride concentration, also affected by change in temperature, because of the fact that the various equilibria (equilibrium constants) are temperature-dependent [33,38,42].

Chloride Complexation of Iron Species

Likewise, iron species can also be complexed with chloride ions, with Fe(III) forming much stronger chloro-complexes than Fe(II) [33,44].

Figure 2.2.6 shows an example of a species diagram for the Fe(III) / Cl^- system, which was also generated from thermodynamic data of the NIST database [40], with Fe^{3+} and $FeCl_2^+$ as the predominant ferric ion species.

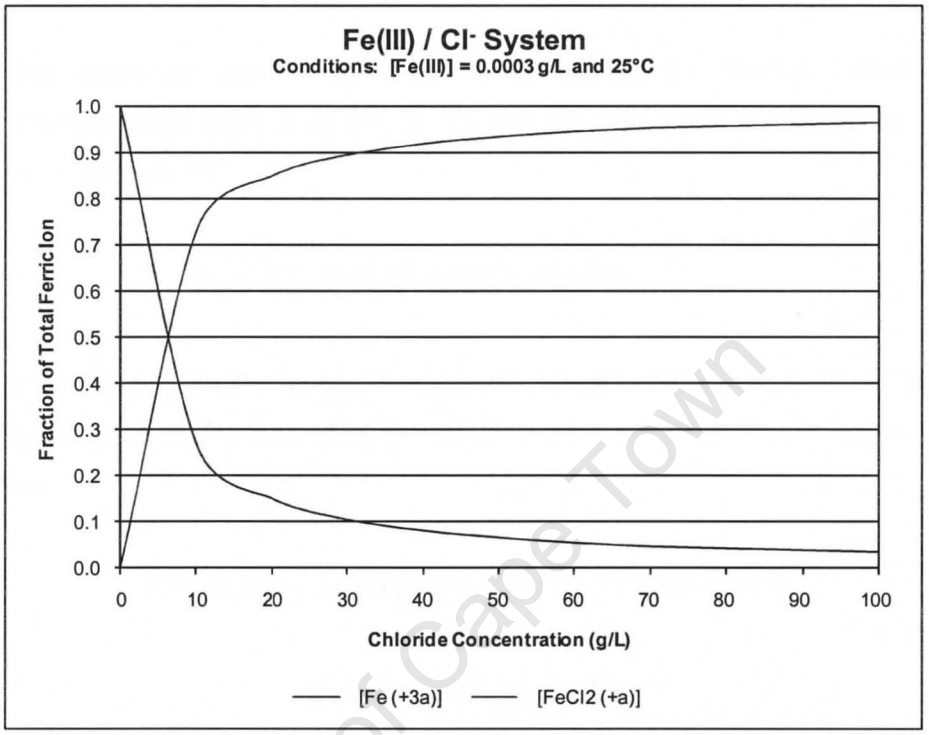

Figure 2.2.6 : Species Distribution Diagram for the Fe(III) / Cl^- System at 25°C by Nicol [41]

Effect of Complexation on the Oxidation-Reduction Potential

The formation of complexes between a metal ion and a ligand can have a significant effect on the value of the oxidation-reduction potential [33]. For example, consider the half-cell reaction for the cupric / cuprous couple:

$$Cu^{2+} + e^- = Cu^+ \qquad (2.2.1)$$

The value for the standard potential (E°) is 0.162 V (vs. SHE), i.e. under conditions where all gaseous species are at a fugacity (thermodynamic pressure)

of 1 atmosphere and all the dissolved species at an activity (thermodynamic concentration) of 1 molal, at 25°C (298.15 K) [38]. However, for diluted solutions, activity and fugacity can be approximated by concentration and (partial) pressure, respectively [33,39].

Thus, the potential under non-standard conditions (or formal potential), at concentrations other than unity (at 25°C), can be calculated by using the Nernst equation as follows [33,38].

$$E = E° - 0.0591\log([Cu^{+}]/[Cu^{2+}]) \qquad (2.2.2)$$

And, at a total chloride concentration of 50 g/L: $[Cu^{+}] = 1.45 \times 10^{-11}$ M (data from Figure 2.2.4) and $[Cu^{2+}] = 5.37 \times 10^{-3}$ M (data from Figure 2.2.5). Therefore,

$$E = 0.162 - 0.0591\log(1.45 \times 10^{-11} / 5.37 \times 10^{-3})$$

$$E = 0.668 \text{ V (vs. SHE)}$$

Thus, in the presence of a ligand such as chloride ions, the potential will change due to complexation of the cupric and cuprous ions rendering altered concentrations of both the free cupric (Cu^{2+}) and cuprous (Cu^{+}) ions. In other words, the effect of complexation can be viewed as a reduction in the activity of both the free Cu^{2+} and Cu^{+} ions.

Thermodynamics of the Oxidation of Covellite in Chloride Solutions

Figure 2.2.7 schematically shows the oxidation of covellite in an acidic, oxygenated, sulphate system (in the presence of ferric ions) in comparison to an acidic, oxygenated, chloride system (in the absence of ferric ions).

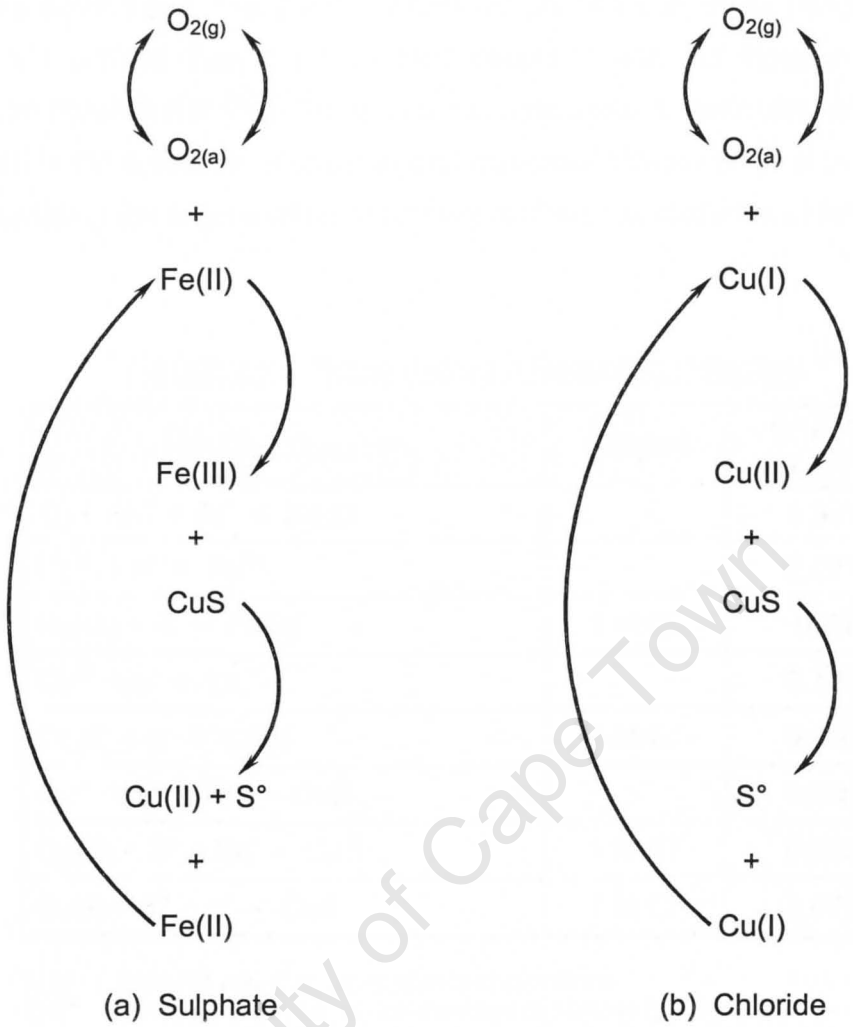

Figure 2.2.7 : Oxidants for the Leaching of Covellite in (a) the Sulphate System and (b) the Chloride System - Adapted from Nicol [37]

From a thermodynamic viewpoint (Table 2.2.1), both O_2 / H_2O ($E° = 1.229$ V) and Fe(III) / Fe(II) ($E° = 0.771$ V) redox couples can facilitate oxidation of covellite to cupric ions and elemental sulphur in a sulphate system ($E° = 0.631$ V). However, from a kinetic consideration, it is known that the O_2 / H_2O couple is very irreversible with respect to the covellite surface [18,41,45], and that the kinetics of oxidation by dissolved oxygen are very slow under atmospheric conditions [49,50].

On the other hand, the Fe(III) / Fe(II) couple is much more reversible on the mineral's surface than the O_2 / H_2O couple [41] and the kinetics of oxidation proceed much faster [49,50]. Thus, in a sulphate system, ferric ions act as primary oxidant in the oxidation of covellite and dissolved oxygen plays a secondary role by facilitating the regeneration of primary oxidant, i.e. oxidation of ferrous to ferric ions.

Table 2.2.1 : Some Relevant Reduction Potentials [45]

Reaction Equation	Solution	E° or E°' (vs. SHE)
$O_2 + 4H^+ + 4e^- = 2H_2O$		1.229
$Fe^{3+} + e^- = Fe^{2+}$		0.771
$Fe(III) + e^- = Fe(II)$	1 M Cl^-	0.74
$Cu^{2+} + e^- = Cu^+$		0.162
$Cu(II) + e^- = Cu(I)$	1 M Cl^-	0.492
$Cu^{2+} + S° + 2e^- = CuS$		0.631
$Cu(II) + S° + 2e^- = CuS$	1 M Cl^-	0.583
$Cu(I) + S° + e^- = CuS$	1 M Cl^-	0.675

1) E° standard potential, i.e. at standard conditions
2) E°' formal potential, i.e. at non-standard conditions (25°C)

In a chloride system, cuprous ions are stabilized by complexation, which introduces a fast and very reversible redox couple, namely the Cu(II) / Cu(I) couple [33,41,45]. In fact, it has been shown that this redox couple has a higher degree of reversibility than the Fe(III) / Fe(II) couple on platinum [33], on a corroding chalcopyrite surface [51,52], as well as on a corroding covellite surface [53].

Thus, under appropriate conditions, the Cu(II) / Cu(I) redox couple can also oxidize covellite as can be seen from the thermodynamics presented in Figure 2.2.8.

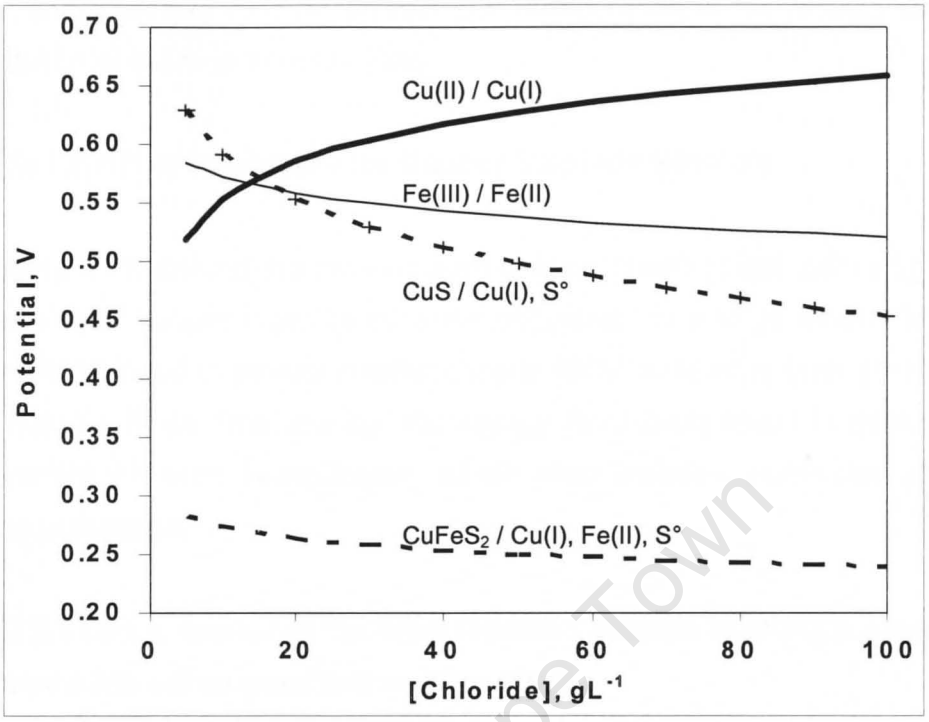

Figure 2.2.8 : Potentials of Various Couples in the Cu(II) / Cu(I) / S° System at 25°C by Nicol [47]

Figure 2.2.8 summarizes the thermodynamics of the various redox couples involved in a system with initial concentration ratios of Cu(II) / Cu(I) = 100 and Fe(III) / Fe(II) = 0.001, which is so constructed that these couples are in equilibrium with the following couple,

$$CuS = Cu(I) + S° + e^- \qquad (2.2.3)$$

for a total chloride concentration of 15 g/L and a total copper concentration of 1 g/L [47]. The graphs show that covellite is unstable in the presence of cupric ions under these conditions. Thus, as a result of the increased stability of cuprous ions in chloride solutions, cupric ions can oxidize covellite.

For the same reasons as mentioned before, cupric ions will act as the primary oxidant and dissolved oxygen will facilitate regeneration of the primary oxidant, i.e. oxidation of cuprous to cupric ions.

2.3 Chloride Leaching Processes for Copper Sulphide Minerals

The driving force behind the development of hydrometallurgical technologies for the leaching of copper sulphide minerals originated, to a large extent, from an environmental need to control sulphur dioxide (SO_2) emissions from smelters [54]. Consequently, much time, money and energy have been spent to date on the development of such technologies, which also includes numerous chloride leaching processes.

Table 2.3.1 lists a number of the more important chloride leaching processes of which only a few will be described in some detail.

Table 2.3.1 : Chloride Leaching Processes for Copper Sulphide Minerals

Process	Feed Material	Scale	Reference
Hoepfner	Concentrate	Laboratory (small)	42, 55
U.S. Bureau of Mines	Concentrate	Laboratory (large)	44, 54
MINTEK	Concentrate	Pilot plant	44, 54
Noranda	Concentrate	Laboratory	56, 57
ELKEM	Concentrate	Pilot plant (small)	44
CYMET	Concentrate	Pilot plant	44, 54, 56, 57
CLEAR	Concentrate	Industrial plant	44, 54, 56
Minemet Recherches	Concentrate	Pilot plant	44, 54
CUPREX	Concentrate	Pilot plant	44, 54, 56
Hydrocopper (GCM)	Concentrate	Laboratory (large)	54
Intec	Concentrate	Demonstration plant (ready for commercialization)	56, 57
Sumitomo	Concentrate	Pilot plant	57
BHAS	Matte	Industrial plant	56, 57
PLATSOL™	Concentrate	Pilot plant (ready for commercialization) NorthMet mine, USA	57
HydroCopper™ (Outotec)	Concentrate	Demonstration plant (ready for commercialization) Erdenet mine, Mongolia	56, 57, 58
CESL	Concentrate	Semi-industrial plant (Sossego mine, Brazil) Industrial plant (Highland Valley Copper)	57
Cuprochlor	Low-grade,whole ore (supergene material)	Industrial heap leach operation (Michilla mine, Chile)	59
Company A	Concentrate / milled ore	Laboratory (small)	60
Company A	Low-grade, whole ore (chalcopyrite-bearing)	Column-scale (1 m and 6 m)	60
Company A	Low-grade,whole ore (mixed oxides / sulphides)	Industrial heap leach operation (mine)	60

Hoepfner Process [42,55]

As early as the 1890's, Hoepfner discovered that copper could be solubilised from copper sulphide minerals in chloride solutions with elemental sulphur as a product of the reaction. This led to a patented process in 1893, which drew considerable interest again during the 1970's. A modified version of this process comprised the following process steps:

- Leach: Cupric chloride leaching in acidic, inert (oxygen-free) chloride solutions at ambient pressure and 105°C, e.g.

$$CuFeS_2 + 3Cu^{2+} \xrightarrow[H_2O]{NaCl} 4Cu^{+} + Fe^{2+} + 2S^{\circ} \qquad (2.3.1)$$

$$Cu_2S + 2Cu^{2+} \xrightarrow[H_2O]{NaCl} 4Cu^{+} + S^{\circ} \qquad (2.3.2)$$

$$CuS + Cu^{2+} \xrightarrow[H_2O]{NaCl} 2Cu^{+} + S^{\circ} \qquad (2.3.3)$$

- Purification: Elemental sulphur recovery from the solids residue followed by removal of any concomitant, solubilised metals (such as iron) from solution by metal hydroxide precipitation, e.g.

$$Fe^{2+} + 2OH^{-} \rightarrow Fe(OH)_2 \qquad (2.3.4)$$

$$M^{n+} + nOH^{-} \rightarrow M(OH)_n \qquad (2.3.5)$$

- Electrolysis: One-electron electrolysis in a diaphragm cell to deposit copper at the cathode with regeneration of cupric ions at the anode, e.g.

Cathode:

$$Cu^{+} + e^{-} \rightarrow Cu^{\circ} \qquad (2.3.6)$$

Anode:

$$Cu^{+} \rightarrow Cu^{2+} + e^{-} \qquad (2.3.7)$$

- Recycling: Finally, recycling of the anolyte as leach reagent. Additional cupric ions could also be generated by oxidation of cuprous ions (in cell effluent) with hydrochloric acid and oxygen, e.g.

$$2Cu^{+} + 2HCl + \tfrac{1}{2}O_2 \rightarrow 2Cu^{2+} + 2Cl^{-} + H_2O \qquad (2.3.8)$$

The process is relatively straightforward without multi-phased steps and its closed-recycle nature and possible adaptation to other substrates adds to its appeal. One-electron electrolysis of cuprous ions also has the potential to save energy and to reduce much of the size of the facility. Furthermore, using cupric chloride as the oxidant, especially so with chalcocite- and covellite-bearing concentrates, introduces no foreign ions into solution that may render process complications.

However, concentrates, especially chalcopyrite-bearing, present problems with respect to leaching (excess leach reagent necessary and incomplete reaction), elemental sulphur recovery, separation of concomitant metals due to co-precipitation of copper and incomplete material balances.

CYMET Process [44,54,56,57]

The Cyprus Metallurgical Processes Corporation (CYMET) originally conducted anodic dissolution of copper mineral sulphide concentrates in slurries with direct electrowinning of copper in an electrolytic, membrane cell.

Thereafter, they developed a process, which comprised a two-stage, counter-current leach with ferric and cupric chloride in the presence of sodium chloride. The process operated at ambient pressure and 98°C and achieved 99% overall copper dissolution after 3 hours in each stage.

After thickening and filtration, the pregnant leach solution was vacuum-cooled to about 40°C to crystallize about half the copper as cuprous chloride. The latter was centrifuged, washed, dried and then reduced with hydrogen in a fluidized-bed reactor (500°C). Copper nodules suitable for fire-refining to copper wire-bars were produced in this way.

The spent leaching solution was regenerated by oxidation of cuprous and ferrous ions by hydrochloric acid and oxygen to cupric and ferric ions, respectively. In addition, the iron level in the solution was controlled by β-goethite and sodium jarosite precipitation.

A continuous pilot plant, which treated about 20 t / d of chalcopyrite-bearing concentrate, was operated for a period of four years until 1982. The results demonstrated that high copper dissolutions were achievable and that copper could be successfully recovered from solution by non-electrowinning methods. All parts of the process were reported as technically feasible and all corrosion problems to have been overcome. However, a major drawback of this process was that silver in the concentrate was extensively solubilised in the leaching circuit; consequently, much of the latter reported to the cuprous chloride crystals and, from there, to the metallic copper.

CLEAR (Copper Leaching Electrowinning and Recycle) Process [44,54,56]

The Duval Corporation developed a process for the treatment of chalcopyrite-bearing concentrates and attained an output of about 100 t Cu / d.

The process entailed a two-stage, counter-current leach in which the concentrate is only partially leached during the first stage at 105°C and according to:

$$CuFeS_2 + 3CuCl_2 \rightarrow 4CuCl + FeCl_2 + 2S° \quad (2.3.9)$$

$$FeCl_3 + CuCl \rightarrow FeCl_2 + CuCl_2 \quad (2.3.10)$$

The solution from the first stage was treated with copper metal to ensure that all the copper was present as cuprous ions in solution and the clarified solution was sent to electrolysis to produce copper metal powder by electrolysis. The anolyte, which contained cupric ions, was recycled to the second-stage leach.

The solids residue from the first stage was further leached, at 330 kPa O_2 and 150°C, in a second stage. Sulphate and iron control was affected by potassium jarosite and β-goethite precipitation in this stage.

A large-scale, demonstration plant was continuously operated until 1982, which demonstrated the general viability of the chloride processing route for chalcopyrite-bearing concentrates. However, needs for improvement of solution purification, recovery of by-products and control of the anodic and cathodic reactions in chloride electrowinning circuits were identified.

CUPREX Process[44,54,56]

In this process, concentrate is leached with ferric chloride at atmospheric pressure and 95°C to produce cupric ions and elemental sulphur. Excess oxidant (ferric chloride) is necessary to ensure that all the copper is present as cupric ions in solution. The leaching reactions are given as:

$$CuFeS_2 + 4FeCl_3 \rightarrow CuCl_2 + 5FeCl_2 + 2S° \quad (2.3.11)$$

$$CuFeS_2 + 3FeCl_3 \rightarrow CuCl + 4FeCl_2 + 2S^\circ \quad (2.3.12)$$

$$CuCl + FeCl_3 = CuCl_2 + FeCl_2 \quad (2.3.13)$$

After liquid-solids separation, the pregnant leach solution is cooled, treated with calcium chloride to precipitate gypsum and then contacted with a kerosene solution (DS 5443) to selectively (solvent) extract cupric chloride according to:

$$Cu(II)_{(aq)} + 2Cl^-_{(aq)} + 2L_{(org)} = L_2CuCl_{2\,(org)} \quad (2.3.14)$$

The loaded organic is scrubbed to remove minor impurities and then stripped with water at 65°C. The concentrated cupric chloride solution is sent to the electrowinning cell. The Metchlor-diaphragm cell allows separation between the anolyte and catholyte solutions by a cation-selective (ion-exchange) membrane. This allows maintaining the charge balance in the catholyte solution by transfer of sodium ions from the anolyte solution.

Copper is deposited as powder (granules) at the cathode, while chlorine gas is generated at the anode. The chlorine gas is recovered and used to oxidize cuprous to cupric ions, which are generated during electrolysis. The resultant cupric ions are extracted in a separate ("reforming") solvent extraction stage. The loaded organic from this stage is mixed with the organic feed to the main solvent extraction circuit.

The process produces high-purity copper powder at high current efficiency (94%) and with a specific energy consumption of 2.66 kWh / kg Cu. The silver content of the copper powder is less than 1 ppm and, in fact, this process should allow for the recovery of high-grade silver by-product from the raffinate. The solvent extraction circuit is relatively straightforward and does not require in-circuit pH control.

However, the overall flowsheet is somewhat complex and the ion-selective, membrane cells may be difficult to maintain in an industrial environment. Finally, it may also well be argued that this process suffers from a double disadvantage: 1) eletrowinning of cupric ions and 2) copper powder is produced.

HydroCopper™ Process [56,57,58]

Outotec's process is tailored for the leaching of copper sulphide mineral concentrates in continuous, stirred-tank reactors. A block diagram of the process is presented in Figure 2.3.1.

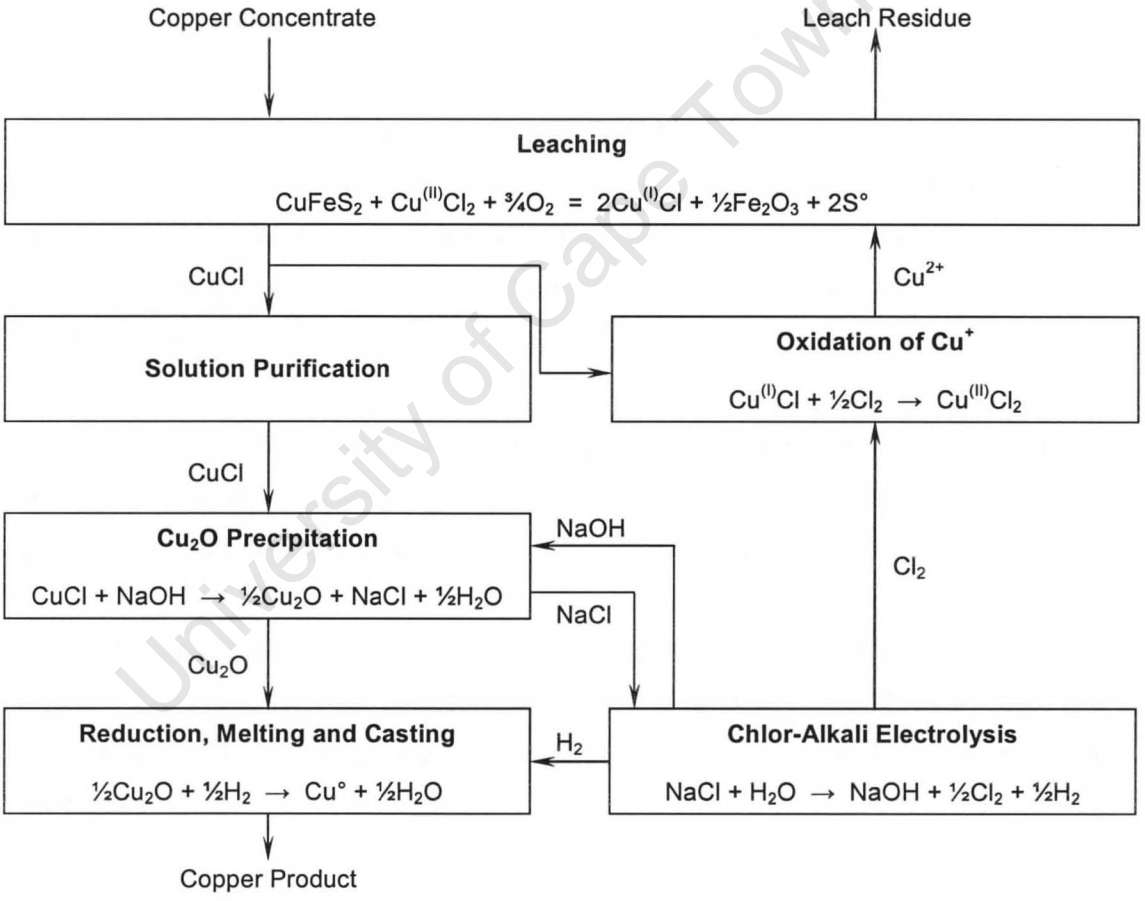

Figure 2.3.1 : HydroCopper™ Process [58]

The concentrate is leached in strong sodium chloride solutions at atmospheric pressure and 85°C to 95°C. The purified, pregnant leach solution is treated with sodium hydroxide to recover copper by precipitation of cuprous oxide. Air or oxygen is sparged into the leach reactors to oxidize ferrous to ferric ions, which are precipitated at pH 1.5 to pH 2.5. Sulphide sulphur is removed in its elemental form; however, about 10% to 15% is oxidized to sulphate, which is removed by gypsum precipitation.

After removal of all the sulphides, the solution potential in the final stage of the counter-current leach increases high enough to allow for gold dissolution as a chloro-complex. Recovery of the latter is achieved by either activated carbon or chemical precipitation. Silver is recovered by cementation with copper powder.

Chlor-alkali electrolysis is used to regenerate reactants, e.g. sodium chloride is decomposed into chlorine gas, hydrogen gas and sodium hydroxide. Chlorine is used for the oxidation of cuprous to cupric ions in the leach, sodium hydroxide solution is recycled for the precipitation of cuprous oxide and hydrogen is used for the reduction of cuprous oxide.

Cuprous oxide is reduced with hydrogen gas in a rotary kiln at 500°C to produce a very fine copper powder. This is then melted in an induction furnace to produce copper-wire rod or other cast products of copper.

This technology has been tested at demonstration scale (1 t Cu / day) on various copper sulphide mineral concentrates and eventually resulted in the first HydroCopper™ industrial plant being constructed at the Erdenet mine in Mongolia.

Table 2.3.2 lists some of the identified strengths and weaknesses of chloride technologies for the leaching of copper sulphide minerals.

Table 2.3.2 : Strengths and Weaknesses of Chloride Leaching Processes [54,56,57]

Strengths	Weaknesses
Fast kinetics for copper dissolution (making atmospheric conditions viable)	Corrosion (special materials of construction)
High extents of copper dissolution	High capital and maintenance costs
No sulphur dioxide (SO_2) emissions	Direct electrowinning does not produce LME grade A copper (cathode)
Elemental sulphur formation (little sulphate formation)	Poor quality (purity and morphology) copper products requires further (electro-) refining
Atmospheric pressures viable	Large energy requirements (mixing and oxygen dispersion)
Low temperatures (below 100°C) viable	Recovery of elemental sulphur from the solids residue requires additional attention
Smaller solution volumes (due to high copper solubility)	Total sulphide sulphur removal required if gold is to be recovered from the solids residue
Oxidants easily regenerated (cupric and ferric ions)	Selenium content of elemental sulphur remains a general concern
Pyrite (FeS_2) inert	
Silver dissolution	
Recovery of valuable by-products (gold and silver)	
Decoupling of metal production (from acid manufacture)	
Economically competitive (for unconventional concentrates)	

It is almost certain that traditional smelting and refining processes will remain unchallenged with regard to the processing of large tonnage of concentrates for many years to come.

However, hydrometallurgical processes, including chloride leaching technologies, will certainly find a niche application in the copper industry, e.g. for the treatment of complex concentrates [54], for concentrates containing high-value elements (such as gold and silver) [54], as well as for high-impurity [56] or so-called "dirty" [57] (such as arsenic-bearing) concentrates. In addition, these processes may also find usefulness in extending the life of existing, but obsolete, solvent extraction / electrowinning capital equipment [56].

2.4 Leaching Studies on Covellite

The chemistry, deportment of reaction products, kinetics and proposed mechanisms of the leaching of covellite are presented with regard to studies conducted on either natural or synthetically produced samples. Investigations on so-called secondary (or second-stage) covellite, which was produced from the leaching of natural or synthetic chalcocite, djurleite or digenite, are also included.

These investigations were performed at atmospheric pressures (except one [61]), over the temperature range 20°C to 105°C and, as far as the author is aware of, in the absence of active microorganisms.

2.4.1 Chemistry of Reaction

Covellite

One of the earliest fundamental leaching studies on covellite was conducted by Sullivan [49]. He investigated the dissolution behaviour of the mineral, sourced from crystalline (Kennecott, Alaska) and massive (Butte, Montana) natural samples, in acidic, ferric sulphate solutions. He found that the mineral dissolved according to the overall reaction:

$$CuS + Fe_2(SO_4)_3 = CuSO_4 + 2FeSO_4 + S^\circ \qquad (2.4.1)$$

Subsequent studies performed in the same medium, on both natural and synthetic samples, produced overall reaction equations similar to the one shown above (Equation 2.4.1) [62,63,64]. However, one of these works reported that, apart from elemental sulphur (S°), some sulphate sulphur was also produced. The latter constituted 4% of the leached sulphur with the remainder as elemental sulphur [62].

Dutrizac and MacDonald also found that a small amount of sulphate was formed in their experiments on pure, synthetic covellite disks and high-grade, natural covellite [65]. The following equation was reported to describe this reaction:

$$CuS + 8Fe^{3+} + 4H_2O \rightarrow Cu^{2+} + 8Fe^{2+} + SO_4^{2-} + 8H^+ \qquad (2.4.2)$$

Consequently, they proposed a more general, overall equation for the dissolution of covellite in acidic, ferric sulphate solutions:

$$CuS + (2 + 8x)Fe^{3+} + 4xH_2O \rightarrow Cu^{2+} + (2 + 8x)Fe^{2+} + (1 - x)S° + xSO_4 \qquad (2.4.3)$$

With the values of x such that 0% to 10% of the leached sulphur reported in the sulphate form.

Apart from ferric ion as the oxidant, leaching of the mineral sulphide can also be achieved by means of cupric ions as was discussed earlier [42,47,50,61,66-73]. For example, in the presence of ligands such as chloride ions, the cuprous ion is stabilized [33,38,44,74,75]. This then introduces a very fast and reversible redox couple, which can oxidize covellite effectively, namely the Cu(II) / Cu(I) couple [33,41,45]. However, in an acidic sulphate system, cuprous ions are unstable and, as a result of this, the Cu(II) / Cu(I) couple is not functional to mediate leaching in this medium [75].

McDonald and Langer investigated the leaching characteristics of synthetic covellite powder in cupric chloride ($CuCl_2$) / sodium chloride (NaCl) solutions under inert gas sparging [42]. They described the leaching process by:

$$CuS + Cu^{2+} \underset{H_2O}{\overset{NaCl}{\rightleftharpoons}} 2Cu^{+} + S^{\circ} \qquad (2.4.4)$$

It was found that, when the ratio of cuprous to cupric ion was 4 : 1 under their conditions, the leaching reaction did not continue to completion. This was attributed to an equilibrium attained, which arrested the net forward reaction. Furthermore, once this occurred, experimental evidence in support of their proposed reaction showed a decrease in elemental sulphur and an increase in "bonded" sulphur, i.e. sulphide sulphur bonded to copper in the solids residue.

In addition, they introduced another reaction for the slow oxidation of elemental sulphur to sulphate:

$$3Cu^{2+} + 4S^{\circ} + 4H_2O = 3CuS + SO_4^{2-} + 8H^{+} \qquad (2.4.5)$$

This accompanied the leaching reaction (Equation 2.4.4) and became dominant with the attainment of the equilibrium. Equation 2.4.5 attempted to explain the slow deposition of covellite, the continued slow consumption of cupric ions, as well as additional sulphate formation and sulphur consumption, which they observed.

Cheng and Lawson [50] studied the kinetics of leaching synthetic covellite in acid, oxygenated, chloride solutions and suggested that the overall reaction was most probably:

$$CuS + \tfrac{1}{2}O_2 + 2H^{+} + Cl^{-} = CuCl^{+} + H_2O + S^{\circ} \qquad (2.4.6)$$

They discovered that about 10% of the leached sulphur was oxidized to sulphate in solution, with the remainder as xylene-soluble, elemental sulphur.

Secondary (or Second-Stage) Covellite

By means of quantitative experiments on a pure, natural chalcocite (Cu_2S) sample in acidic, ferric sulphate solutions, Sullivan [76] concluded that the mineral dissolved in two stages:

First Stage:

$$Cu_2S + Fe_2(SO_4)_3 = CuSO_4 + 2FeSO_4 + CuS \quad (2.4.7)$$

Second Stage:

$$CuS + Fe_2(SO_4)_3 = CuSO_4 + 2FeSO_4 + S^\circ \quad (2.4.8)$$

With the overall reaction as:

$$Cu_2S + 2Fe_2(SO_4)_3 = 2CuSO_4 + 4FeSO_4 + S^\circ \quad (2.4.9)$$

It was found that very little free sulphur was formed during the first stage of leaching (until about 50% of the total copper was extracted) to produce a residue with the approximate formula, CuS. However, this residual CuS did not remain constant, but continued to undergo change as more copper was dissolved (during the second stage) until the ratio of Cu : S became 0.8 - 0.9 : 1. This was different from what was found for covellite, where this ratio remained more or less 1 : 1 over the duration of the leach [49].

Many other investigations on chalcocite, which were conducted in either acidic ferric sulphate [63,77,78,79] or ferric chloride solutions [80,81,82], confirmed a two-stage

process of dissolution with the formation of an intermediate product ("CuS") as was found by Sullivan [76].

In their study on massive, natural samples, Fisher *et al.* observed that the dissolution of chalcocite in acidic, oxygenated, chloride solutions (in the absence of ferric ions) occurred in two, distinct steps [61]. They found that blue-remaining (*blaubleibender*) covellite, $Cu_{1.0-1.2}S$, was the final product of the first-stage reaction.

First Stage:

$$2Cu_2S + 1/2O_2 + 2H^+ + 6Cl^- = 2CuS + 2CuCl_3^{2-} + H_2O \qquad (2.4.10)$$

Second Stage:

$$2CuS + 7/2O_2 + H_2O + 6Cl^- = 2CuCl_3^{2-} + 2SO_4^{2-} + 2H^+ \qquad (2.4.11)$$

These investigators stated that the dissolution curves all showed a transition from first to second stage at about 40% copper dissolution, which corresponded to a *blaubleibender* covellite formula of $Cu_{1.2}S$. However, the formula, CuS, was used in the reaction equations for simplicity.

Equation 2.4.11 shows sulphate sulphur as one of the major reaction products. To the author's knowledge, this has not been confirmed by any other study performed under similar conditions. Most studies performed in acidic, chloride solutions report the formation of largely elemental sulphur [67,68,69,70,71,73] and, in a few cases, also together with small amounts of sulphate [67,69].

The conventional Pourbaix diagram (Figure 2.2.3; 2.2 Thermodynamics) for the sulphur-water system predicts that elemental sulphur can be oxidized to bisulphate ($HSO_4^-{}_{(aq)}$) or even sulphate ($SO_4^{2-}{}_{(aq)}$) at potentials of greater than

about 0.3 V, over the range pH 0 to pH 2. Therefore, it might be expected that when a mineral sulphide such as CuS is oxidized in acidic solutions, only soluble copper ions and bisulphate and / or sulphate ions would be obtained. However, in practise, it is found that the dissolution reaction produces elemental sulphur and very little sulphate.

Furthermore, if it is assumed that the sulphate is produced from the oxidation of elemental sulphur (Equation 2.4.12), then catalysis by sulphur-oxidizing microorganisms would be required to make the reaction of any kinetic significance (cited from reference in [83]).

$$2S^\circ + 3O_2 + 2H_2O \rightarrow 2H^+ + 2HSO_4^- \qquad (2.4.12)$$

In addition, consider the following general reaction equation, which describes the oxidation of a mineral sulphide (MS) in acidic, ferric ion solutions:

$$MS + 2Fe^{3+} \rightarrow M^{2+} + 2Fe^{2+} + S^\circ \qquad (2.4.13)$$

It has been shown that the sulphur produced from the above reaction could be oxidized according to the equation (cited from reference in [84]):

$$3M^{2+} + 4S^\circ + 4H_2O \rightarrow 3MS + 7H^+ + HSO_4^- \qquad (2.4.14)$$

Although the reaction is thermodynamically feasible, the reaction kinetics are very slow; therefore, this reaction may also explain the small amounts of sulphate sulphur observed by some investigators. This is essentially the same reaction that has been proposed by McDonald and Langer (Equation 2.4.5) to explain the presence of some additional sulphate sulphur [42]. Another way of writing their reaction would be:

$$3Cu^{2+} + 4S^\circ + 4H_2O = 3CuS + HSO_4^- + 7H^+ \qquad (2.4.15)$$

Cheng and Lawson investigated the kinetics of leaching of synthetic chalcocite in acidic, oxygenated, chloride solutions [67]. They suggested that the dissolution of the mineral essentially occurred via two, sequential stages and according to:

First Stage:

$$Cu_2S + 2H^+ + \tfrac{1}{2}O_2 = Cu^{2+} + CuS + H_2O \qquad (2.4.16)$$

Second Stage:

$$CuS + 2H^+ + \tfrac{1}{2}O_2 = Cu^{2+} + S^\circ + H_2O \qquad (2.4.17)$$

It was found that a series of copper-deficient (chalcocite) intermediate products were formed during the first stage before "stable" covellite was produced. For example, *blaubleibender* covellite, covellite and trace amounts of sulphate sulphur were identified after about 46% copper dissolution. However, no elemental sulphur was detected, which led them to conclude that: 1) very small (trace) amounts of elemental sulphur were formed on the particle surface during the first stage, 2) the elemental sulphur was subsequently oxidized to sulphate and 3) the second stage proceeded in parallel with the first stage and that the rate of leaching of the second stage only became significant once about 40% of the copper initially present had been extracted.

In addition these workers found that less than 1% of the sulphide sulphur initially present in the chalcocite was converted to sulphate with more than 95% of the copper dissolved. This was far less than the 10% they found when leaching covellite under similar conditions [50]. They attributed this to the possibility that the secondary (or second-stage) covellite was more "active" and therefore yielded a higher conversion to elemental sulphur.

Vračar *et al.* [70] studied the leaching of finely-grained, Cu(I) sulphide samples in acidic, oxygenated (calcium) chloride solutions and proposed a two-stage process with reactions the same as by Cheng and Lawson [67]. Furthermore, they found that apart from elemental sulphur, their solids residue also contained: $CaSO_4 \cdot 0.5H_2O$, $Ca(ClO_3) \cdot 2H_2O$ and $Cu_2Cl(OH)_3$.

It is interesting to note the presence of gypsum ($CaSO_4 \cdot 0.5H_2O$), which indicates that some sulphate (or bisulphate) sulphur was produced during the leach.

Studies executed in acidic, chloride solutions (in the absence of ferric ions) on chalcocite intermediate products such as djurleite ($Cu_{1.97}S$) [72,73] and digenite ($Cu_{1.8}S$) [69,73] in general showed a similar two-stage process for the dissolution of these minerals, with the formation of secondary covellite. Some of the reaction equations suggested from these investigations:

Djurleite [72]

First Stage:

$$Cu_{1.97}S + 0.97Cu^{2+}_{(chloro\text{-}complexes)} = CuS + 1.94Cu^{+}_{(chloro\text{-}complexes)} \qquad (2.4.18)$$

Digenite [69]

First Stage:

$$Cu_{1.8}S + 1.6H^{+} + 0.4O_2 = CuS + 0.8Cu^{2+} + 0.8H_2O \qquad (2.4.19)$$

Second Stage:

$$CuS + 2H^{+} + 0.5O_2 = Cu^{2+} + H_2O + S^{\circ} \qquad (2.4.20)$$

In summary of what has been presented on the reaction chemistry of the leaching of both covellite and secondary covellite, it seems that:

- Cupric ions can oxidize covellite in acidic, chloride solutions;
- Ferric ions can oxidize covellite in both acidic, chloride and acidic, sulphate solutions;
- Oxygen can oxidize covellite;
- Cupric ions are reduced to cuprous ions during the oxidation of covellite;
- Ferric ions are reduced to ferrous ions during the oxidation of covellite;
- The oxidation of covellite produces soluble copper and mostly elemental sulphur;
- Small amounts of sulphate sulphur may be produced during the process of oxidation, and
- Less sulphate sulphur is produced during the oxidation of secondary covellite.

2.4.2 Deportment of Reaction Products

It was shown that cupric ions oxidized covellite to produce cuprous ions and elemental sulphur in acidic, chloride solutions (in the absence of ferric ions) under inert gas sparging [42].

However, in the presence of dissolved oxygen, cuprous ions can be oxidized back to cupric ions and the rate of oxidation is appreciable fast [85,86]. Likewise, ferrous ions can also be oxidized back to ferric ions, but the rate of chemical oxidation in acidic sulphate and chloride solutions is much slower, even when catalyzed by copper ions in the latter medium [33,86,87,88].

Studies in acidic, chloride and sulphate solutions showed that ferric ions oxidized covellite to produce soluble copper ions, ferrous ions and elemental sulphur. The latter seemed to retain the mineral particle's original outline, which only disintegrated once the sulphur had been dissolved by carbon bisulphide (CS_2) [49].

The sulphur formed a thin, coating layer across the mineral's leached surface, although most of the sulphur was concentrated in a few areas. In addition, it was found that the sulphur always contained some retained, fine-divided covellite[65].

Cheng and Lawson observed the formation of a growing layer of large, well-defined sulphur crystals in chloride solutions [50]. They believed that this allowed the leaching reagents to penetrate the sulphur product layer and made the mineral surface more accessible for reaction. Nevertheless, the formation of sulphur on the mineral surface still had a retarding effect on the kinetics of dissolution, which improved markedly once the sulphur had been removed with xylene.

King *et al.* found that elemental sulphur appeared in the second-stage of leaching synthetic chalcocite in acidic, ferric chloride solutions [81]. The sulphur always appeared in the holes or pores of a porous structure of fibrous, residual covellite and never formed a massive layer under the conditions tested. He also observed that material with the compositions $Cu_{0.79}S$ and $Cu_{0.9}S$, which were produced from partially leached synthetic chalcocite, were the first to show the presence of orthorhombic sulphur in the XRD pattern.

Some investigators discovered that, apart from elemental sulphur, some sulphate sulphur was also produced in solution [42,50,62,65,67,69,70] and the formation thereof seemed more pronounced closer to the melting point (112.8°C [89]) of sulphur [42]. However, it seemed that significantly less sulphate was formed during the leaching of secondary covellite as compared to covellite [42,50], which was attributed to the greater "reactivity" of secondary covellite [67].

And finally, Sullivan found that the Cu : S ratio for residual, covellite remained more or less constant at about 1 : 1 [49], whereas the ratio for secondary covellite continued to decrease to as low as 0.8 - 0.9 : 1 over the duration of the leach [76].

No explanation for this difference in behaviour is given, but it may well be due to the greater "reactivity" of secondary covellite, because of the mineral's large surface area.

2.4.3 Kinetics of Dissolution

The kinetics of dissolution of covellite and secondary covellite will be discussed with respect to the following: acidity, chloride ion concentration, cupric ion concentration, cuprous ion concentration, dissolved oxygen concentration (or oxygen partial pressure), particle size / surface area and temperature in acidic, chloride solutions.

In addition, some examples of typical rates of dissolution will also be presented under the temperature section.

Acidity

King *et al.* found that the rate of dissolution of secondary covellite was independent of the hydrochloric acid (HCl) concentration from 0.05 M to 0.8 M [81]. This finding was confirmed by Fisher *et al.* [61] from 0.175 M H^+ to 1.4 M H^+, by Deng *et al.* [68] from 0.07 M H_2SO_4 to 0.36 M H_2SO_4 (under oxygen-free conditions) and by Ruiz *et al.* [69] over the ranges: 0.6 M HCl to 1.2 M HCl at 1.5 M Cl^- (total) and 0.2 M HCl to 2 M HCl at 2.5 M Cl^- (total) and 3.4 M Cl^- (total), respectively. However, the latter investigator observed the precipitation of what was thought to be cupric oxychloride, $CuCl_2 \cdot 3Cu(OH)_2$, at initial acid concentrations lower than 0.2 M HCl. This was attributed to the depletion of acid in the leaching system.

In contrast to the above findings, the results of Cheng and Lawson showed that the rate of dissolution of secondary covellite increased slightly with increased acidity from 0.02 M H_2SO_4 to 0.5 M H_2SO_4 [67]. Further increase in the sulphuric

acid concentration to 2 M H_2SO_4 resulted in a slight decrease in the rate of dissolution. This was attributed to decreased dissolved oxygen at combined, high chloride and sulphate concentrations.

In oxygenated solutions, Deng *et al.* also noticed a small increase in the rate of secondary covellite dissolution with increased sulphuric acid concentration from 0.1 M to 0.6 M [68]. However, it was stated that the effect was not that significant, provided that at least 0.1 M H_2SO_4 was maintained in solution. These investigators emphasized the importance to operate at conditions well-below pH 3 in order to prevent the precipitation of the basic cupric chloride - atacamite ($Cu_2(OH)_3Cl$).

Cheng and Lawson found that the rate of covellite dissolution increased slightly with increased sulphuric acid concentration over the range 0.005 M to 0.5 M [50]. Further increase in acidity to 2 M H_2SO_4 again rendered a slight decrease in the kinetics. In addition, it was found that at acidities of about pH 4, a yellow-green solid precipitated, which was identified as basic copper chloride ($Cu_2(OH)_3Cl$).

The effect of acidity on the rate of dissolution of covellite was difficult to evaluate since the pH of the leaching medium was not maintained constant in the above studies to the author's knowledge. In addition, in some cases, more than one variable was also changed at a time, either directly or indirectly, which clouded interpretation even further.

In conclusion, the author is of the opinion that, if there is an effect of acidity on the rate of dissolution of covellite, it does not seem to be significant. More importantly it seems, under the above conditions, is to maintain the leaching medium well-below pH 3 in order to prevent cupric ions to precipitate from solution as basic cupric chlorides.

Chloride Ion Concentration

Sullivan observed that the rate of dissolution of covellite was slower in acidic, ferric chloride than in acidic, ferric sulphate solutions at low temperature (35°C) [49]. However, the rates of dissolution were virtually the same at high temperature (98°C). The latter observation was confirmed by other workers [90,91].

The same investigator also found that, at low temperature (35°C), the rate of dissolution of secondary covellite was virtually identical in both systems [76]. However, at elevated temperature (98°C), the rate of dissolution was faster in an acidic, ferric chloride solution. No explanation was given for these observations.

Many investigators observed that the rate of dissolution of both covellite and secondary covellite was enhanced appreciably in the presence of some chloride ions in acidic, oxygenated solutions (in the absence of ferric ions) and that the rate of dissolution increased with increased chloride concentration up to a specific value [50,61,67,68,71]. However, above this value, the kinetics were found to be independent of chloride concentration. In other words, the rate of dissolution did not increase with further increase in chloride concentration above such a value.

For example, Cheng and Lawson found that the rate of dissolution of covellite increased linearly when the chloride ion concentration was increased from 0.01 M to 0.5 M; thus, the reaction was found to be first order with respect to the chloride ion concentration over this range [50]. However, a further increase in chloride concentration to 2 M had no effect on the rate of dissolution. This was attributed to a decrease in dissolved oxygen concentration at high chloride concentration.

Also, Deng and Muir showed that the rate of dissolution of secondary covellite increased with increased chloride ion concentration over the range 0.04 M to 0.5 M; however, the increase in kinetics from 0.1 M Cl^- to 0.5 M Cl^- was only marginal [68]. These workers stated that there was no advantage with respect to the kinetics with a further increase in chloride concentration. This finding was confirmed by Fisher *et al.* [61] for 0.2 M Cl^- to 1 M Cl^-, Vračar *et al.* [70] for 0.25 M Cl^- to 0.75 M Cl^- and Deng *et al.* [71] over the range 0.25 M Cl^- to 2 M Cl^-.

On the other hand, the results of Cheng and Lawson showed that the rate of dissolution of secondary covellite increased with increased chloride ion concentration from 0.1 M to 2 M [67]. And, likewise, Ruiz *et al.* [69] observed an increase in the kinetics over the range 1 M Cl^- to 5 M Cl^-; thus, increased kinetics up to much higher chloride concentrations.

An analysis of the former workers' data shows that the rate of dissolution is second order with respect to the chloride ion concentration over the range 0.1 M to 0.5 M. Over this range, the dissolved oxygen concentration is more or less similar (14 mg/L to 16 mg/L) according to the method of Narita *et al.* [92]. A further increase in chloride concentration to 2 M shows a small decrease in the rate of dissolution, which may, in all likelihood, be due to the lower dissolved oxygen concentration of 8.9 mg/L.

The data of Ruiz *et al.* show a 0.7^{th} order dependency of the chloride ion concentration on the rate of the reaction over the range 1 M to 5 M.

Cupric Ion Concentration

In contrast to the leaching of brass and copper scrap metal with cupric ions in acidic, oxygen-free, chloride solutions [93], McDonald and Langer found that minerals such as chalcocite and covellite did not leach to completion in such systems [42,55].

Their explanation, which entails the establishment of a thermodynamic equilibrium (Equation 2.4.4) arresting the dissolution process, has already been discussed (see 2.4.1 Chemistry of Reaction).

Deng and Muir emphasized the importance of high concentrations of cupric ions in order to promote fast kinetics in acidic, oxygen-free, chloride solutions [68]. These investigators believed that the dissolution of secondary covellite was potential (E_h) controlled and that as the concentration of cuprous ions in solution increased, the potential decreased until an equilibrium (Equation 2.4.4) was reached at the rest potential of the residual mineral. Therefore, they believed that the extent of dissolution was limited by pulp density and the Cu(II) : Cu(I) ratio.

Their results showed that the extent of dissolution increased with decreased pulp density for a fixed, initial cupric chloride concentration. In other words, an increase in the extent of dissolution with an effective increase in the Cu(II) : mineral molar ratio.

Ruiz *et al.* also found that the extent of dissolution of secondary covellite increased with increased cupric chloride concentration, at a constant total chloride ion concentration of 3 M, in acidic, chloride solutions under nitrogen sparging [69]. These workers ascribed this to the displacement of the equilibrium (Equation 2.4.4) to the right with an increase in cupric ions in solution. In addition, they also made the important comment that, if the leaching of the mineral sulphide proceeded by reaction with cupric ions, then the rate of dissolution should be affected by the initial cupric ion concentration, which they found to be so.

On the other hand, in the presence of dissolved oxygen, some studies seem to indicate that, once present, cupric ions have only a small effect on the rate of dissolution of both covellite and secondary covellite in acidic, chloride solutions

(in the absence of ferric ions) [68,69]. The reason for this is that dissolved oxygen facilitates the regeneration of cupric ions by oxidation of any cuprous ions in solution. Therefore, if the dissolution reaction were to be limited by an equilibrium such as presented in Equation 2.4.4, the regeneration of cupric ions will drive the reaction to the right and, consequently, mineral dissolution to (near-) completion [69].

An explanation according to mixed potential theory and, somewhat more accurate than that of Deng and Muir [68], can also be presented in order to explain the above from a kinetic point of view. This will be discussed in some detail under 2.5 Electrochemistry.

Cuprous Ion Concentration

As already discussed, McDonald and Langer reported that an increase in cuprous ion concentration to a substantial level prevented the dissolution of covellite in acidic, oxygen-free, chloride solutions to proceed to completion [42]. They found this occurred at a cuprous to cupric ion ratio of about 4 : 1 under their experimental conditions. This finding was supported by other workers [68,69].

Under similar experimental conditions, but in the presence of dissolved oxygen where cuprous ions could be oxidized back to cupric ions, the dissolution of covellite was not arrested and continued to high extents of dissolution [50,61,67,68,69].

From the presented observations with regard to both cupric and cuprous ion concentrations, it can be concluded that high Cu(II) : Cu(I) ratios would be advantageous to the leaching of covellite and secondary covellite in acidic, chloride solutions.

Dissolved Oxygen Concentration

Cheng and Lawson observed that the rate of dissolution of covellite in acidic, chloride solutions increased with increased oxygen partial pressure over the range 5% O_2 to 100% O_2 [50]. Rate constants were generated by fitting their data to the following equation:

$$1 - (1 - \alpha)^{1/3} = kt \qquad (2.4.21)$$

With:

α Fraction of covellite leached
k Apparent rate constant
t Reaction time

The relationship between their apparent rate constant (k) and oxygen partial pressure (P_{O2}) was of the form:

$$k = A(P_{O2})^{0.3} \qquad (2.4.22)$$

With:

A Proportionality constant
P_{O2} Oxygen partial pressure

Thus, they reported that their apparent rate constant (k) showed a 0.3 order relationship with respect to oxygen partial pressure; however, they could not assign any physical significance to this.

An analysis of their data, where ln(initial rate) vs. ln(P_{O2}) was plotted for copper dissolution intervals of 0% to 10%, 10% to 20% ... 50% to 60%, is presented in Table 2.4.1

Table 2.4.1 : Reaction Orders (Covellite)

Range (% Cu)	x	R^2
0 - 10	0.32	0.95
10 - 20	0.28	0.96
20 - 30	0.28	0.98
30 - 40	0.30	0.97
40 - 50	0.22	0.92
50 - 60	0.24	0.98

1) Data adapted from Cheng and Lawson [50]
2) 0.5 M H_2SO_4, 0.5 M NaCl, 13 µm, 1 g/L solids and 90°C
3) x denotes the reaction order with respect to oxygen partial pressure

The reaction order remains about 0.3 up to 40% copper dissolution; thereafter, it seems that the rate of dissolution of covellite becomes slightly less dependent on the oxygen partial pressure, which may be due to the thickening layer of elemental sulphur forming over time. Although one would expect a value for x closer to 0.5, the determined values, at least, indicate the likelihood of electrochemical reactions.

A similar analysis of the same investigators' data for secondary covellite over the copper dissolution intervals 0% to 20%, 20% to 40% and 40% to 60%, is shown in Table 2.4.2.

Table 2.4.2 : Reaction Orders (Secondary Covellite)

Range (% Cu)	x	R^2
0 - 20	1.10	0.97
20 - 40	0.97	0.99
40 - 60	0.78	0.99

1) Data adapted from Cheng and Lawson [67]
2) 0.5 M H_2SO_4, 0.5 M NaCl, 23 µm, 1 g/L solids and 85°C
3) x denotes the reaction order with respect to oxygen partial pressure

The results show a linear dependency of the rate of dissolution of secondary covellite with respect to oxygen partial pressure, as was reported by Cheng and Lawson, up to 40% copper dissolution [67]. Thereafter, the rate of dissolution again becomes somewhat less dependent on the oxygen partial pressure, which is in all likelihood again due to the thickening layer of elemental sulphur.

In addition, the results show that the rate of dissolution of secondary covellite has a greater dependency on oxygen partial pressure than that of covellite. This is probably the result of the greater "reactivity" of the former, because of the residual mineral's large, effective surface area [49,61,76,81,94].

Other workers have also reported on the kinetic advantage with respect to the leaching of secondary covellite by operation at increased oxygen flow rates [68,69,71,73], improved oxygen distribution [71] and pre-oxygenation of the leach solution [68].

In contrast to the above, Fisher *et al.* found that the rate of dissolution of secondary covellite was independent of oxygen pressure over the range 53 kPa to 165 kPa in acidic, chloride solutions [61]. However, these authors conducted their experiments at much higher oxygen pressures than the other studies presented in this text. This might be the reason for their finding.

Particle Size / Surface Area

It is well-known that the kinetics of dissolution are much faster for secondary covellite than for covellite and this phenomenon has been observed and reported on for a variety of systems [32,49,50,67,76,95]. An example to illustrate this in acidic, oxygenated, chloride solutions is presented in Figure 2.4.1.

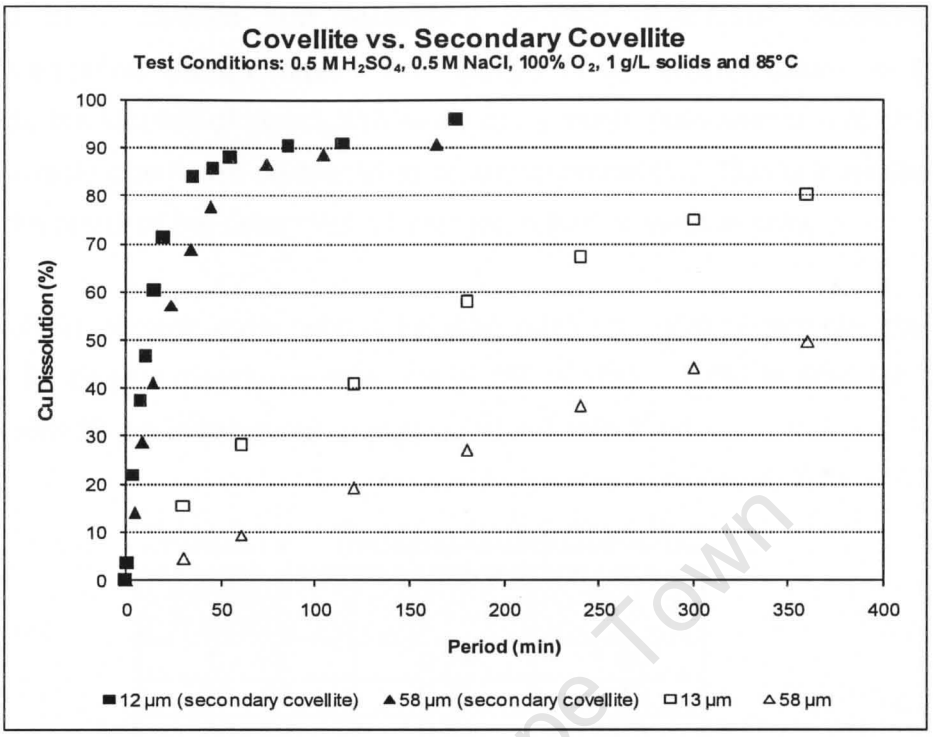

Figure 2.4.1 : Copper Dissolutions (adapted from Cheng and Lawson [50,67])

The data indicate that the kinetics of dissolution for secondary covellite are more than an order of magnitude faster than that for covellite for virtually the same initial (mean) particle sizes. This means that, in the case of secondary covellite, the apparent surface area (available for reaction) is more than ten times that of the superficial area for both the 12 µm and 58 µm sizes. Thus, a much larger, effective surface area is formed for secondary covellite during the first stage of chalcocite leaching [61].

The increased surface area is the result of the higher porosity [61,76,81,95] of secondary covellite from diffusion of cuprous ions from the mineral lattice [81] giving the residual covellite an almost fibrous appearance [81,94].

In addition, it can also be seen (and reported by Cheng and Lawson [50,67]) that the rate of both covellite and secondary covellite dissolution increases with decreased initial particle size. Not highlighted by these workers, is that for covellite, the kinetics of dissolution seem to be much more sensitive to change in initial particle size when compared to secondary covellite. This is in all likelihood again the result of the latter mineral's larger, effective surface area.

An analysis of their data, where ln(initial rate) vs. ln(initial particle size) was plotted for copper dissolution intervals of 0% to 10% ... 40% to 50% for 13 µm, 28 µm and 58 µm mean sizes, is presented in Table 2.4.3.

Table 2.4.3 : Reaction Orders (Covellite)

Range (% Cu)	x	R^2
0 - 10	-0.74	1.00
10 - 20	-0.79	0.99
20 - 30	-0.61	1.00
30 - 40	-0.45	1.00
40 - 50	-0.55	0.99

1) Data adapted from Cheng and Lawson [50]
2) 0.5 M H_2SO_4, 0.5 M NaCl, 100% O_2, 1 g/L solids and 85°C
3) x denotes the reaction order with respect to initial particle size

The results show that the rate of dissolution of covellite is inversely proportional to the initial particle size, with the reaction order ranging from more or less 0.8 to 0.5 up to 50% copper dissolution. Therefore, as noted previously, the rate of dissolution also seems to become slightly less dependent on the initial particle size over time.

For secondary covellite, over the copper dissolution intervals 0% to 20% ... 60% to 80% for 12 µm, 36 µm and 58 µm mean sizes, the results are shown in Table 2.4.4.

Table 2.4.4 : Reaction Orders (Secondary Covellite)

Range (% Cu)	x	R^2
0 - 20	-0.28	0.99
20 - 40	-0.36	0.99
40 - 60	-0.35	0.98
60 - 80	-0.25	0.99

1) Data adapted from Cheng and Lawson [67]
2) 0.5 M H_2SO_4, 0.5 M NaCl, 100% O_2, 1 g/L solids and 85°C
3) x denotes the reaction order with respect to initial particle size

The reaction order ranges from 0.3 to 0.4 up to 80% copper dissolution, with the rate of dissolution of secondary covellite inversely proportional to the initial particle size. In addition, the results show that the kinetics of dissolution have a greater dependency on the initial particle size for covellite than for secondary covellite.

In their study, Fisher *et al.* found that the rate of dissolution of secondary covellite was independent of initial (average) particle size over the range 126 µm to 252 µm [61]. They attributed this to the extraordinary porosity of the residual mineral, which increased the effective surface area to such an extent that it lost any relationship to the initial surface area. This was found to be the case by some other investigators as well [76,94,96].

Temperature

All the presented studies showed that the rate of dissolution of both covellite and secondary covellite increased with increased temperature and that the dependency on temperature was strong [32,42,50,61,66-73,81].

The reported apparent activation energies for some of these studies are summarized in Table 2.4.5, together with the author's own determined apparent activation energy (on the relevant data) by the method employed by King *et al.* [81].

It was found that some of these workers [50,61,67] corrected their rates of dissolution (or apparent rate constants) for decreased dissolved oxygen concentration with increased temperature prior to their Arrhenius plots, while others [69,81] (including the author of this text) did not.

Nevertheless, as it can be seen from the data presented in Table 2.4.5, the author's apparent activation energies agree reasonably well with those of the investigators (especially so, during the initial stages of leaching), except for one study [61], of which the data rendered much poorer linear regression fits than all the other studies.

The high values for the apparent activation energy, which spans a range of 50 $kJ.mol^{-1}$ to 122 $kJ.mol^{-1}$ (author's values), indicate that the reaction at the mineral surface is most likely controlled by a chemical (or electrochemical) reaction for both covellite and secondary covellite, since these values exceed 40 $kJ.mol^{-1}$ [33].

From the results of the two studies conducted at virtually the same experimental conditions (except for initial particle size) [50,67], it is interesting to note a slightly larger value of 77 $kJ.mol^{-1}$ for covellite than the 69 $kJ.mol^{-1}$ for secondary covellite. The uncorrected values show similar results during the initial stages of leaching; thereafter, the values for covellite increase over time, whereas those for secondary covellite show a decrease. The reason for this is unknown at this stage.

King *et al.*, whose study was conducted in the presence of ferric ions, also found that the apparent activation energy increased over time, from 101 $kJ.mol^{-1}$ to 122 $kJ.mol^{-1}$, and contributed this to the progressive formation of elemental sulphur [81]. The values they obtained are higher than for all the other studies.

Table 2.4.5 : Reported Activation Energies from Leaching Studies on Covellite

Test Conditions	E_a [a] ($kJ.mol^{-1}$)	E_a [b] ($kJ.mol^{-1}$)	Range (% Cu)	Temp. (°C)	Ref.
• CuS (synthetic) • 28 µm, 1 g/L solids • 0.5 M H_2SO_4, 0.5 M NaCl • Pre-oxygenation (2 h) • 600 mL O_2 / min • Stirred reactor, 1000 rpm	77	68 77 78 86 [c] 89 [c]	0 - 10 10 - 20 20 - 30 30 - 40 40 - 50	75 - 95	50
• Secondary CuS (from synthetic chalcocite) • 212 µm, 2.5 g/L solids • 0.2 M HCl, 0.5 M Fe(III) (as $FeCl_3$) • Fe(III) / Fe(II) = 10 • Stirred reactor, 900 rpm	101 103 112 122	-	0 - 20 20 - 40 40 - 60 60 - 80	22.5 - 80	81
• Secondary CuS (from synthetic chalcocite) • 49 µm, 1 g/L solids • 0.5 M H_2SO_4, 0.5 M NaCl • Pre-oxygenation (2 h) • 600 mL O_2 / min • Stirred reactor, 1000 rpm	69	67 62 58 50 [d]	0 - 20 20 - 40 40 - 60 60 - 80	65 - 94	67
• Secondary CuS (from natural chalcocite) • 193 µm, 10 g/L solids • 0.35 M H^+, 0.5 M Cl^- • Pre-oxygenation, oxygen sparging • 86 kPa O_2 • Stirred reactor, 1000 rpm	38	50 [e] 55 [e] -	0 - 20 20 - 40 40 - 60	30 - 74	61
• Secondary CuS (from natural digenite) • 63 µm, 1.33 g/L solids • 0.6 M HCl, 2.4 M NaCl • Pre-oxygenation • 260 mL O_2 / min • Stirred reactor, 675 rpm	84	85 80 [f] 77 [f] 91 [f] 85 [g] 79 [g] 85 [g]	0 - 9.1 9.1 - 18.2 18.2 - 27.3 27.3 - 36.4 36.4 - 45.5 45.5 - 54.6 54.6 - 63.7	50 - 90	69

a) Apparent activation energy reported by investigator(s)
b) Apparent activation energy determined by author of this text
c) Temperature range: 80°C to 95°C
d) Temperature range: 75°C to 94°C
e) Temperature range: 45°C to 74°C
f) Temperature range: 60°C to 90°C
g) Temperature range: 70°C to 90°C

Table 2.4.6 : Reported Rates of Dissolution from Leaching Studies on Covellite

Test Conditions	Rate of Dissolution (mol Cu $cm^{-2}.s^{-1}$) [a]											Ref.
	35°C	45°C	50°C	60°C	65°C	70°C	75°C	80°C	85°C	90°C	95°C	
• Covellite (natural sample) • Butte • -147+74 µm • 0.358 M $FeCl_3$, 0.137 M HCl • Atmospheric air • Stirred vessel	-	-	-	-	-	-	-	-	-	-	1.65×10^{-9} (98°C)	49
• Covellite (natural sample) • Kennecott N° 2 • -74 µm, 20 g/L solids (35°C) • -147+74 µm (98°C) • 0.179 M $FeCl_3$, 0.137 M HCl (35°C) • 0.358 M $FeCl_3$, 0.137 M HCl (98°C) • Atmospheric air • Roll-bottle tests (35°C) • Stirred vessel (98°C)	8.11×10^{-12}	-	-	-	-	-	-	-	-	-	3.71×10^{-9} (98°C) [b]	49
• Covellite (synthetic sample) • -38+25 µm, 10 g/L solids • 0.0079 M Cu (as $CuSO_4$), 0.2 M HCl • Atmospheric air • Stirred reactor, 800 rpm • Solution potential control (0.58 V) [c] • Solution potential control (0.66 V) [c]	4.86×10^{-12} (0.58 V) 6.61×10^{-12} (0.66 V)	-	-	-	-	-	-	-	-	-	-	19
• Covellite (synthetic sample) • 28 µm, 1 g/L solids • 0.5 M H_2SO_4, 0.5 M NaCl • Pre-oxygenation (2 h) • 600 mL O_2 / min • Stirred reactor, 1000 rpm	-	-	-	-	-	-	-	5.35×10^{-10}	8.39×10^{-10}	1.13×10^{-9}	1.48×10^{-9}	50

a) Rates of dissolution for covellite determined up to 40% copper dissolution
b) Rate of dissolution for covellite determined up to 46% copper dissolution
c) Solution potential vs. Standard Hydrogen Electrode (SHE)

Table 2.4.7 : Reported Rates of Dissolution from Leaching Studies on Secondary Covellite

Test Conditions	Rate of Dissolution (mol Cu $cm^{-2}.s^{-1}$) [a]											Ref.
	35°C	45°C	50°C	60°C	65°C	70°C	75°C	80°C	85°C	90°C	95°C	
• Secondary covellite (natural Cu_2S) • Kennecott • -147+74 µm, 20 g/L solids • 0.179 M $FeCl_3$, 0.137 M HCl • Atmospheric air • Roll-bottles	2.23×10^{-10}	-	-	-	-	-	-	-	-	-	-	76
• Secondary covellite (natural Cu_2S) • 193 µm, 10 g/L solids • 0.35 M H^+, 0.5 M Cl^- • Pre-oxygenation, oxygen sparging • 86 kPa O_2 • Stirred reactor, 1000 rpm	-	2.56×10^{-9}	-	3.99×10^{-9}	-	-	1.39×10^{-8} (74°C)	-	-	-	-	61
• Secondary covellite (synthetic Cu_2S) • 212 µm, 2.5 g/L solids • 0.2 M HCl, 0.5 M Fe(III) (as $FeCl_3$) • Fe(III) / Fe(II) = 10 • Stirred reactor, 900 rpm	-	-	7.08×10^{-9}	2.16×10^{-8}		6.49×10^{-8}	-	1.37×10^{-7}	-	-	-	81
• Secondary covellite (synthetic Cu_2S) • 49 µm, 1 g/L solids • 0.5 M H_2SO_4, 0.5 M NaCl • Pre-oxygenation (2 h) • 600 mL O_2 / min • Stirred reactor, 1000 rpm	-	-	-	-	3.08×10^{-9}	-	5.17×10^{-9}	-	1.20×10^{-8}	-	1.72×10^{-8} (94°C)	67
• Secondary covellite (natural $Cu_{1.8}S$ • 63 µm, 1.33 g/L solids • 0.6 M HCl, 2.4 M NaCl • Pre-oxygenation • 260 mL O_2 / min • Stirred reactor, 675 rpm	-	-	-	-	-	1.57×10^{-8}	-	3.86×10^{-8}	-	5.79×10^{-8}	-	69

a) Rates of dissolution for secondary covellite determined up to 40% copper dissolution

2.4.4 Mechanisms of Dissolution

Since this work entails the anodic dissolution of covellite in acidic, chloride solutions, only mechanisms relevant to covellite and secondary covellite in this medium, and in the absence of ferric ions, will be considered.

Fisher *et al.* [61] suggested that oxygen adsorbed on the mineral surface was reduced by:

$$O_2 + H^+ + e^- = HO_2 \qquad (2.4.23a)$$

$$HO_2 + H^+ + e^- = H_2O_2 \qquad (2.4.23b)$$

$$H_2O_2 + H^+ + e^- = H_2O + OH \qquad (2.4.23c)$$

$$OH + H^+ + e^- = H_2O \qquad (2.4.23d)$$

The electrons were supplied by the oxidation of *blaubleibender* covellite as shown in Figure 2.4.2. The reaction occurred as a sequence of simple electrochemical steps, which involved one-electron transfers. They postulated the rate-controlling step to be one of the electron transfer steps in the anodic reaction; thus, the rate of dissolution of secondary covellite was electrochemically controlled.

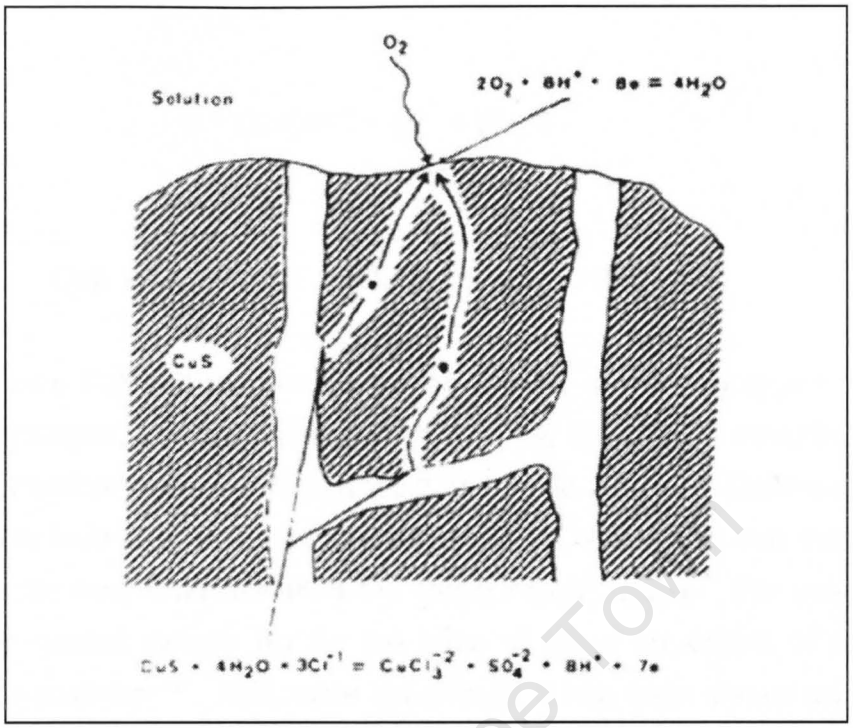

Figure 2.4.2 : Electrochemical Model of Second Stage Chalcocite Dissolution in the Chloride System by Fisher *et al.* [61]

In this study, the variables were: acidity, chloride ion concentration, initial particle size, oxygen pressure and temperature. Except for temperature, none of these variables showed any effect on the rate of dissolution. This was attributed to the extraordinary porosity of the *blaubleibender* covellite formed, which increased the surface area to an extent that it lost any relationship to the initial surface area. The apparent activation energy, over the temperature range 30°C to 74°C, was reported as 38.3 $kJ.mol^{-1}$.

The value of the apparent activation energy (although slightly low) seems to indicate that the process is controlled by a chemical (or electrochemical) reaction since the reported value is close to 40 $kJ.mol^{-1}$ [33].

The proposed mechanism suggests the following anodic and cathodic reactions:

Cathodic:

$$O_2 + 4H^+ + 4e^- = 2H_2O \qquad (2.4.24)$$

Anodic:

$$CuS + 4H_2O + 3Cl^- = CuCl_3^{2-} + SO_4^{2-} + 8H^+ + 7e^- \qquad (2.4.25)$$

The cathodic half-cell reaction (Equation 2.4.24) assumes oxygen to be the electron-acceptor, i.e. the primary oxidant in the leaching of covellite. This is thermodynamically feasible (Figure 2.2.2 and Table 2.2.1; 2.2 Thermodynamics), but unlikely from a kinetic point of view since it is well-known that the O_2 / H_2O couple is far less reversible than the Cu(II) / Cu(I) couple. For example, the exchange current density (i_o) for the latter is about six orders of magnitude greater on platinum [33]. And, more specifically, it has been shown recently that the cathodic current density (i_c) for the reduction of Cu(II) is larger than that for dissolved oxygen on a synthetic covellite surface in acidic, chloride solutions [18,41].

The anodic half-cell reaction (Equation 2.4.25) shows sulphate instead of elemental sulphur as one of the major reaction products. The unlikelihood of this has already been discussed (2.4.1 Chemistry of Reaction and 2.2 Thermodynamics)

Finally, the overall reaction (Equation 2.4.11) shows that the oxidation of secondary covellite is acid-producing. Studies in acidic, chloride solutions show that the process is acid-consuming and that, if the acidity of the solution is not controlled below pH 3 to pH 4 (depending on chloride concentration), copper may in fact precipitate out as a Cu(II)-hydroxychloride [42,50,71].

Therefore, based on the above arguments, the above reaction mechanism cannot be accepted.

Cheng and Lawson [50,67] thought the leaching reaction for covellite to be electrochemical in nature and proposed the following anodic and cathodic half-cell reactions at the mineral surface for both covellite and secondary covellite, in acidic, oxygenated chloride solutions:

Cathodic:

$$2H^+ + \tfrac{1}{2}O_2 + 2e^- = H_2O \qquad (2.4.26)$$

Anodic:

$$CuS = Cu^{2+} + S^\circ + 2e^- \qquad (2.4.27)$$

These took place at different, mobile sites on the mineral surface as illustrated in Figure 2.4.3.

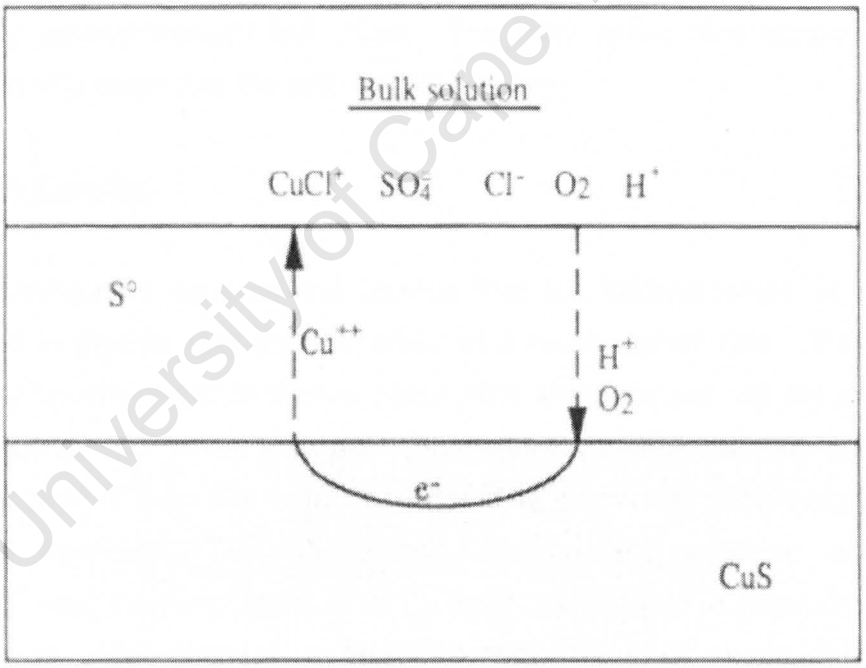

Figure 2.4.3 : A Schematic Illustration of the Electrochemical Leaching Model of Covellite in Oxygenated, Acidic, Sulphate-Chloride Solutions by Cheng *et al.* [50]

In general, cuprous ions were oxidized at the mineral surface to cupric ions, with $CuCl^+$ as the main chloro-complexed, cupric species, which then diffused into the bulk solution through a growing, porous layer of well-defined, elemental sulphur crystals, which surrounded a reducing ("shrinking") core of unreacted covellite. Electrons passed through electrical-conducting covellite from the anodic to the cathodic sites.

Covellite

It was concluded that the rate of dissolution of covellite was controlled by a chemical (or electrochemical) reaction at the mineral surface, which was supported by an apparent activation energy of 77 $kJ.mol^{-1}$ over the range 75°C to 95°C. In addition, these workers claimed that a plot of the apparent rate constant (k) vs. the reciprocal of the initial particle diameter (d_p) gave a straight line, which essentially passed through the origin. The latter result also supported their conclusion with respect to the rate-controlling step.

Secondary Covellite

These investigators were of the opinion that the second stage of leaching proceeded in parallel with the first albeit at a much slower rate. The second stage only became significant once about 40% of the copper, initially present in the chalcocite, had been leached. Secondary covellite reacted and left a thickening shell of elemental sulphur surrounding a reducing ("shrinking") core of unreacted covellite. They determined an apparent activation energy of 69 $kJ.mol^{-1}$ over the range 65°C to 94°C, which made them to conclude that the process was under chemical or mixed control. In other words, the rate of dissolution of secondary covellite was limited by a dominant surface chemical (or electrochemical) reaction initially and then by both chemical and diffusion processes in the latter stages of the leach.

The determined apparent activation energies of 69 $kJ.mol^{-1}$ (secondary covellite) and 77 $kJ.mol^{-1}$ (covellite) seem to indicate that the leaching of covellite and secondary covellite in acidic, oxygenated chloride solution is indeed controlled by a chemical (or electrochemical) reaction, since these values are well above 40 $kJ.mol^{-1}$ [33].

However, Equation 2.4.26 shows that Cheng and Lawson also assume oxygen to be the primary oxidant (electron-acceptor), which is again contested from a kinetic viewpoint as discussed earlier. Therefore, their reaction mechanism cannot be accepted.

The scheme of electrochemical reactions, for the leaching of secondary covellite in acidic, oxygenated chloride solutions by Vračar *et al.*, is rejected for the same reason [70].

In their investigation of the leaching kinetics of digenite in acidic, oxygenated chloride solutions, Ruiz *et al.* found that the experimental data for the second-stage of leaching fitted Equation 2.4.28 excellently [69].

$$1 - \tfrac{2}{3}\alpha_{cv} - (1 - \alpha_{cv})^{\frac{2}{3}} = k_{cv}t_{cv} \qquad (2.4.28)$$

With:

α_{cv} Fraction of secondary covellite leached
k_{cv} Apparent rate constant
t_{cv} Reaction time

These investigators were of the opinion that this was an indication that the leaching of secondary covellite was controlled by the transport of cupric species through a porous sulphur layer. In conjunction, an apparent activation energy of 84 $kJ.mol^{-1}$ was determined over the range 50°C to 90°C.

The above results were considered to be consistent with the dissolution of secondary covellite by an electrochemical mechanism, for which they proposed:

Cathodic:

$$Cu^{2+} + e^- = Cu^+ \qquad (2.4.29)$$

Anodic:

$$CuS = Cu^+ + S^\circ + e^- \qquad (2.4.30)$$

They suggested that the formed cuprous ions were subsequently oxidized to cupric ions by dissolved oxygen according to:

$$2Cu^+ + \tfrac{1}{2}O_2 + 2H^+ = Cu^{2+} + H_2O \qquad (2.4.31)$$

Figure 2.4.4(b) illustrates the reaction mechanism schematically for the case of a spherical particle.

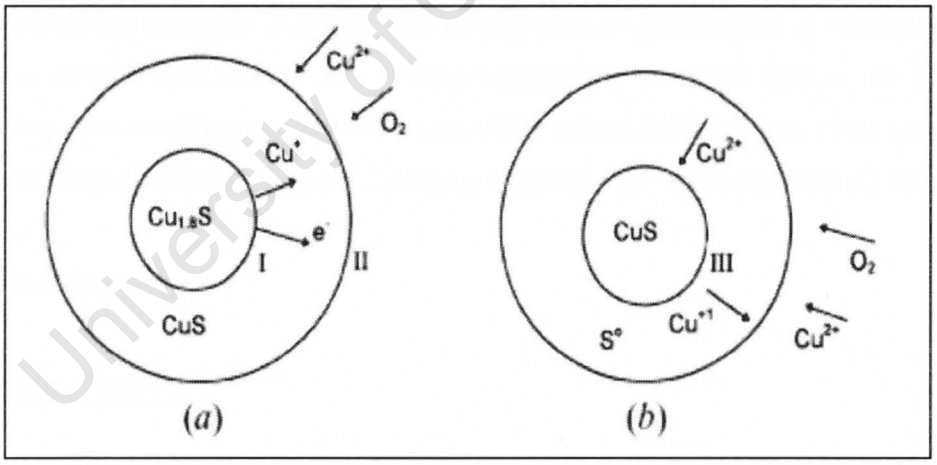

Figure 2.4.4 : Schematic Diagram of Electrochemical Dissolution of Digenite in Oxygenated Chloride Media: (a) First-Stage Galvanic Couple and (b) Second-Stage Corrosion Couple by Ruiz *et al.* [69]

The scheme shows the formation of a growing sulphur layer product over the surface of a shrinking core of secondary covellite. The oxidant, which is the cupric ion, has to diffuse through the sulphur layer towards the surface of the unreacted mineral, since elemental sulphur is not capable of electronic conduction. Therefore, the anodic and cathodic half-cell reactions occur at the CuS / S° interface (III), which represents a corrosion couple.

The diffusion of the oxidant species (cupric ions), through the growing, porous layer of sulphur, was considered to be the rate-limiting process. In other words, the leaching of secondary covellite was mass transport controlled.

The problem with their explanation is that the apparent activation energy of 84 $kJ.mol^{-1}$ is characteristic of a process, which is controlled by a chemical (or electrochemical) reaction and not by a mass transport limitation [33]. The investigators attempt to rationalize this by stating that the high value for the activation energy could be due to the fact that the rate of production of cuprous ions is slower than the rate of oxidation of cuprous ions. However, this in itself implies that the process is controlled by the rate of production of cuprous ions, which is in fact the rate of the anodic dissolution reaction (Equation 2.4.30). Therefore, the leaching of secondary covellite, at least during the initial stages, is not controlled by mass transport, but by a chemical (or electrochemical) reaction.

2.5 Electrochemistry

Reference Electrodes

Oxidation-reduction (redox) potentials may be measured and reported against various reference electrodes, e.g. the saturated, potassium sulphate, mercury / mercurous sulphate (sat.K_2SO_4, Hg / Hg_2SO_4) electrode, the saturated potassium chloride, mercury / mercurous chloride or calomel (sat. KCl, Hg / Hg_2Cl_2) electrode, the saturated potassium chloride, silver / silver

chloride (sat. KCl, Ag / AgCl) electrode and the 3 M potassium chloride, silver / silver chloride (3 M KCl, Ag / AgCl) electrode, with the latter being commonly used in practise today. These have respective potentials of 244.4 mV, 651.3 mV, 197.0 mV and 207.0 mV against the standard hydrogen electrode (SHE) at 25°C [34]. Therefore, when a redox potential is reported against the standard hydrogen scale (vs. SHE), it is usually referred to as E_h [10,33,97].

Redox Potential Measurements in Solution

A redox potential is established when oxidant and reductant, i.e. two phases, exchange electrons with each other, in such a way, that the electrons in both phases are in equilibrium. Therefore, in order to obtain a redox potential in equilibrium, it is required that no transport of metal ions occurs from metal to electrolyte and *vice versa* [98]. In other words, the metal must remain inert under the conditions of measurement.

The oxidation state in solution, pertaining to typical leaching processes of copper sulphide minerals, is usually monitored by measurement of the redox potential with a platinum electrode against that of a suitable reference electrode. The reason for this is that the indicator electrode (platinum) remains inert under the reigning, leaching conditions. However, it is also possible to use other materials such as vitreous carbon and lead as indicator electrodes [99] provided these remain inert under the conditions of measurement.

Typically in leaching processes, the potential is measured in the bulk solution with a stationary, platinum (indicator) electrode. However, it is also possible to measure the potential in solution close to a mineral electrode's surface with more sophisticated equipment such as a rotating-ring-disk electrode (RRDE) [10,34,97,99]. Also, it is important to realize that these measurements, i.e. in the bulk and close to the mineral's surface, can be significantly different under certain conditions [97].

Equilibrium Redox Potential Properties

Consider the general redox couple:

$$Ox + ne^- = Red \qquad (2.5.1)$$

The equilibrium potential (E) is expressed by the Nernst equation as follows [33,39,100].

$$E = E° - \frac{RT}{nF} \ln\left(\frac{[Red]}{[Ox]}\right) \qquad (2.5.2)$$

With:

E Potential, in V (vs. SHE)
E° Standard potential, in V (vs. SHE)
R Universal gas constant, 8.31441 $J.mol^{-1}.K^{-1}$
T Temperature, in K
n Number of electrons (e^-)
F Faraday's constant, 96 487 $C.mol^{-1}$ e^-
[Red] Activity of Red, in molal, or
Fugacity of Red, in atmosphere
[Ox] Activity of Ox, in molal, or
Fugacity of Ox, in atmosphere

The standard potential (E°) refers to a potential when all gaseous species are at a fugacity (thermodynamic pressure) of 1 atmosphere and all dissolved species at an activity (thermodynamic concentration) of 1 molal, i.e. 1 mole per 1000 g of water, at 25°C (298.15 K) [38]. For diluted solutions, activity and fugacity are approximated by concentration and (partial) pressure, respectively [33,39].

Consider the following reaction for the anodic dissolution of covellite:

$$CuS = Cu^{2+} + S° + 2e^- \quad (2.5.3)$$

Then, the equilibrium electrode potential (E) at 25°C is given by:

$$E = 0.633 - \frac{0.0591}{2} \log \frac{1}{[Cu^{2+}]} \quad (2.5.4)$$

With:

$[Cu^{2+}]$ Concentration of uncomplexed or free cupric ions, in $mol.dm^{-3}$

Table 2.5.1 presents the reduction potentials for couples encountered in the leaching of some copper sulphide minerals.

Table 2.5.1 : Some Relevant Reduction Potentials [45]

Reaction	Solution	E° or E°' (vs. SHE)
$CuS + Cu^{2+} + 2e^- = Cu_2S$		0.494
$CuS + Cu(II) + 2e^- = Cu_2S$	1 M Cl^-	0.443
$Cu^{2+} + S° + 2e^- = CuS$		0.633
$Cu(II) + S° + 2e^- = CuS$	1 M Cl^-	0.583
$Cu(I) + S° + e^- = CuS$	1 M Cl^-	0.675
$5Cu^{2+} + Fe^{2+} + 4S° + 12e^- = Cu_5FeS_4$		0.543
$5Cu(II) + Fe(II) + 4S° + 12e^- = Cu_5FeS_4$	1 M Cl^-	0.493
$Cu^{2+} + Fe^{2+} + 2S° + 4e^- = CuFeS_2$		0.427
$Cu(II) + Fe(II) + 2S° + 4e^- = CuFeS_2$	1 M Cl^-	0.377
$Cu(I) + Fe(II) + 2S° + 3e^- = CuFeS_2$	1 M Cl^-	0.341
$CuS + Fe^{2+} + 2S° + 2e^- = CuFeS_2$		0.220

1) E° standard potential, i.e. at standard conditions
2) E°' formal potential, i.e. at non-standard conditions (25°C)

The total Cu(I), Cu(II), Fe(II) and Fe(III) concentrations were all set at 3 g/L each in the case of the above potentials (Table 5.1). It should also be noted that the potentials in 1 M chloride ions are formal rather than standard values, because the metal ions are not present as aqua-ions at unit activity, but as chloro-complexes.

Thus, from a thermodynamic point of view, it can be seen that covellite should be oxidized at potentials above 0.633 V (vs. SHE) in a solution containing cupric ions at unit activity, at 25°C. However, in a solution of 1 M chloride ions, the mineral should be oxidized at potentials above 0.583 V (vs. SHE) at 25°C.

The formal potential (as presented in Table 5.1) is also sometimes referred to as the so-called open-circuit potential (OCP) or rest potential of the mineral.

Kinetic Potential

It is important to realize that the thermodynamics do not specify the rate at which the oxidation process occurs. In general, kinetic limitations will require a significant overpotential as a driving force for the above reaction [33].

Mixed potential theory was first introduced in 1938 (cited from reference in [10]), which was later used by others to explain the kinetic and mechanistic features of electrochemical reactions pertaining to many hydrometallurgical processes [31,101,102]. More specifically to its application in leaching studies, the reader is referred to the pioneer-work of Nicol *et al.* with regard to an electrochemical model established for the leaching of uranium dioxide [103,104].

Although the measured redox potential of a solution is a useful parameter, it does not necessarily reflect the actual potential at the surface of a dissolving mineral - the so-called mixed potential (E_m). This potential is established when two or more electrochemical reactions (anodic and cathodic) occur at the mineral surface, independently of each other [31,33].

Consider the oxidative dissolution of covellite in an acidic, ferric sulphate solution:

$$CuS_{(s)} + 2Fe^{3+}_{(aq)} = Cu^{2+}_{(aq)} + 2Fe^{2+}_{(aq)} + S° \quad (2.5.5)$$

In reality, this process occurs as the following coupled anodic and cathodic reactions, which occur at equal rates at the mineral surface, under freely dissolving conditions.

Cathodic:

$$2Fe^{3+}_{(aq)} + 2e^- = 2Fe^{2+}_{(aq)} \quad (2.5.6)$$

Anodic:

$$CuS_{(s)} = Cu^{2+}_{(aq)} + S° + 2e^- \quad (2.5.7)$$

Figure 2.5.1 depicts schematic current density (i) - potential (E) curves for the anodic dissolution of covellite and the cathodic reduction of ferric ions on the mineral surface, as well as the anodic oxidation of ferrous ions thereon.

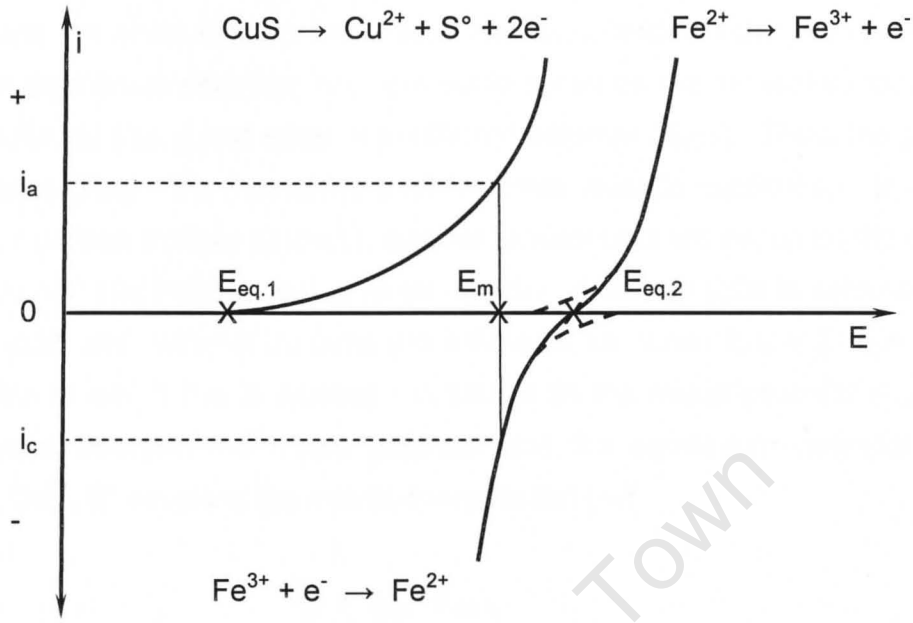

Figure 2.5.1 : Mixed Potential Model (Type I) adapted from Nicol [33,36,103]

With:

- i Current density, in $A.m^{-2}$
- i_a Anodic current density, in $A.m^{-2}$
- i_c Cathodic current density, in $A.m^{-2}$
- E Potential, in V (vs. SHE)
- $E_{eq.1}$ Equilibrium potential for the reaction in Equation 2.5.7 ($i_a = i_c = 0$), in V (vs. SHE)
- $E_{eq.2}$ Equilibrium potential for the reaction in Equation 2.5.6 ($i_a = i_c = 0$), in V (vs. SHE)
- E_m Mixed potential ($i_a = -i_c \neq 0$), in V (vs. SHE)
- η Overpotential, in V (vs. SHE)
- η_a Anodic overpotential, in V (vs. SHE)
- η_c Cathodic overpotential, in V (vs. SHE)

The moment when covellite is in contact with the solution containing the oxidant (ferric ions), both anodic (Equation 2.5.7) and cathodic (Equation 2.5.6) half-cell reactions are at equilibrium, i.e. at $E_{eq.1}$ and $E_{eq.2}$, respectively. However, this is not an equilibrium situation, because some areas on the mineral surface are at one potential ($E_{eq.1}$) and other at a different potential ($E_{eq.2}$). Thus, the potential difference ($E_{eq.2}$ - $E_{eq.1}$) provides a driving force towards equilibrium. In order to attain a uniform surface potential, electrochemical cells are set up on the covellite surface and electrical current is forced to flow. A steady state is achieved when the anodic and cathodic currents are balanced, i.e. when $\Sigma\, i_a = \Sigma\, -i_c \neq 0$. The potential at which this is achieved is known as the mixed potential (E_m). The difference between the mixed potential and the equilibrium potential of the CuS / Cu^{2+}, S° couple is the anodic overpotential (η_a).

$$\eta_a = E_m - E_{eq.1} \qquad (2.5.8)$$

The anodic overpotential represents the driving force for the leaching reaction (Equation 2.5.5) and the corresponding anodic current density (i_a) is equivalent to the specific rate of leaching of covellite.

The difference between the mixed potential and the equilibrium potential of the Fe^{3+} / Fe^{2+} couple is the cathodic overpotential (η_c).

$$\eta_c = E_m - E_{eq.2} \qquad (2.5.9)$$

For the case presented in Figure 2.5.1, the anodic current density (i_a) and the cathodic current density (i_c) are equal, but opposite in sign, at the mixed potential:

$$i_a = -i_c \qquad (2.5.10)$$

In the above example, the reverse reaction for Equation 2.5.7 was ignored in the region of the mixed potential. Generally, this approximation is true for the cathodic behaviour of most copper sulphide minerals, which exhibit highly irreversible electrochemical behaviour [31,33,97]. However, the electrochemical characteristics of the oxidizing reagent (ferrous ion) or reducing reagent (ferric ions) are sometimes considerably more reversible on the mineral surface and one cannot always make the above assumption, which implies that the reverse reaction, i.e. the oxidation of ferrous to ferric ions, can be neglected in the region of the mixed potential [33,36,97]. However, at high Fe(III) : Fe(II) ratios, the anodic oxidation of ferrous to ferric ions can be ignored (Type I) [36,97].

Figure 2.5.2 shows the case (Type III) for the above system, where the mixed potential is fixed by the current-potential characteristics of the Fe(III) / Fe(II) couple, because of the negligible contribution of the anodic oxidation reaction (Equation 2.5.7) of covellite in establishing the mixed potential.

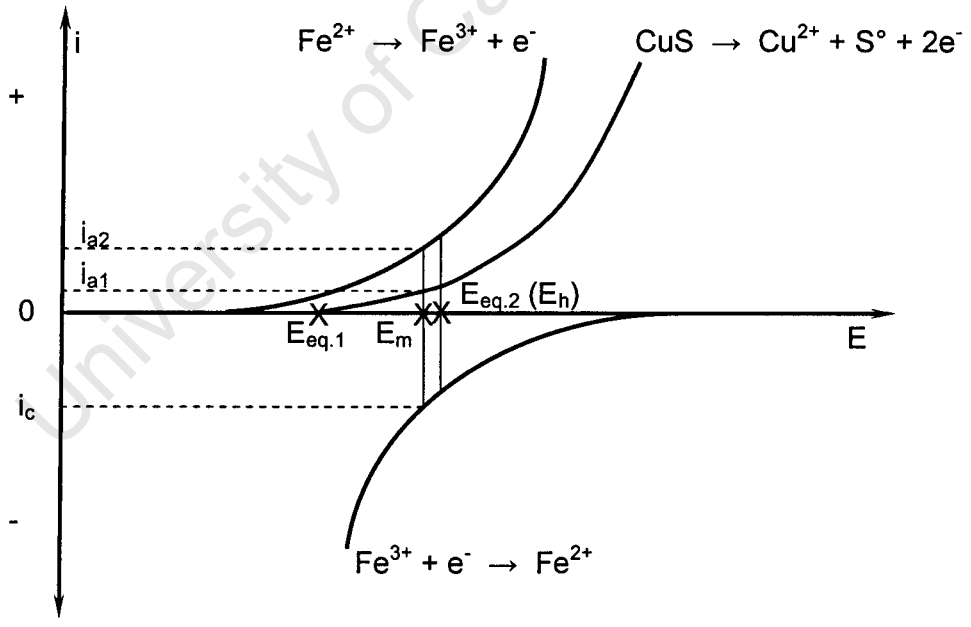

Figure 2.5.2 : Mixed Potential Model (Type III) by Nicol [10,33,36,97,103]

The anodic oxidation of covellite introduces an additional current, which must be balanced by an additional cathodic current. Thus, the mixed potential is the potential where:

$$i_{a1} + i_{a2} = -i_c \qquad (2.5.11)$$

With:

i_{a1} Anodic current density due to the anodic oxidation of covellite, which is equivalent to the rate of dissolution of covellite, in $A.m^{-2}$

i_{a2} Partial anodic current density for the oxidation of ferrous to ferric ions, in $A.m^{-2}$

i_c Partial cathodic current density for the cathodic reduction of ferric to ferrous ions, in $A.m^{-2}$

The relationship between current density and potential is expressed by the so-called Butler-Volmer equation [10,31,33,34,36,97,99,101,102,103,104] and writing each of the current densities of Equation 2.5.11 in terms of the latter, renders:

$$i_{a1} = k_{a1}\exp(\beta_{a1}E_m) \qquad (2.5.12)$$

$$i_{a2} = k_{a2}[Fe(II)]\exp(\beta_{a2}E_m) \qquad (2.5.13)$$

$$-i_c = k_c[Fe(III)]\exp(-\beta_cE_m) \qquad (2.5.14)$$

With:

k An electrochemical rate constant

β Tafel slope, in $V.decade^{-1}$

Electrochemical Studies on Covellite

Lázaro-Báez compared the anodic responses from linear sweeps (5 $mV.s^{-1}$) for rotating (200 rpm) bornite (Cu_5FeS_4), chalcopyrite ($CuFeS_2$) and covellite (CuS) electrodes in 0.1 M H_2SO_4 + 0.05 M Fe(III) at 60°C [10]. These are essentially plots of the anodic current density (i_a) against the applied electrode potential (E), where the electrodes were swept in the positive direction from the open circuit potential (OCP), up to slightly above 0.8 V (vs. SHE).

She showed that the reactivity for bornite was higher than that for covellite, which was much higher than that for chalcopyrite. In addition, it was found that the open circuit potential for all three minerals were negative to the anodic process on chalcopyrite and followed the order:

$$OCP(CuFeS_2) > OCP(CuS) > OCP(Cu_5FeS_4) \qquad (2.5.15)$$

The values were 0.42, 0.4 and 0.27 V (vs. SHE), respectively.

The open circuit potential for the three minerals in 0.1 M HCl + 0.05 M Fe(III) at 60°C, followed the order:

$$OCP(CuS) > OCP(CuFeS_2) > OCP(Cu_5FeS_4) \qquad (2.5.16)$$

The values for these were measured at 0.46, 0.41 and 0.4 V (vs. SHE), respectively.

Bornite showed the same reactivity in both solutions, while the reactivity of chalcopyrite was only marginally higher in the chloride solution.

On the other hand, covellite was found to be much less reactive in this medium, with almost half the anodic current density for the sulphate solution. This was also reflected by a mixed potential, which was about 90 mV lower in the chloride than in the sulphate solution, whereas the mixed potential for bornite was virtually the same in both solutions and slightly higher (20 mV) for chalcopyrite in the chloride solution. Thus, it was demonstrated that the rate of covellite was potential-dependent with an increase in anodic current density with increased potential in both media. Furthermore, although this was not pointed out by the investigator, covellite also showed some indication of active-passive behaviour in the chloride solution.

The above findings with respect to reactivity were confirmed by the cathodic reduction of ferric ions on these minerals in both solutions.

Lázaro-Baez's observation, although obtained at higher temperature and by different technique, seems to be in agreement with the findings of Sullivan, who showed that the rate of dissolution of covellite was slower in acidic, ferric chloride than in acidic, ferric sulphate solutions, in his leaching studies conducted at 35°C [49].

Ghali *et al.* conducted an electrochemical study to investigate the anodic dissolution behaviour of impure commercial and pure synthetic covellite electrodes in acidic, chloride solutions ranging from 0.01 M HCl to 1 M HCl [105].

These investigators found that the rate of dissolution of covellite was potential-dependent and strongly influenced by the acidity (pH) and chloride ion concentration of the solution. In other words, the rate of dissolution increased with increased acidity and chloride ion concentration. An increase in the porosity of covellite also had a positive effect on the kinetics of dissolution. However, an increase in Cu(II) ion concentration seemed to decrease the rate of dissolution, but this effect was less marked than that of acidity and chloride ion concentration.

Furthermore, the mineral showed typical active-passive behaviour with the formation of elemental sulphur.

Unfortunately, the above workers performed their experiments over a very wide applied potential range, which spanned up to about 1.5 V (vs. SCE). At such high potentials, oxygen will evolve due to the oxidation of water, which may lead to bias towards the measured anodic current density. Also, it is unlikely that mineral surface potentials up to such high values can be obtained by redox couples such as Cu(II) / Cu(I) and Fe(III) / Fe(II), even at very high temperatures. This may make some of their findings less relevant to atmospheric leaching processes.

Jones *et al.* produced anodic and cathodic polarization curves for a suite of oxide and sulphide minerals, including covellite, in both chloride (1 N HCl) and sulphate (1 N H_2SO_4) solutions [106]. Their results showed that the anodic oxidation of covellite was potential-dependent, the rate of dissolution increased with increased temperature and the mineral electrode showed active-passive behaviour.

The above investigators also made the interesting conclusion that electrochemical polarization measurements may be useful for rapid, screening tests prior to more focused leaching tests by conventional methods.

Very little work has been reported on the electrochemistry of covellite in acidic, chloride solutions and, especially so, on the anodic processes involved at relatively low potentials, e.g. 0.55 V (vs. SHE) to 0.62 (vs. SHE). This is somewhat surprising, since this medium is attractive for leaching and electrolysis due to the high solubility of cupric chloride and expected low overpotentials associated with chloride ions. Nevertheless, the above workers all seem to be in agreement on the potential-dependency of covellite, as well as the mineral's active-passive behaviour in acidic, chloride solutions. Also, it seems that acidity

(pH), chloride ion and copper ion concentration are important parameters to be considered in the leaching of covellite in this medium.

In general, electrochemical techniques can be very useful in mechanistic or screening tests pertaining to the leaching of copper sulphide minerals. However, care has to be taken that the applied potential range is relevant to that induced during the conventional leaching process. Also, purity of the mineral electrode used, is also very important, because impurities oxidizing at applied potentials will cause bias towards measured anodic (and cathodic) currents. Furthermore, it should also be remembered that these techniques are conducted over relatively short periods of time, which may again introduce bias towards the rate of leaching in view of passivation of the mineral electrode later on. Therefore, it is essential to conduct these in conjunction with longer-duration, conventional leaching tests.

CHAPTER 3

EXPERIMENTAL

3.1 Materials

3.1.1 Electrodes

Covellite Electrode

The mineral electrode was manufactured from a synthetically produced covellite sample, which constituted synthesis of cupric ion with gaseous hydrogen sulphide or sulphide ion at high temperature according to a published method [65]. XRD analysis showed that the sample was relatively pure with 98.5% covellite and only trace amounts of chalcocite present.

The synthesis process produced cylindrical samples of 1 mm in diameter, which were typically about 10 mm in length. A copper layer was electro-plated on one end of the covellite sample to which a thin copper wire was soldered using silver epoxy resin. The other end of the copper wire was connected to a stainless steel screw, also using silver epoxy resin. The mineral electrode was finally imbedded in a cylindrical, resin (Araldite LY 568) disk (Figure 3.1).

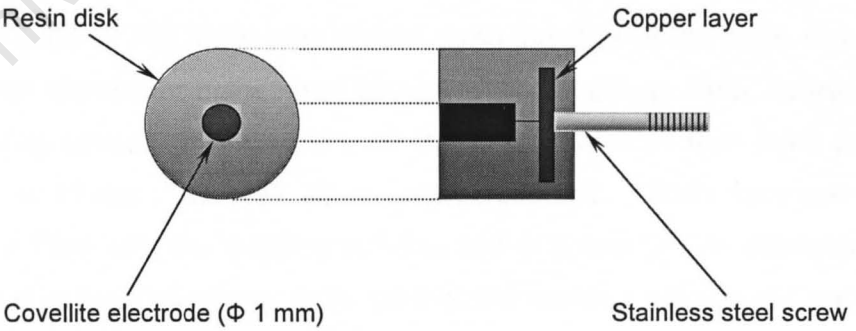

Figure 3.1 : Covellite Electrode

The calculated surface area of the mineral electrode exposed to the solution was 0.0079 cm^2.

Counter Electrode

The counter electrode used, was a thin, platinum (Pt) wire of about 10 mm in length, of which the one end was coiled for improved electrical contact.

Reference Electrode

The reference electrode was a saturated, potassium sulphate, mercury-mercurous sulphate (sat. K_2SO_4, Hg / Hg_2SO_4) electrode with a potential of 0.651 V against the standard hydrogen electrode (SHE) at 25°C [107]. All potentials in this study have been reported against SHE.

3.1.2 Apparatus

A schematic diagram of the apparatus used in this study is presented in Figure 3.2. This shows an aluminium holder in which the resin disk, containing the mineral electrode, was inserted for support. The holder was open at the bottom to allow for electrical contact with the stainless steel screw of the stationary, resin disk.

A polyvinylchloride (PVC) fitting was placed upon the face of the resin disk and tightened to an aluminium holder (not shown) with a stainless steel, screw-ring. The PVC fitting contained a capillary of 2 mm in diameter and fixed length (2 mm, 5 mm or 10 mm), as well as a larger reservoir. Both reservoir and capillary were filled with the working solution and a 2 mm (inside diameter) O-ring, imbedded in the PVC fitting, ensured that the working solution did not leak from the capillary and reservoir. The platinum wire was inserted into the solution-filled capillary and the reference electrode into the reservoir.

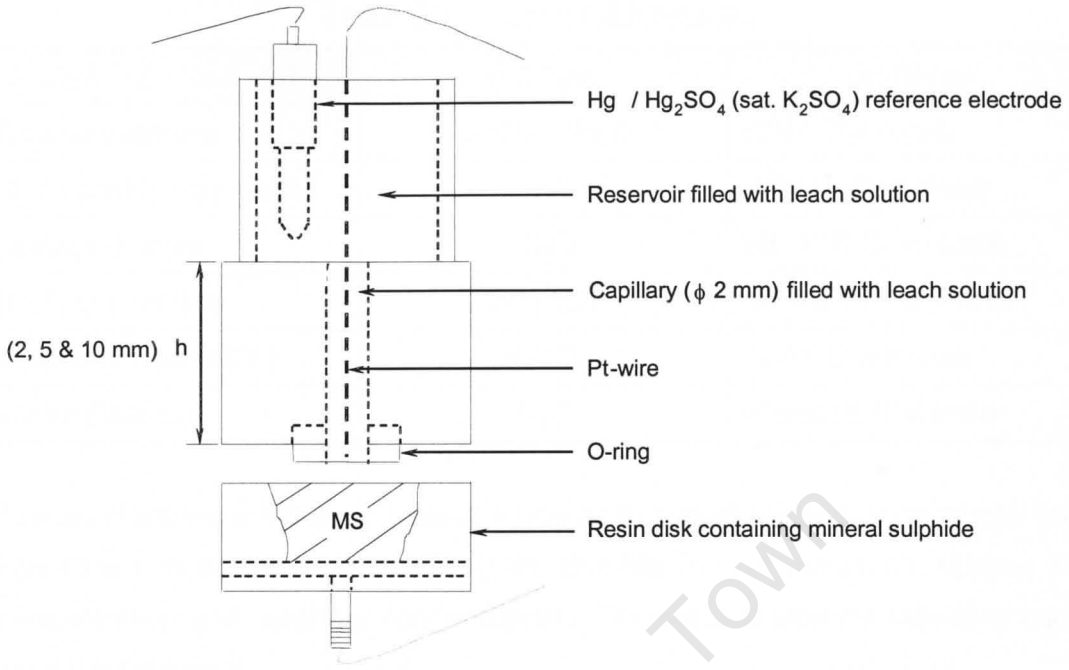

Figure 3.2 : Experimental Set-Up

The above three-electrode system was used in conjunction with an EG & G Princeton Applied Research Model 173 Potentiostat / Galvanostat and an EG & G Princeton Applied Research Model 175 Universal programmer to conduct electrochemical measurements. Current and potential readings from the potentiostat were captured using a National Instrument data acquisition card, which was controlled by Labview™ software. The latter also allowed for the recorded data to be exported to a suitable spreadsheet program, e.g. Microsoft's Excel®.

3.1.3 Working Solutions

The solutions used as electrolytes in this study were all prepared using analytical grade (AR) chemicals and Millipore-quality (Milli-Q) water. A list of the chemicals with their respective formulae and suppliers is presented in Table 3.1.

Table 3.1 : Chemical Reagents

Chemical Reagent	Formula	Supplier
Copper sulphate	$CuSO_4 \cdot 5H_2O$	BDH Chemicals
Hydrochloric acid (32%)	HCl	SIGMA Chemicals
Sodium chloride	NaCl	MERCK Chemicals
Sodium sulphate	Na_2SO_4	MERCK Chemicals
Sulphuric acid (98%)	H_2SO_4	AJAX Chemicals
Water (Milli-Q)	H_2O	Murdoch University

The solutions were made up in such a way as to ensure initial change of only one constituent at a time, e.g. acidity (pH), chloride ion concentration, copper ion concentration and sulphate concentration. The various working solutions used were the following:

Hydrochloric Acid Solutions

- 0.01 M HCl
- 0.02 M HCl
- 0.2 M HCl
- 1 M HCl
- 2 M HCl

Hydrochloric Acid / Sodium Chloride Solutions

- 0.2 M HCl + 0.3 M Cl^- (as NaCl)
- 0.2 M HCl + 0.8 M Cl^- (as NaCl)
- 0.2 M HCl + 1.8 M Cl^- (as NaCl)

Hydrochloric Acid / Sodium Sulphate Solutions

- 0.2 M HCl + 10 g/L SO_4^{2-} (as Na_2SO_4)
- 0.2 M HCl + 50 g/L SO_4^{2-} (as Na_2SO_4)
- 0.2 M HCl + 100 g/L SO_4^{2-} (as Na_2SO_4)

Hydrochloric Acid / Copper Sulphate Solutions

- 0.2 M HCl + 0.5 g/L Cu (as $CuSO_4$)

Sulphuric Acid Solutions

- 0.01 M H_2SO_4
- 0.02 M H_2SO_4
- 0.2 M H_2SO_4
- 1 M H_2SO_4
- 2 M H_2SO_4

Sulphuric Acid / Sodium Chloride Solutions

- 0.01 M H_2SO_4 + 0.2 M Cl^- (as NaCl)
- 0.02 M H_2SO_4 + 0.2 M Cl^- (as NaCl)
- 0.2 M H_2SO_4 + 0.2 M Cl^- (as NaCl)
- 1 M H_2SO_4 + 0.2 M Cl^- (as NaCl)
- 2 M H_2SO_4 + 0.2 M Cl^- (as NaCl)
- 0.2 M H_2SO_4 + 2 M Cl^- (as NaCl)

Sulphuric Acid / Sodium Chloride / Copper Sulphate Solutions

- 0.2 M H_2SO_4 + 0.2 M Cl^- (as NaCl) + 0.05 g/L Cu (as $CuSO_4$)
- 0.2 M H_2SO_4 + 0.2 M Cl^- (as NaCl) + 0.1 g/L Cu (as $CuSO_4$)
- 0.2 M H_2SO_4 + 0.2 M Cl^- (as NaCl) + 0.5 g/L Cu (as $CuSO_4$)
- 0.2 M H_2SO_4 + 0.2 M Cl^- (as NaCl) + 1 g/L Cu (as $CuSO_4$)
- 0.2 M H_2SO_4 + 2 M Cl^- (as NaCl) + 0.05 g/L Cu (as $CuSO_4$)
- 0.2 M H_2SO_4 + 2 M Cl^- (as NaCl) + 0.1 g/L Cu (as $CuSO_4$)
- 0.2 M H_2SO_4 + 2 M Cl^- (as NaCl) + 0.5 g/L Cu (as $CuSO_4$)
- 0.2 M H_2SO_4 + 2 M Cl^- (as NaCl) + 1 g/L Cu (as $CuSO_4$)

3.2 Methods

3.2.1 Electrochemical Measurements

All electrochemical tests were conducted on stationary mineral electrodes using the apparatus and set-up already described. Unless otherwise stated, a Φ 2 mm PVC fitting with a 2 mm capillary length was used in these tests. Also, all tests were conducted at atmospheric conditions of 101.325 kPa (abs) and ± 25°C.

Open Circuit Potential (OCP)

Potential measurements were collected over time at zero current for the mineral electrode and the platinum wire with respect to the sat. K_2SO_4, Hg / Hg_2SO_4, reference electrode.

Cyclic Voltammetry

In general, this is a very useful technique to investigate the occurrence of intermediate species in an electrochemical reaction and can be applied to a stationary electrode [75].

In the hydrometallurgical field, more specifically in the leaching of mineral sulphides, this technique is applied to identify the appropriate potential regime for mineral dissolution, as well as the likely anodic and cathodic reactions taking place at the mineral surface. The technique involves the application of a linear, potential sweep to a mineral electrode by means of a potentiostat. The corresponding current measurement is an indication of reaction at the mineral surface [75,99,108].

All voltammograms in this study were generated by sweeping the mineral electrode in the anodic (positive) direction from the OCP, at a sweep rate of 10 $mV.s^{-1}$ (unless otherwise stated). Before sweeping commenced, the mineral electrode was maintained for three minutes at the OCP within the working solution. This was to aid in generating reproducible results.

A typical voltammogram for a stationary, covellite electrode in 0.2 M HCl at 25°C is shown in Figure 3.3. An enlargement of only the anodic region of the above is presented in Figure 3.4.

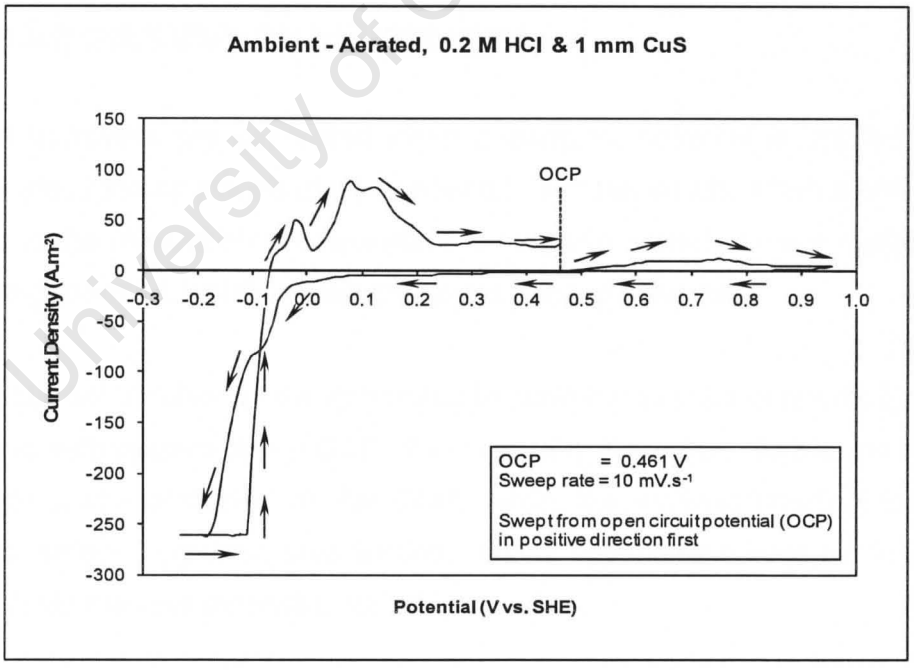

Figure 3.3 : A Typical Voltammogram for a Covellite Electrode

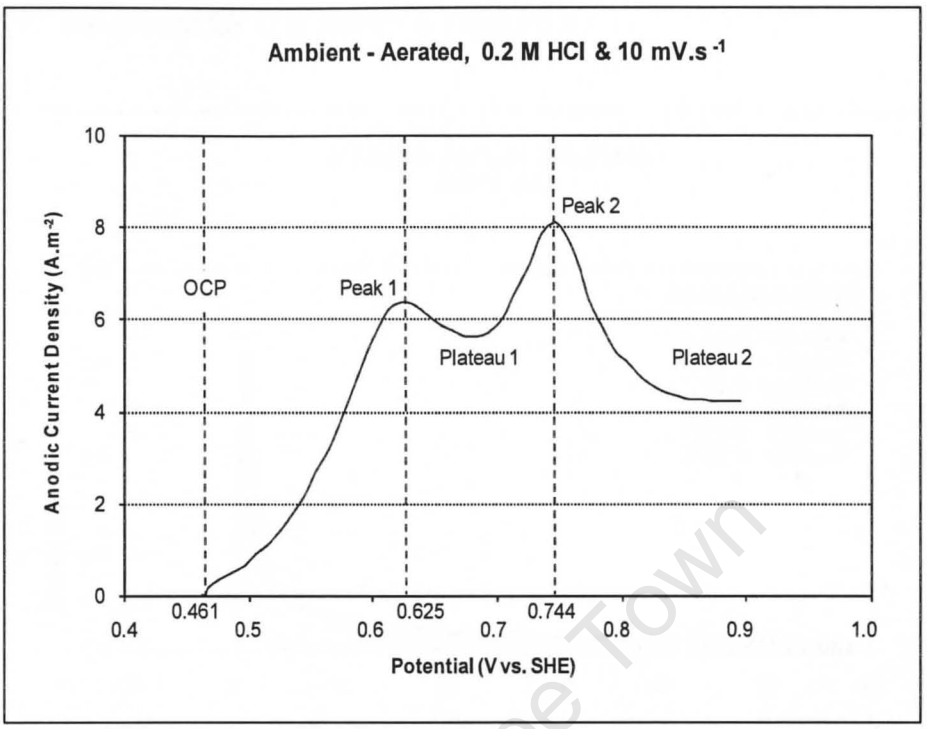

Figure 3.4 : Anodic Region for a Covellite Electrode

Current Transients (Potentiostat Experiments)

Current transients are generated when a constant potential is applied to the mineral electrode by means of a potentiostat. In other words, when a potential is applied to the mineral electrode surface for a given period, current against time data are generated, which correspond to the applied potential.

Anodic current transients were generated by applying a range of anodic (positive) potentials with respect to the OCP of the covellite electrode. Again, the mineral electrode was maintained at the OCP, within the working solution for three minutes, before a potential was applied. These experiments were all conducted over one hour unless otherwise stated.

Typical anodic current density profiles for a stationary, covellite electrode in a 0.2 M HCl solution at 25°C is shown in Figure 3.5.

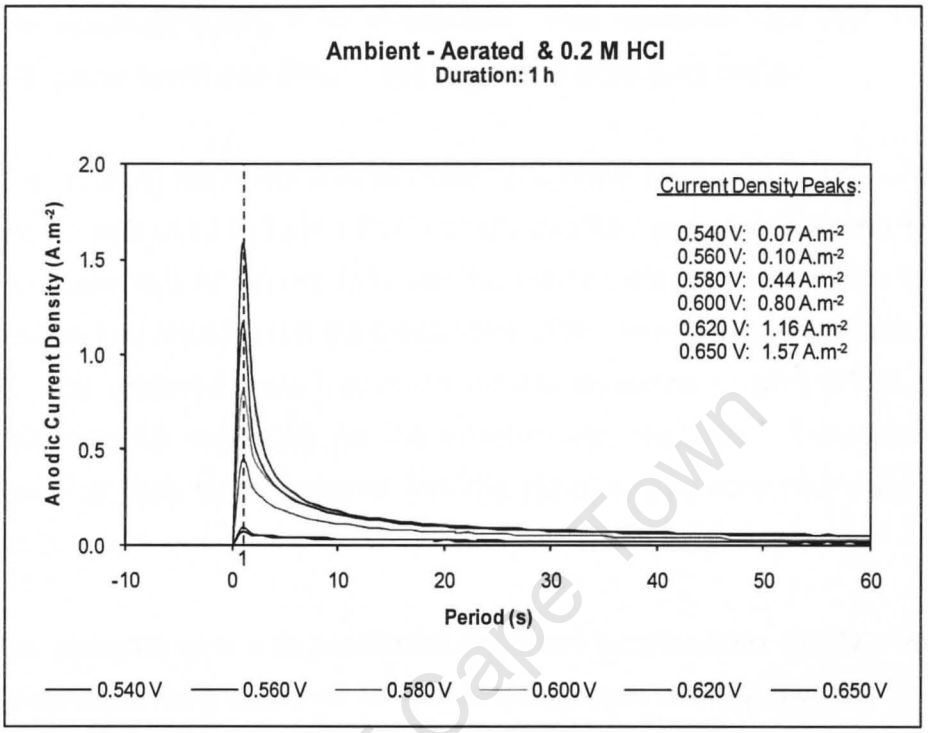

Figure 3.5 : Typical Anodic Current Density Profiles for a Covellite Electrode

3.2.2 Experimental Procedure

Prior to each experiment, the electrode surface, which exposed the mineral, was very gently sanded with P 800 silicon carbide paper for a few seconds. This was performed with the aid of a revolving, polishing wheel to which the silicon paper was attached. A small stream of tap water was used to wet the silicon paper during the sanding process. Thereafter, the mineral was wet-polished in the same way using a finer grind (P 2400) silicon paper. This was done to rid the mineral electrode surface from any reaction products formed during the previous experiment. Care was taken not to skew the electrode's surface during the sanding and polishing processes.

After polishing, the mineral electrode was immersed in Milli-Q water and ultrasonically cleaned in a small bath for five minutes. This ensured that the electrode surface was clean from any sanding and polishing debris, which might affect the readings during experimentation. The electrode was then carefully dried with paper towel and fitted in the apparatus described earlier.

Once the mineral electrode was in place, a syringe fitted with a thin, stainless steel needle was used to fill the PVC fitting's capillary and reservoir with working solution. Care was taken not to touch the mineral electrode's surface with the needle since this would affect the electrode's OCP. In addition, the solution-filled capillary and reservoir were inspected for the presence of air bubbles, which might also impact negatively on the experimental readings. If bubbles were found present, they were removed with the aid of a thin, non-conducting, glass needle.

Next, the platinum wire was positioned down the length of the capillary with the front tip as close as possible to the mineral electrode surface, but not touching. Thereafter, the reference electrode was positioned in the reservoir.

Finally, the mineral electrode, platinum wire and reference electrode were all electrically connected to the potentiostat and the three-electrode system was ready for use.

CHAPTER 4

RESULTS AND DISCUSSION

4.1 Potential Measurements

4.1.1 OCP and the Effect of Capillary Length on Solution Potential

Unlike in the leaching of fine-milled concentrates and ores, where the target copper sulphide mineral is usually well-liberated, this is not the case in heap leaching of whole ores, where a substantial portion of the target mineral is often locked in the gangue matrix. Some of the mineral may also occur in capillaries or pores in the gangue material, which the leach lixiviant has to penetrate in order to establish solid / liquid contact for leaching. An example of this situation is shown in Figure 4.1.

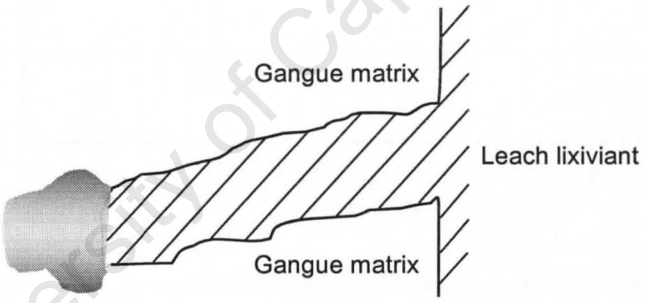

Figure 4.1 : Covellite Partially Exposed in a Capillary Filled with Solution

Therefore, in order to investigate whether the length of such a capillary or pore would have any effect on the solution potential close to the covellite surface and thereby also on the rate of dissolution of the mineral, experiments were conducted with the set-up described earlier in Chapter 3.

Capillary Length of 10 mm

Figure 4.2 shows the OCP behaviour of a stationary, covellite electrode in an aerated, 0.2 M HCl + 0.5 g/L Cu (as $CuSO_4$) solution at ambient conditions. Also shown are the potential of the solution in the capillary (Φ = 2 mm, h = 10 mm) close to the mineral surface, as well as the initial potential of the bulk solution in the reservoir.

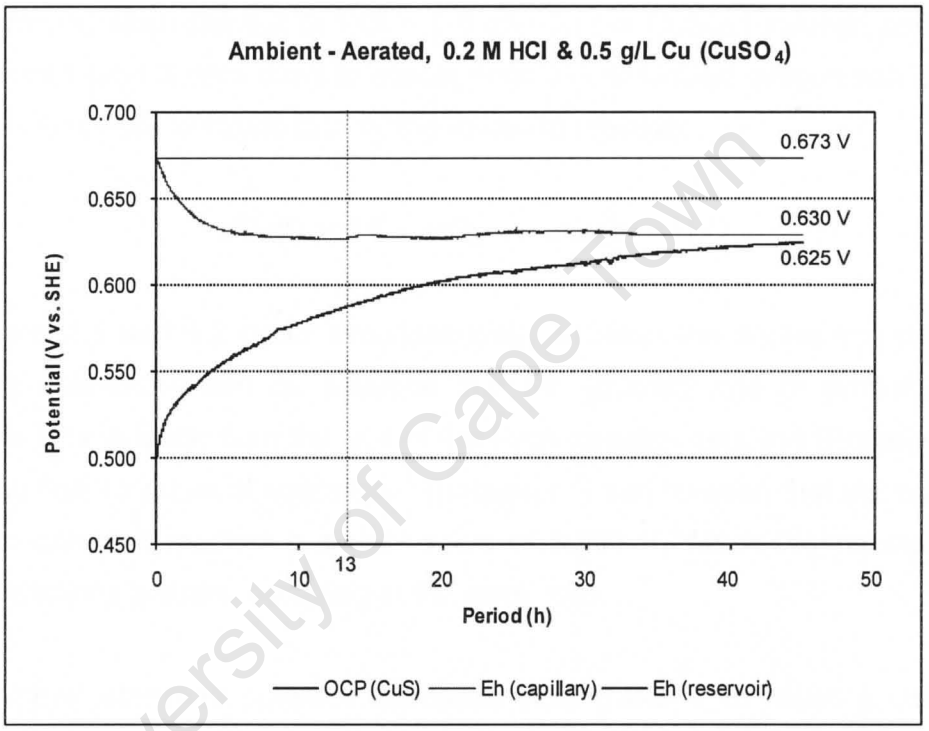

Figure 4.2 : OCP and Solution Potential Transients for Covellite in a Capillary (Φ = 2 mm, h = 10 mm)

Initially, the capillary solution potential is the same as the reservoir solution potential of 0.673 V. As time progresses, the former decreases as a result of a decreasing Cu(II) / Cu(I) ratio due to the reduction of cupric to cuprous ions at the mineral electrode's surface. In other words, the mineral electrode is being oxidized by cupric ions at the solid / liquid interface and the process can be described by the following reaction equation:

$$CuS + Cu(II) \rightarrow 2Cu(I) + S^{\circ} \quad (4.1)$$

It is expected that elemental sulphur instead of bisulphate and / or sulphate will be preferentially produced under the reigning test conditions of low potential and temperature for reasons already discussed under 2.2 Thermodynamics and 2.4.1 Chemistry of Reaction.

Furthermore, since the 0.2 M HCl + 0.5 g/L Cu (as $CuSO_4$) solution has been pre-aerated (and is also open to atmospheric air), dissolved oxygen can oxidize cuprous ions back to cupric ions by the following reaction:

$$2Cu(I) + 2H^{+} + \tfrac{1}{2}O_2 \rightarrow 2Cu(II) + H_2O \quad (4.2)$$

Equations 4.1 and 4.2 occur simultaneously, but from the decreasing capillary solution potential it can be deduced that the (overall) rate of production of cuprous ions is faster than the rate of the back-oxidation reaction (Equation 4.2) over the first 13 hours of operation. Thereafter, it can be seen that the capillary solution potential reaches a steady value of 0.630 V, which means that both these reactions are now occurring at the same rate.

The mineral electrode potential increases from 0.498 V to reach a value of 0.625 V after about 47 hours. This value is very similar to that of the capillary solution potential (0.630 V), which means that the mineral electrode potential is actually determined by the Cu(II) / Cu(I) couple.

From the measured capillary solution potentials, cupric and cuprous ion concentrations were calculated by means of thermodynamic data obtained from the NIST database [40], which in turn was used to determine the equilibrium potentials for the following anodic processes for the dissolution of covellite:

$$CuS = Cu(I) + S^{\circ} + e^{-} \quad (4.3)$$

$$CuS = Cu(II) + S^{\circ} + 2e^{-} \quad (4.4)$$

The results are presented in Table 4.1.

Table 4.1 : Equilibrium Potentials for Covellite (10 mm Capillary)

Time (h)	$E_{h,\ capillary}$ (V)	[Cu(II)] (M)	[Cu(I)] (M)	$[Cu^{2+}]$ (M)	$[Cu^{+}]$ (M)	E (Cu^{+} / CuS) (V)	E (Cu^{2+} / CuS) (V)
0	0.673	7.87×10^{-3}	3.94×10^{-7}	6.18×10^{-3}	1.41×10^{-11}	0.465	0.566
47	0.630	7.87×10^{-3}	2.05×10^{-6}	6.18×10^{-3}	7.34×10^{-11}	0.507	0.566

1) [Cu(II)] total cupric ion concentration
2) [Cu(I)] total cuprous ion concentration
3) $[Cu^{2+}]$ free or uncomplexed cupric ion concentration
4) $[Cu^{+}]$ free or uncomplexed cuprous ion concentration

As the capillary solution potential (determined by the Cu(II) / Cu(I) couple) is greater than the equilibrium potential for the covellite electrode, the latter can be oxidized by cupric ions in solution. Both reactions (Equations 4.3 and 4.4) are feasible, but the one-electron process is thermodynamically more favourable, because of the greater difference between the capillary solution potential and the covellite equilibrium potential for this reaction (Equation 4.3).

Therefore, the decreasing capillary solution potential is a result of a net increase in cuprous ion concentration with time and, very likely, due to: 1) anodic dissolution of the covellite electrode according to Equation 4.3, and 2) reduction of cupric ions at the surface of the covellite electrode according to Equation 4.5.

$$Cu(II) + e^{-} = Cu(I) \quad (4.5)$$

The above two half-cell reactions present the respective oxidation and reduction components of the electrochemical reaction already presented in Equation 4.1. And, in conjunction with Equation 4.2, the overall reaction is given by:

$$CuS + 2H^+ + \tfrac{1}{2}O_2 \rightarrow Cu(II) + S^\circ + H_2O \qquad (4.6)$$

It should be mentioned that although all measurements were conducted under open circuit, it has been shown that those for the covellite electrode were in fact obtained under conditions where the mineral is being oxidized. Therefore, these will be referred to as mixed potentials (E_m).

Thus, a Type III situation exists, where E_m is fixed by the Cu(II) / Cu(I) couple under these conditions since the contribution of the anodic current from the oxidation of the mineral is negligible compared to that of the Cu(II) / Cu(I) couple at E_m (see 2.5 Electrochemistry).

Capillary Length of 2 mm

Figure 4.3 shows the results for an experiment conducted under the same conditions as above, i.e. an aerated, 0.2 M HCl + 0.5 g/L Cu (as $CuSO_4$) solution at ambient conditions, except for the use of a fitting with a shorter capillary length (Φ = 2 mm, h = 2 mm).

At the start of the experiment, the capillary and reservoir solution potentials are at 0.674 V, with the covellite electrode at 0.506 V. Again, the capillary solution potential decreases, while the covellite electrode potential increases with time. The former reaches a value of 0.653 V and the latter a value of 0.616 V after 47 hours. The initial and final values for cupric and cuprous ion concentrations in the solution close to the mineral surface, as well as the covellite equilibrium potentials (for Equations 4.3 and 4.4) are presented in Table 4.2.

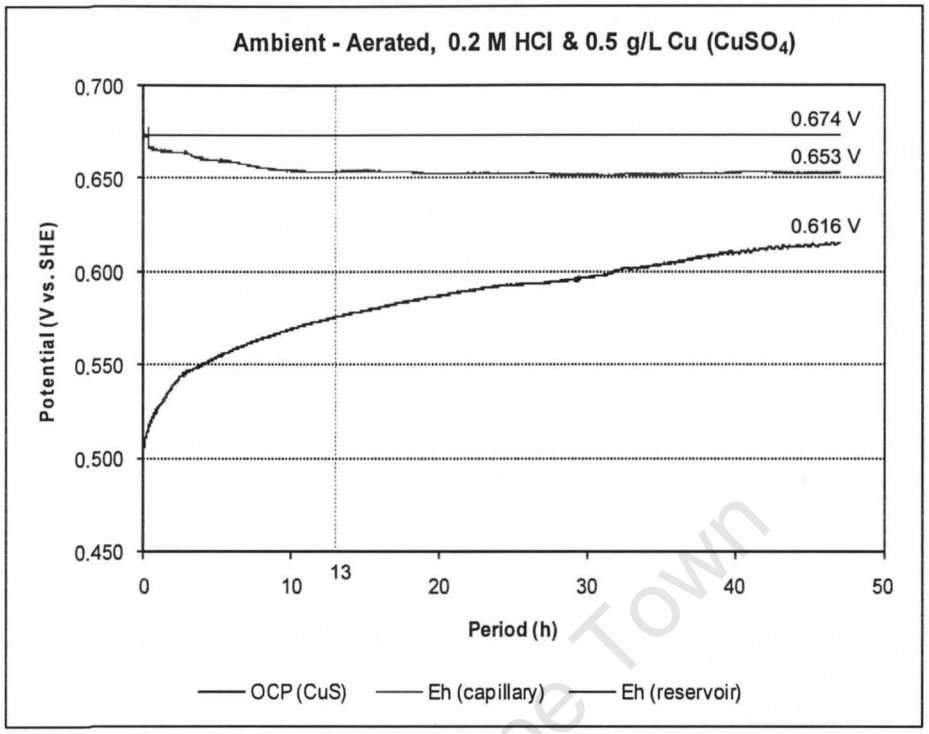

Figure 4.3 : OCP and Solution Potential Transients for Covellite in a Capillary (Φ = 2 mm, h = 2 mm)

Table 4.2 : Equilibrium Potentials for Covellite (2 mm Capillary)

Time (h)	$E_{h,\ capillary}$ (V)	[Cu(II)] (M)	[Cu(I)] (M)	$[Cu^{2+}]$ (M)	$[Cu^{+}]$ (M)	E (Cu^{+} / CuS) (V)	E (Cu^{2+} / CuS) (V)
0	0.674	7.87×10^{-3}	3.78×10^{-7}	6.18×10^{-3}	1.35×10^{-11}	0.464	0.566
47	0.653	7.87×10^{-3}	8.35×10^{-7}	6.18×10^{-3}	2.99×10^{-11}	0.484	0.566

1) [Cu(II)] total cupric ion concentration
2) [Cu(I)] total cuprous ion concentration
3) $[Cu^{2+}]$ free or uncomplexed cupric ion concentration
4) $[Cu^{+}]$ free or uncomplexed cuprous ion concentration

From these results it can be seen that the same conclusions can be derived as for the previous case. I.e. the decreasing capillary solution potential is a result of the oxidation of covellite by cupric ions (according to Equation 4.3) and E_m is fixed by the Cu(II) / Cu(I) couple under these conditions (Type III).

An interesting difference is the behaviour of the capillary solution potential for the different capillary lengths. A comparison between the 2 mm and 10 mm lengths is presented in Figure 4.4.

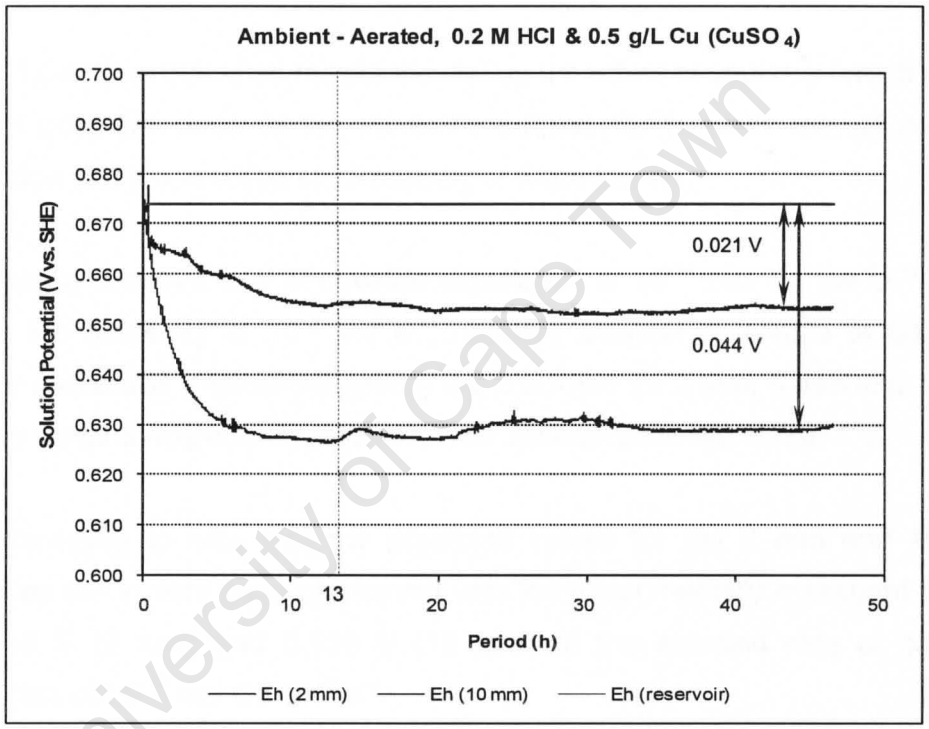

Figure 4.4 : A Comparison of the Solution Potential Transients for Different Capillary Lengths

The capillary solution potential decreases not only with time, but also with increased capillary length. In other words, the potential difference between the bulk solution (in the reservoir) and the solution close to the mineral's surface increases with increased capillary length. For example, this difference is 21 mV

and 44 mV for the 2 mm and 10 mm capillaries respectively, after about 13 hours of operation.

From the data in Tables 4.1 and 4.2 it can be seen that the cupric ion concentration at the mineral's surface is the same for both capillary lengths. However, the cuprous ion concentration for the 10 mm capillary is almost 2.5 times larger than that for the 2 mm capillary (47 hours). Thus, the lower cupric-to-cuprous ion ratio results in a lower solution potential in the case of the 10 mm capillary.

Figure 4.5 shows modelled results simulating the effect of capillary length on the solution potential close to the mineral's surface for a given rate of covellite dissolution and the reaction stoichiometry of Equation 4.1.

Assuming a constant rate of covellite dissolution of 10^{-14} mol Cu $cm^{-2}.s^{-1}$ and a copper ion diffusivity of 10^{-5} $cm^2.s^{-1}$, capillary solution potentials of 0.655 V, 0.640 V and 0.626 V (closed legends) are predicted for 2 mm, 5 mm and 10 mm capillary lengths respectively, at a reservoir solution potential of 0.674 V.

It is interesting to note that the predicted values for the 2 mm and 10 mm capillaries are in very good agreement with the experimentally measured values of 0.653 V (2 mm) and 0.630 V (10 mm) at the selected rate of covellite dissolution of 10^{-14} mol Cu $cm^{-2}.s^{-1}$.

A faster rate of covellite dissolution of 10^{-13} mol Cu $cm^{-2}.s^{-1}$ (same diffusivity) yields even lower capillary solution potentials (open legends), e.g. 0.611 V (2 mm), 0.589 V (5 mm) and 0.571 V (10 mm) for a corresponding reservoir solution potential of 0.674 V.

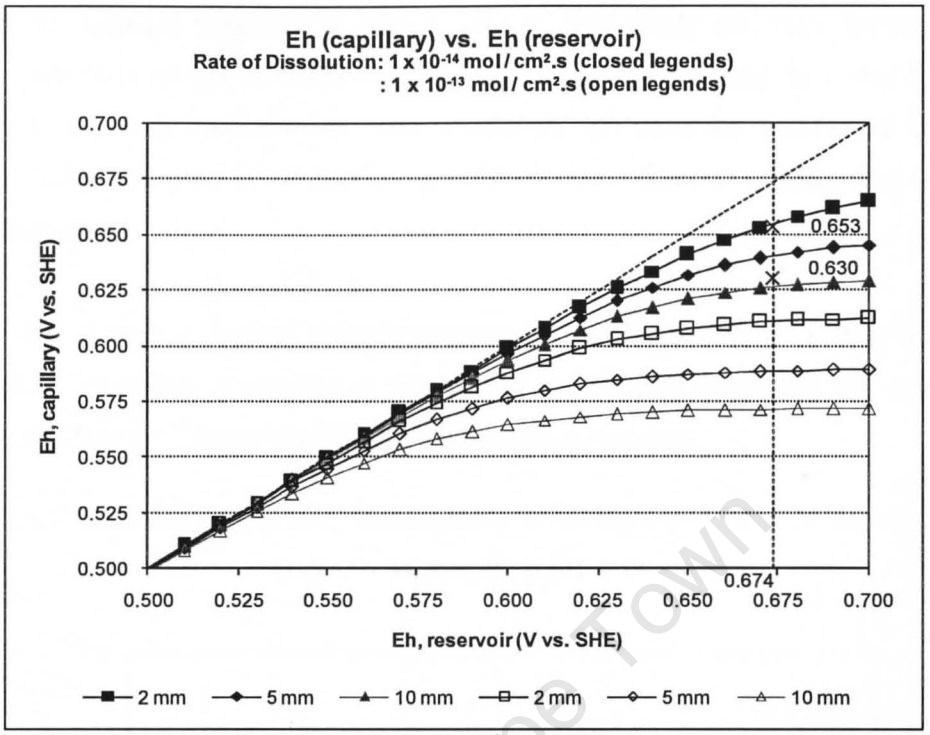

Figure 4.5 : The Effect of Capillary Length and Rate of Mineral Dissolution on the Capillary Solution Potential

In general these results show that the solution potential close to the covellite surface decreases with increased capillary length and also with increased rate of mineral dissolution. Consequently, if the rate of dissolution of covellite is indeed potential-dependent, then capillary length may also affect this rate.

4.2 Cyclic Voltammetry Measurements

Cyclic voltammetry tests were conducted to investigate whether the rate of dissolution of the mineral electrode is dependent on potential, specifically so within the potential range of interest (0.55 V to 0.62 V). Furthermore, this technique was also used to investigate the effect of selected parameters on the rate of mineral dissolution as measured by the anodic current density.

It should be emphasized that although some of the presented data of this section exceed an applied potential of about 0.62 V, this study will only focus on an anodic potential range from the OCP of the mineral electrode to about 0.62 V, which is deemed relevant for the oxidation of covellite facilitated by the Cu(II) / Cu(I) couple in chloride solutions for reasons discussed earlier (see Chapter 1).

Figure 4.6 shows a typical voltammogram for a stationary, Φ 1 mm covellite electrode. This was generated in 0.2 M HCl at 25°C by sweeping the electrode linearly at 10 $mV.s^{-1}$ from the OCP in the anodic direction.

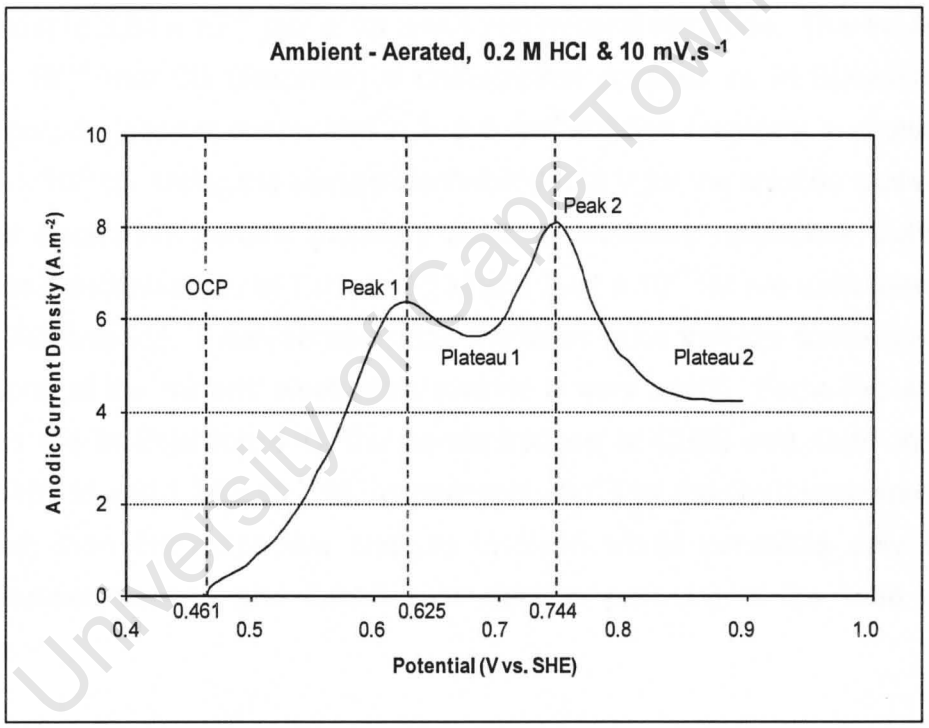

Figure 4.6 : A Typical Voltammogram for a Stationary Covellite Electrode

The graph depicts current density (y-axis) as the anodic response to a potential (x-axis), which is applied to the mineral electrode by means of a potentiostat. The potential is increased in a linear fashion with time and the corresponding anodic current density indicates electrochemical reaction with the formation of

reaction products. In other words, the measured current is the total anodic current, i.e. the sum of all partial anodic currents. These include:

- The current contribution associated with the anodic oxidation of the mineral electrode, and
- The current contribution(s) associated with the anodic oxidation of any reaction product(s).

As the potential increases from the OCP value of 0.461 V, the anodic current density increases as well and reaches 6.4 $A.m^{-2}$ (Peak 1) at a potential of 0.625 V. The cumulative charge up to this potential is 47.1 $C.m^{-2}$, which is equivalent to 3.84×10^{-10} mol e^- for a Φ 1 mm mineral electrode. This equates to 3.84×10^{-10} mol Cu (assuming a one-electron process as in Equation 4.3). Therefore, the copper concentration in a 5 cm^3 solution (capillary and reservoir) is 7.67×10^{-8} M. Using the same potential of 0.625 V for the solution close to the mineral electrode's surface (capillary solution potential), respective Cu(II) and Cu(I) ion concentrations of 7.67×10^{-8} M and 2.42×10^{-11} M are calculated for a 0.2 M HCl solution. It can be seen from the latter value that the concentration of Cu(I) ions at the mineral electrode's surface is very small. For a two-electron process (as in Equation 4.4), the concentrations of Cu(II) and Cu(I) ions are 3.83×10^{-8} M and 1.24×10^{-11} M, respectively. So, if all the Cu(I) ions were to be oxidized, then the respective charges involved would constitute only 0.02% (two electron process) and 0.03% (one-electron process) of the total anodic charge.

Therefore, since the contribution of reaction products such as Cu(I) ions to the measured current density is negligible, it is clear that the rate of dissolution of covellite, as indicated by the anodic current density, increases with increased potential over this range. Thus, for the reaction conditions of Figure 4.6, it can be concluded that the rate of dissolution of covellite is indeed potential-dependent up to 0.625 V.

From Peak 1, the current density decreases slightly up to a potential of 0.674 V (Plateau 1), before it increases again to reach a second peak of 8.1 $A.m^{-2}$ (Peak 2) at 0.744 V. On further increase of the potential, the current density decreases again and forms a second plateau (Plateau 2) from about 0.85 V.

Also, from Figure 4.6 it is to be expected that the rate of dissolution of covellite will not be much affected over the range 0.6 V to 0.7 V since the anodic current density does not change significantly over this potential range for the reigning test conditions. It is also clear that the mineral electrode not only shows active-passive behaviour over the potential range of interest (0.55 V to 0.62 V), but also at higher potentials in a 0.2 M HCl solution.

Equilibrium potentials for a CuS / Cu(I) / Cu(II) system at 25°C were generated for different chloride and total copper concentrations with the aid of thermodynamic data from the NIST database [40]. Figure 4.7 displays a summary of some of the data, which can be found in more detail in Appendix I.

This was done in order to investigate which anodic processes may be involved over the potential range from the OCP (0.461 V) to 0.625 V. In other words, the possibility of the reactions described in Equations 4.3 and 4.4 occurring under the conditions of Figure 4.6, was evaluated from a thermodynamic point of view.

For this purpose, it was assumed that the solution potential close to the mineral electrode's surface (capillary solution potential) is the same as that induced by the potentiostat. Furthermore, although no copper has been introduced to the 0.2 M HCl solution initially, copper ions will come into play due to the anodic oxidation of the mineral electrode, albeit at very small concentrations. These have been estimated from the cumulative charge measured up to a specific potential.

It should be highlighted that such a system, i.e. the dissolving mineral electrode, is in fact not an equilibrium system. The above approach was merely followed to estimate the copper concentration at a specific potential, which would then be used as a typical copper concentration for a solution that is in equilibrium with the mineral electrode.

Figures 4.7(a) to 4.7(f) show the results at selected potentials over the range of interest. These are: 0.476 V, 0.496 V, 0.554 V, 0.575 V, 0.605 V and 0.625 V.

The graphs present the equilibrium potentials for two mineral oxidation reactions (blue and red curves), as well as the "thermodynamic requirement" (horizontal, black line) against chloride concentration. The chloride concentration of interest is indicated by the vertical (black, broken) line on each graph.

At infinitesimal, small copper concentrations, both the anodic oxidation processes of Equations 4.3 and 4.4 are possible since their equilibrium potentials at 0.2 M Cl^- are smaller than the "thermodynamic requirement". However, Equation 4.3 is more favourable than Equation 4.4, because the (solid) blue curve lies below the (solid) red curve over the whole potential range.

On the other hand, at a higher copper concentration of 0.05 g/L (and 0.2 M Cl^-), both these reactions are not feasible up to a potential of 0.496 V, because of the fact that the (broken) blue and red curves exceed the "thermodynamic requirement". Only when the capillary potential is 0.554 V and above, do both these reactions become possible again, with the one-electron process (Equation 4.3) becoming more favourable than the two-electron process (Equation 4.4).

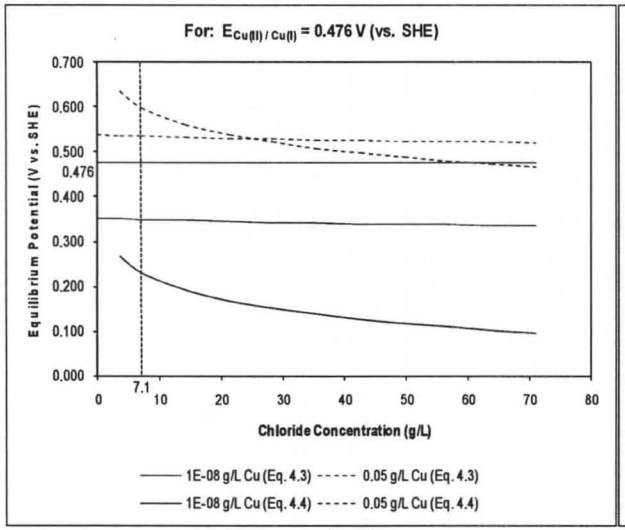

Figure 4.7(a)

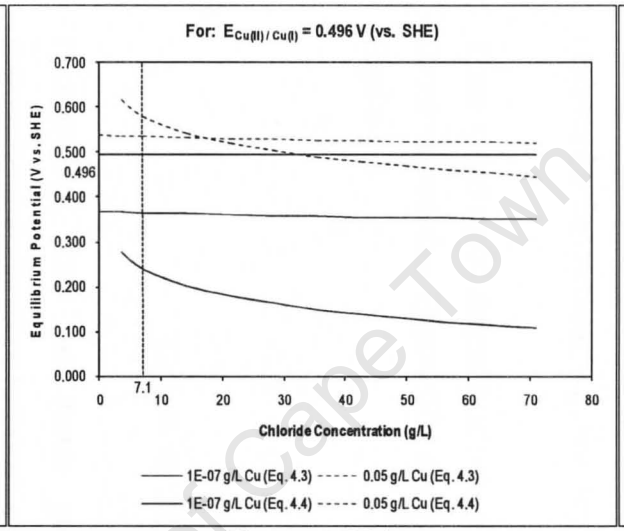

Figure 4.7(b)

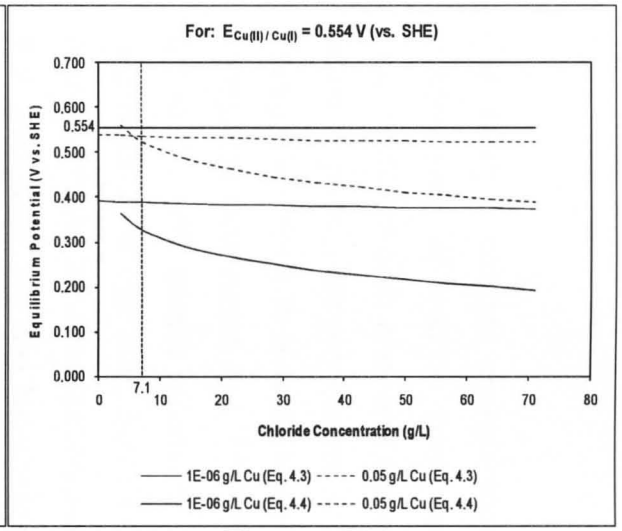

Figure 4.7(c)

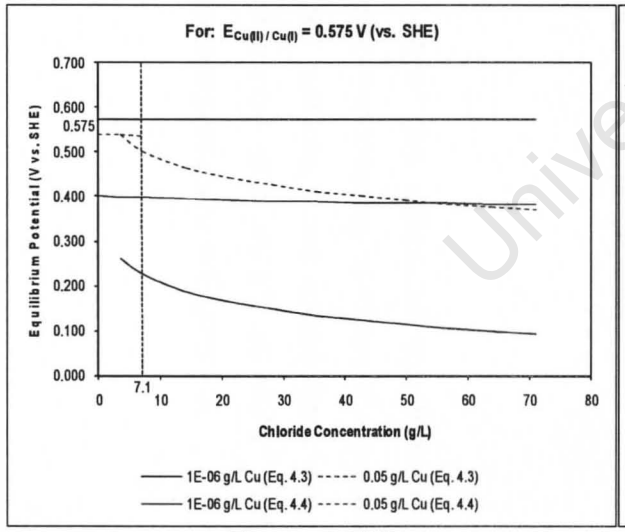

Figure 4.7(d)

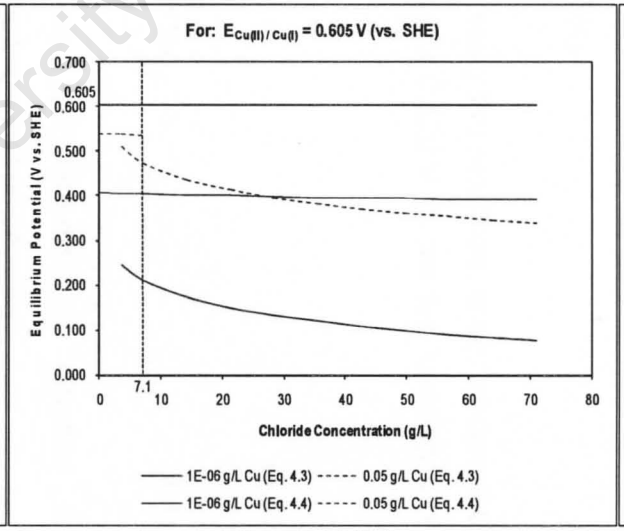

Figure 4.7(e)

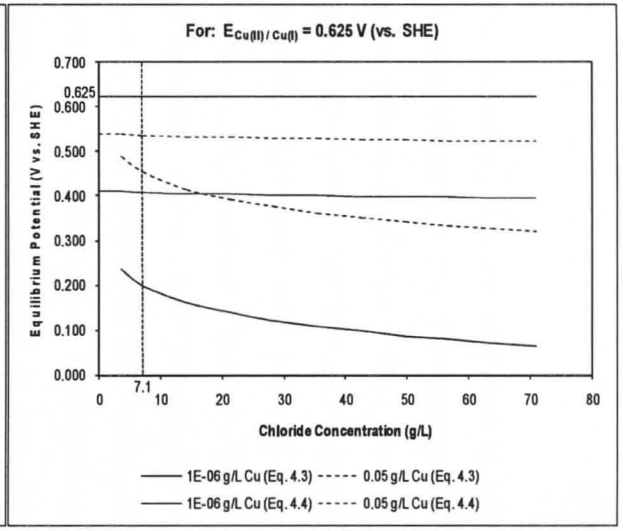

Figure 4.7(f)

Figure 4.7 : Equilibrium Potentials for Reactions in the CuS / Cu(I) / Cu(II) System at 25°C

The effect of chloride concentration is also evident. I.e. an increase in the concentration of chloride ions has a positive effect on the thermodynamic favourability of both one- and two-electron processes (and *vice versa*), but the effect is much more pronounced in the case of the former reaction. This is not unexpected since it is well-known that cuprous ions form stronger chloride-complexes than cupric ions [33,35,38,40,44]. For example, consider Figure 4.7(b) at 0.2 M Cl^-: both anodic processes are not possible since the "thermodynamic requirement" is not met; however, as the chloride concentration increases towards 20 g/L, the one-electron-process becomes feasible again. Furthermore, it is also clear that the two-electron process is more favourable at very low chloride concentrations, e.g. see Figure 4.7(c).

Thus, it has been shown that both the following two reactions, which involve the anodic dissolution of covellite, can occur up to 0.625 V for the test conditions of Figure 4.6:

$$CuS = Cu(I) + S^\circ + e^- \quad (4.3)$$

$$CuS = Cu(II) + S^\circ + 2e^- \quad (4.4)$$

Furthermore, that at these conditions, the one-electron process is thermodynamically more favourable than the two-electron process.

4.2.1 The Effect of Sweep Rate

Important information can be obtained about the nature of the reactions responsible for particular anodic and cathodic responses by variation of the scan or so-called sweep rate [10,108,109]. For this purpose, three experiments were conducted in a 1 M HCl solution at sweep rates of 5 $mV.s^{-1}$, 10 $mV.s^{-1}$ and 20 $mV.s^{-1}$. The respective anodic responses are presented in Figure 4.8.

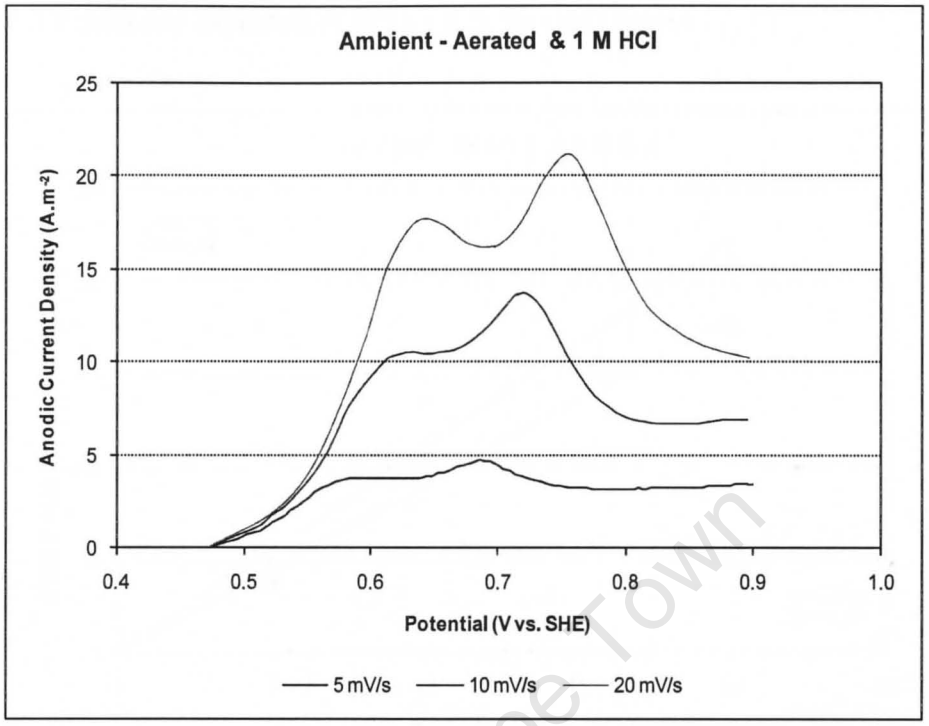

Figure 4.8 : The Effect of Sweep Rate on the Anodic Current Density

It is apparent that the anodic current density increases with increased sweep rate and that the potential associated with the peak current density, i.e. the peak potential, shifts to slightly more positive values. The peak current density (i_p) and peak potential (E_p) values for corresponding sweep rates (v) are summarized in Table 4.3.

Table 4.3 : Anodic Peak Current Densities and Peak Potentials

First Anodic Peak				Second Anodic Peak			
v ($mV.s^{-1}$)	$v^{1/2}$ $(mV.s^{-1})^{1/2}$	i_{p1} ($A.m^{-2}$)	E_{p1} (V)	v ($mV.s^{-1}$)	$v^{1/2}$ $(mV.s^{-1})^{1/2}$	i_{p2} ($A.m^{-2}$)	E_{p2} (V)
5	2.24	3.81	0.604	5	2.24	4.74	0.689
10	3.16	10.6	0.633	10	3.16	13.7	0.714
20	4.47	17.6	0.636	20	4.47	21.2	0.757

Graphical plots of the anodic peak current density against sweep rate for Table 4.3's data are depicted in Figure 4.9, for both peaks.

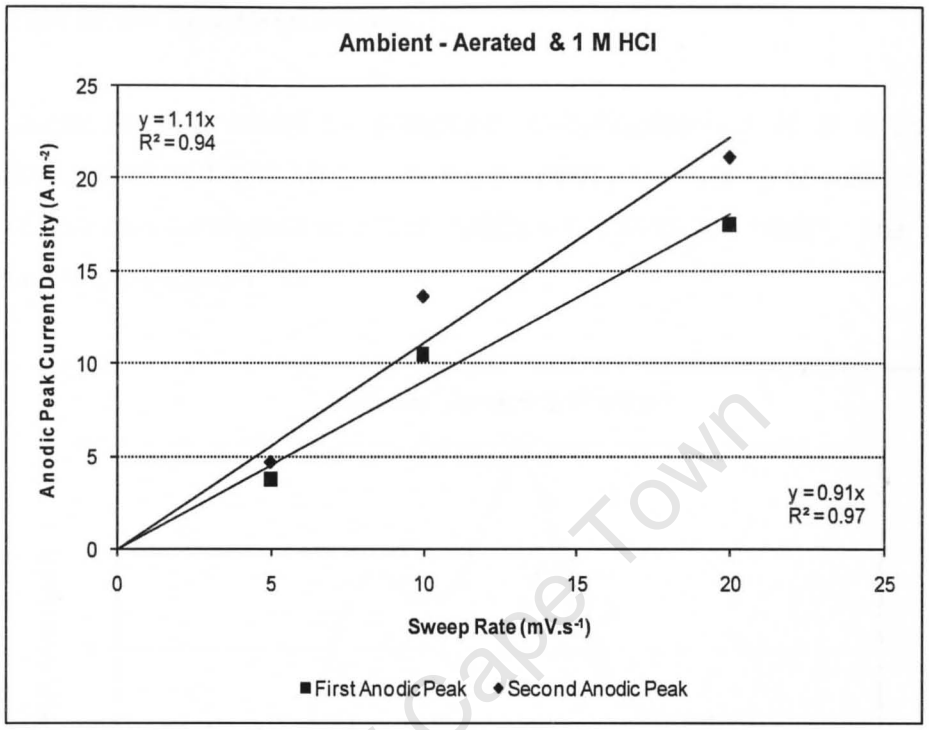

Figure 4.9 : The Relationship between Anodic Peak Current Density and Sweep Rate

Based on extensive analysis, Nicholson and Shain teach us that the peak current density is proportional to the square root of the sweep rate for a simple, reversible charge transfer reaction under diffusion control, but that the peak potential is independent of sweep rate (cited from reference in [108]).

Figure 4.9 shows linear relationships, which indicate that the reigning reactions responsible for these two peaks are not mass transport controlled [108]. In addition, the fact that the peak potentials (for both the first and the second anodic peaks) also shift to slightly more positive values indicates that these processes are irreversible [108]. This is further substantiated by the absence of corresponding cathodic peaks, at least not within proximity of the mixed potential, upon reversal

of the sweep (see Appendix II). This is not unexpected since mineral sulphides (and oxides) invariably exhibit highly, irreversible electrochemical behaviour [33].

4.2.2 The Effect of the Source of Acidity

Since sulphuric acid would be preferred to hydrochloric acid in a potential industrial application for, amongst others, economic reasons, a comparative test to 0.2 M HCl was conducted at 0.2 M H_2SO_4 + 0.2 M Cl^- (as NaCl). The results are presented in Figure 4.10.

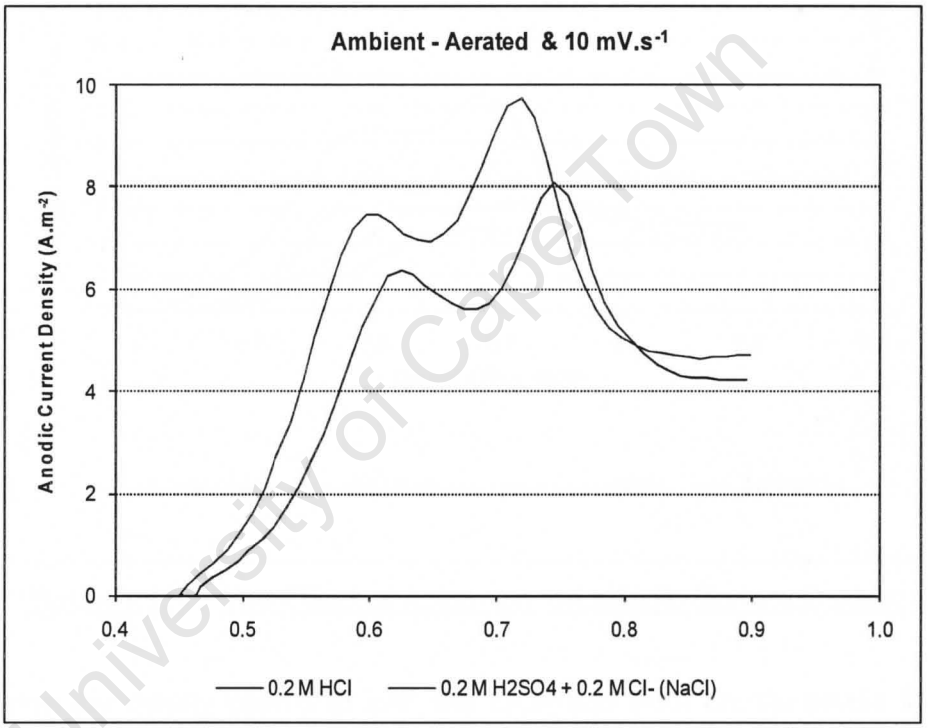

Figure 4.10 : The Effect of the Source of Acidity on the Anodic Current Density

The anodic responses of the mineral electrode for the 0.2 M HCl and 0.2 M H_2SO_4 + 0.2 M Cl^- (as NaCl) solutions are very similar with the current density slightly higher in the case of the latter solution.

4.2.3 The Effect of Acidity

Experiments were conducted to investigate the effect of acidity on the anodic response of the mineral electrode. For this purpose, the chloride concentration was maintained constant at 0.2 M Cl^- (as NaCl) and the acidity increased from 0.01 M H_2SO_4 to 2 M H_2SO_4. The results are shown in Figure 4.11.

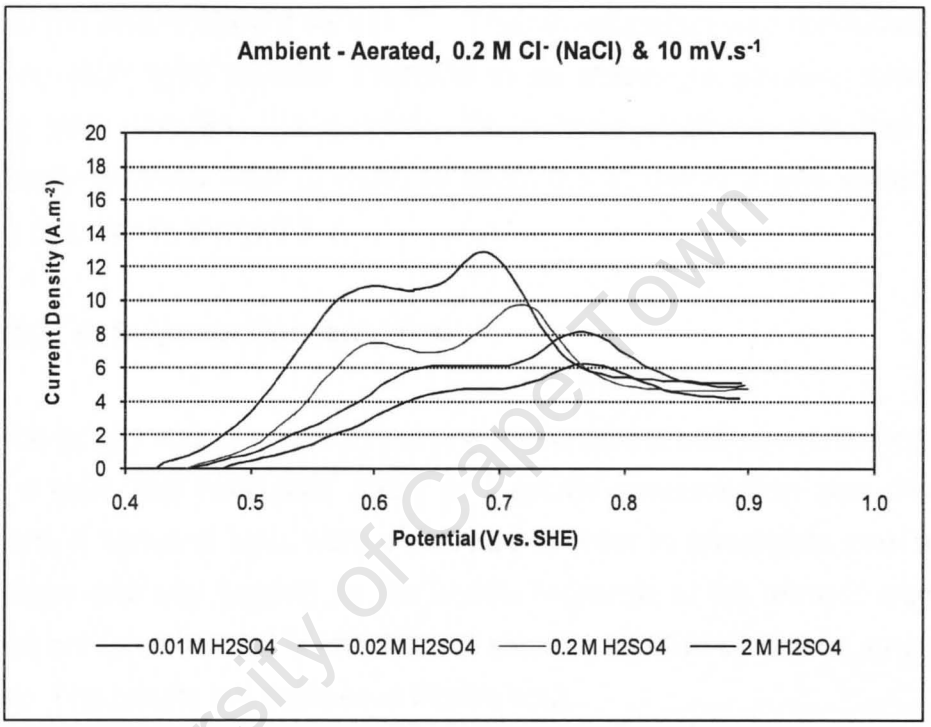

Figure 4.11 : The Effect of Acidity on the Anodic Current Density

Increasing the acidity seems to shift the OCP and both anodic peaks to lower potential values. For example, the OCP shifts from 0.476 V (0.01 M H_2SO_4) to 0.427 V (2 M H_2SO_4), the first anodic peak between 0.6 V and 0.7 V (0.01 M H_2SO_4) shifts to about 0.6 V (2 M H_2SO_4) and the second anodic peak between 0.7 V and 0.8 V (0.01 M H_2SO_4) shifts to about 0.7 V (2 M H_2SO_4). In addition, the current density also increases with increased acidity, especially so at 1 M H_2SO_4 and above.

Ghali *et al.* also observed an increase in anodic current density with increased acidity (0.01 M H^+ to 0.1 M H^+), at more or less constant chloride concentration (1.01 M Cl^- to 1.1 M Cl^-), in their investigation of a stationary (synthetic) covellite electrode in acidic, chloride solutions under argon [105].

On the other hand, Lee *et al.* found that an increase in acidity over the range 0.01 M H_2SO_4 to 2.0 M H_2SO_4 in a 0.2 M Cl^- (as NaCl) solution had no significant effect on the anodic current density [110]. Their investigation was conducted using a rotating (500 rpm) covellite electrode in an electrolyte solution, which was sparged with nitrogen. In addition, the mineral electrode was first swept cathodically from the OCP (0.45 V) to about 0.3 V, before it was swept in the positive direction to about 0.8 V.

4.2.4 The Effect of Sulphate Concentration

Since the acidity was changed by varying the sulphuric acid concentration in the previous tests, the bisulphate and / or sulphate concentration also changed. Therefore, a series of tests were conducted in order to investigate whether this would have had any bearing on the anodic response of the mineral electrode. This was achieved in a 0.2 M HCl solution with the addition of various amounts of Na_2SO_4. The results are depicted in Figure 4.12.

The anodic current density does not seem to be much affected by a change in the Na_2SO_4 concentration. Therefore, it can be concluded that neither Na^+ ions nor HSO_4^- and / or SO_4^{2-} ions have a significant impact on the anodic current density. This is in agreement with the work of Lee *et al.*, who also found that the addition of Na_2SO_4 to a 0.2 M HCl solution showed little difference from the anodic characteristics observed in the absence of Na_2SO_4 [110].

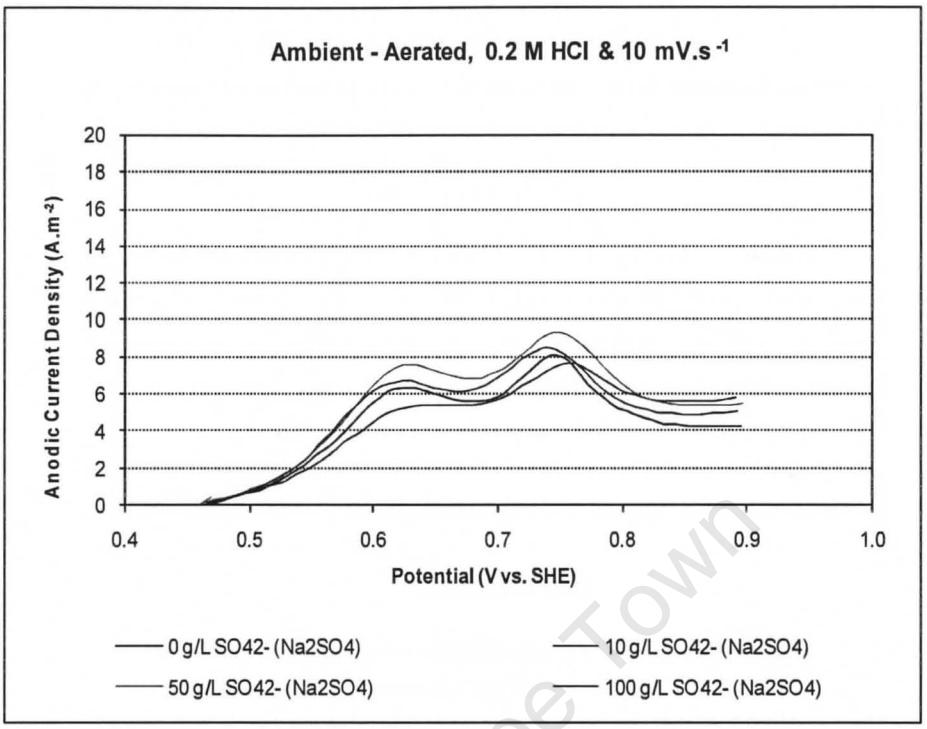

Figure 4.12 : The Effect of Sulphate Concentration on the Anodic Current Density

4.2.5 The Effect of Chloride Concentration

Figure 4.13 shows the effect of increased chloride concentration achieved by the addition of NaCl to a constant acidity of 0.2 M H_2SO_4. In addition, a test at 0.2 M H_2SO_4 (in the absence of chloride ions) was also conducted for comparison purposes.

It can be seen that the presence of chloride ions has a marked effect on the anodic current density, which increases with increased chloride concentration up to 1 M. Above this level no further increase in current density is achieved. This finding is within reasonable agreement with the results of Lee *et al.*, who found that the anodic current density increased up to 0.8 M Cl^- (as NaCl) in a 0.2 M H_2SO_4 solution [110].

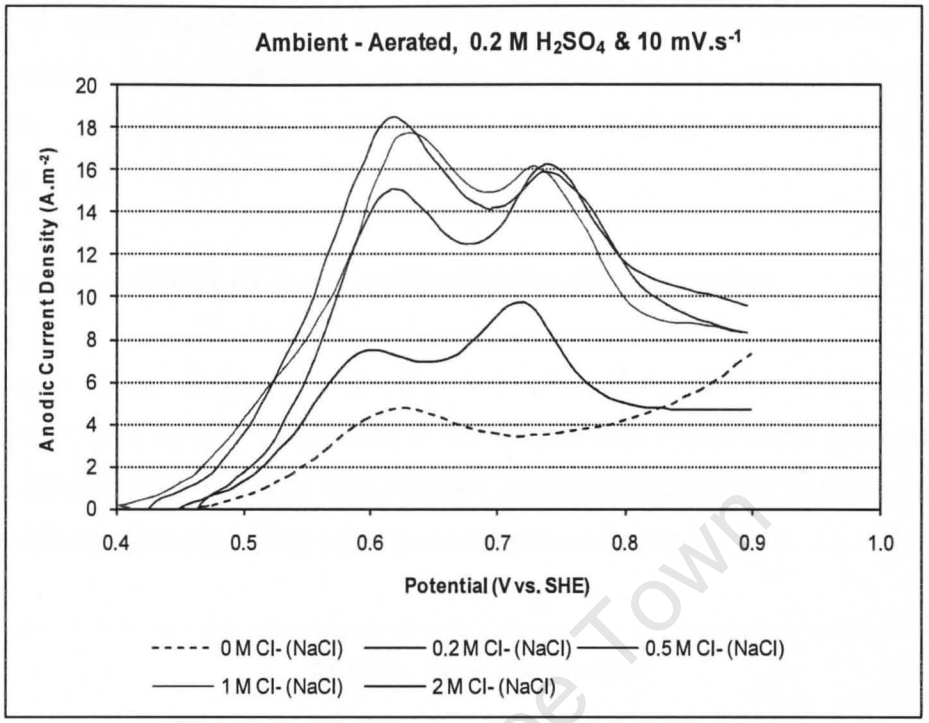

Figure 4.13 : The Effect of Chloride Concentration on the Anodic Current Density

These results are also consistent with the leaching tests of other investigators in acidic, oxygenated chloride solutions (in the absence of ferric ions), which showed that the rate of dissolution of covellite (and secondary covellite) increased with increased chloride concentration, but only up to a specific value [50,61,67,68,70,71]. For example, in the case of covellite, Cheng and Lawson found this value to be 0.5 M Cl^- (as NaCl) in their leaching study where the chloride concentration was increased from 0.01 M to 2 M at 0.5 M H_2SO_4 and 90°C [50].

The chloride solutions all show two distinct anodic peaks with the first one in the vicinity of 0.6 V and the second one between 0.7 V and 0.8 V. In between these two peaks the current forms a plateau, which is indicative of the mineral electrode's passive behaviour over this range. Another plateau is also evident at potentials above 0.8 V.

Unlike in the case of the chloride solutions, only one anodic peak is observed for the 0.2 M H_2SO_4 solution. The mineral electrode also shows passive behaviour in this medium, which spans a wider range of 0.63 V to 0.8 V than in the chloride solutions. Above potentials of about 0.8 V, the current increases with increased potential again.

4.2.6 The Combined Effect of Acidity and Chloride Concentration

Five tests were conducted in the following hydrochloric acid solutions: 0.01 M HCl, 0.02 M HCl, 0.2 M HCl, 1 M HCl and 2 M HCl in order to investigate the combined effect of acidity and chloride concentration on the anodic response of the mineral electrode. The results are portrayed in Figure 4.14.

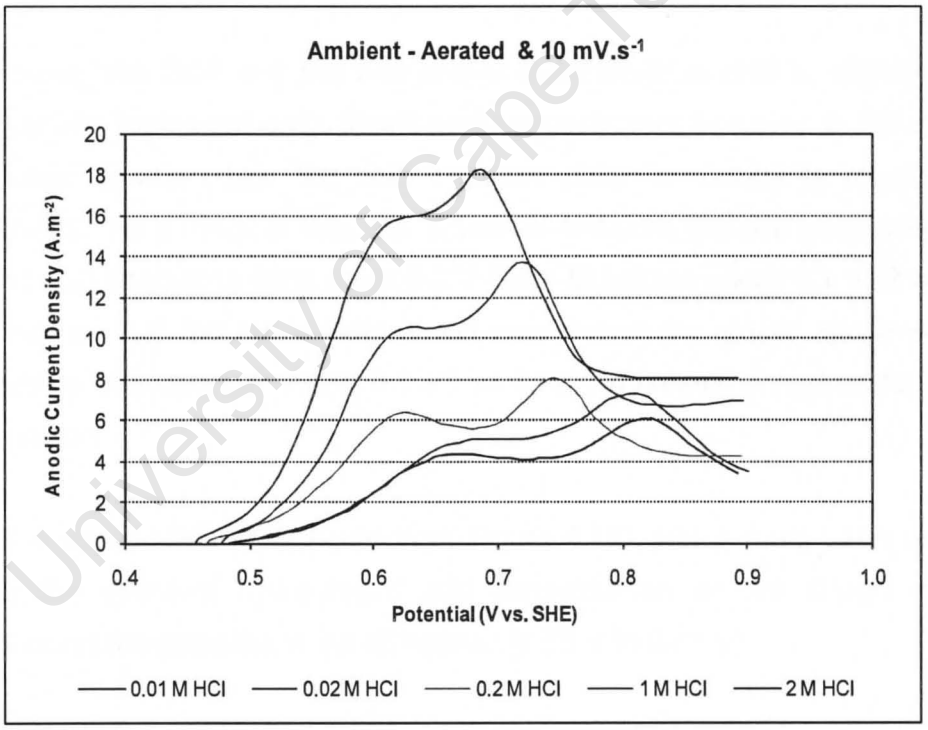

Figure 4.14 : The Combined Effect of Acidity and Chloride Concentration on the Anodic Current Density

It can be seen that the anodic current density not only increases with applied potential, but also with increased hydrochloric acid concentration over a range spanning the OCP and the peak potential corresponding to the first anodic peak (E_{p1}). These observations have also been noted by other investigators [105,110].

Likewise, the current associated with the plateau (between the two peaks) and the second anodic peak, also increases dramatically for concentrations above 0.2 M HCl.

At potentials above the second peak potential (E_{p2}), the anodic current density decreases sharply and eventually forms a second plateau. The current associated with this plateau also increases with increased hydrochloric acid concentration.

Furthermore, the OCP and the first anodic peak seem to shift to slightly lower potentials with increased hydrochloric acid concentration; however, in the case of the second anodic peak, the shift to lower potential values is much more pronounced. As a result of this, the "distance" between the two peak potentials (E_{p1} and E_{p2}) decreases from about 0.2 V (0.01 M HCl) to about 0.1 V (2 M HCl) and it seems that the two anodic peaks may eventually merge into one peak (somewhere between 0.6 V and 0.7 V) on further increase of hydrochloric acid concentration.

Table 4.4 shows data (abstracted from Figure 4.15), which have been used to quantify the effect of hydrochloric acid concentration on the anodic current density within the potential range of interest (0.55 V to 0.62 V).

For this purpose, anodic current densities corresponding to a potential of 0.625 V (i.e. slightly lower than the peak potential, E_{p1}) were selected since the anodic peaks for 0.02 M HCl and 2 M HCl were not sharply defined.

Table 4.4 : Anodic Current Densities at Different HCl Concentrations

[HCl] (M)	E_{p1} (V)	i_{p1} ($A.m^{-2}$)	E (V)	i_a [1] ($A.m^{-2}$)	ln[HCl]	ln(i_a)
0.01	0.671	4.35	0.625	3.50	-4.61	1.25
0.02	-	-	0.625	3.49	-3.91	1.25
0.2	0.625	6.37	0.625	6.37	-1.61	1.85
1	0.633	10.6	0.625	10.6	0	2.36
2	-	-	0.625	15.9	0.69	2.77

1) Anodic current density associated with a potential of 0.625 V

A graphical plot of ln(i_a) against ln[HCl] is presented in Figure 4.15.

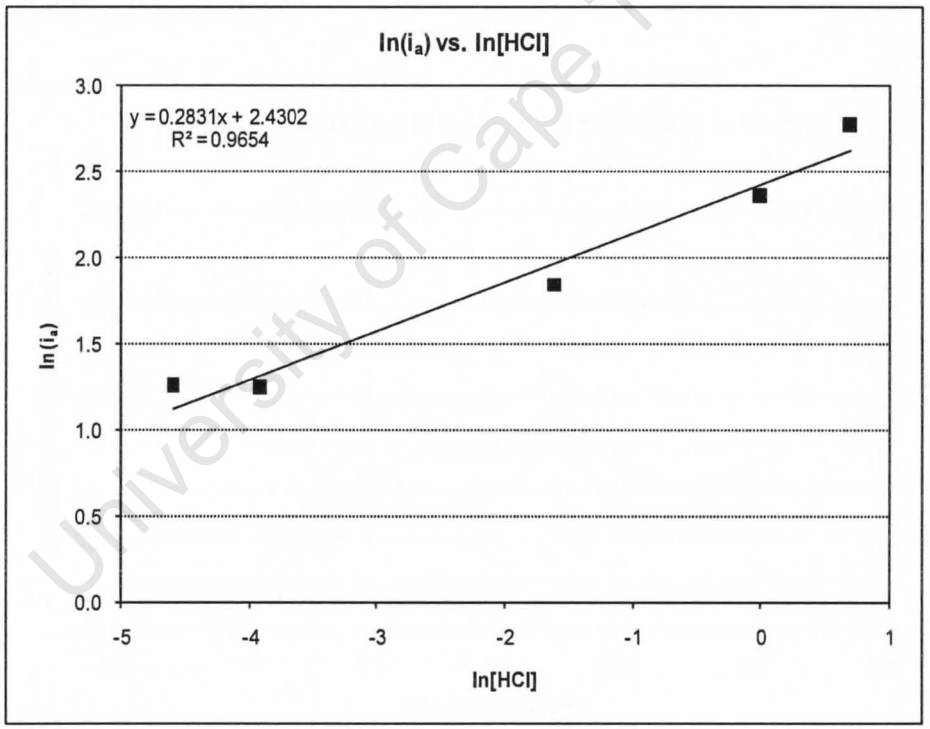

Figure 4.15 : The Relationship between Anodic Peak Current Density and Hydrochloric Acid Concentration

Linearization of the data shows that the order of the reaction with respect to [HCl] is about 0.3, which indicates that the reaction reigning at the first anodic peak at least falls in the realm of electrochemical processes.

4.2.7 The Effect of Copper Concentration

The effect of initial copper concentration on the anodic current density was tested over the range 0.05 g/L to 1 g/L for two acidic, chloride solutions. Figures 4.16 and 4.17 show the respective results for a 0.2 M H_2SO_4 + 0.2 M Cl^- (as NaCl) and a 0.2 M H_2SO_4 + 2 M Cl^- (as NaCl) solution. Also included in these figures are the corresponding results in the absence of additional copper (as $CuSO_4$), which are denoted by 0 g/L Cu.

Low Chloride Concentration

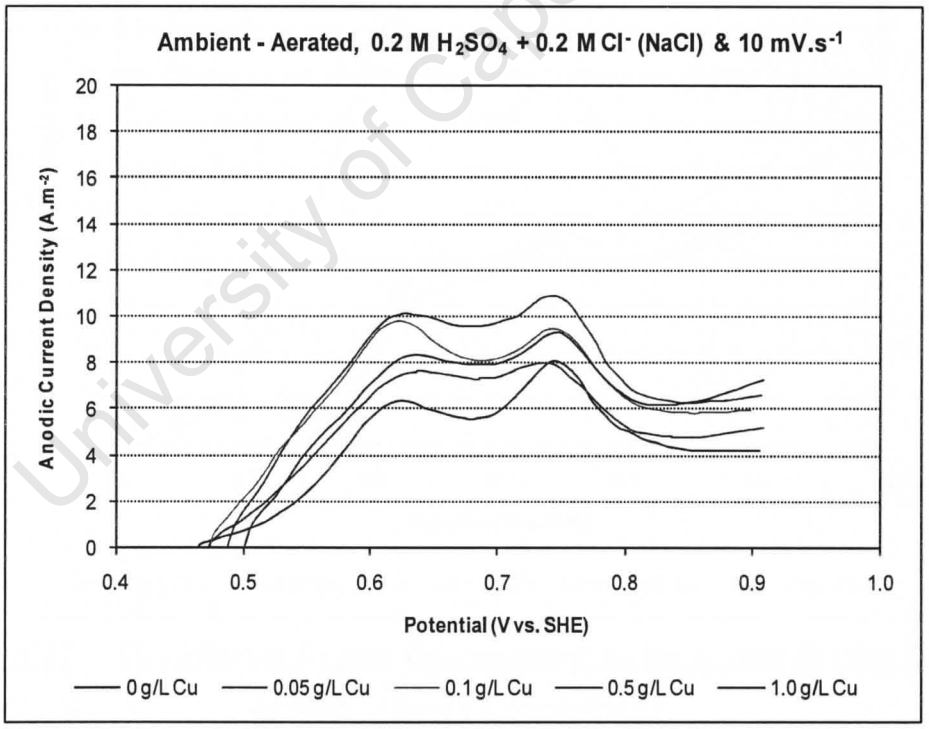

Figure 4.16 : The Effect of Copper Concentration on the Anodic Current Density at Low Chloride Concentration

It can be seen that the OCP shifts to slightly more positive values (from 0.461 V to 0.501 V) in the presence of copper ions and that the anodic current forms sharper intersections with the potential-axis over the range 0.05 g/L Cu to 1 g/L Cu. This phenomenon is characteristic of the mixed potential being established by the highly reversible Cu(II) / Cu(I) couple [33,41].

Furthermore, copper ions initially present also seem to result in somewhat higher anodic current densities as indicated by the measured peaks and steeper slopes, (for example over the potential range 0.5 V to 0.550 V), which indicates a positive effect on the rate of oxidation of the mineral electrode.

High Chloride Concentration

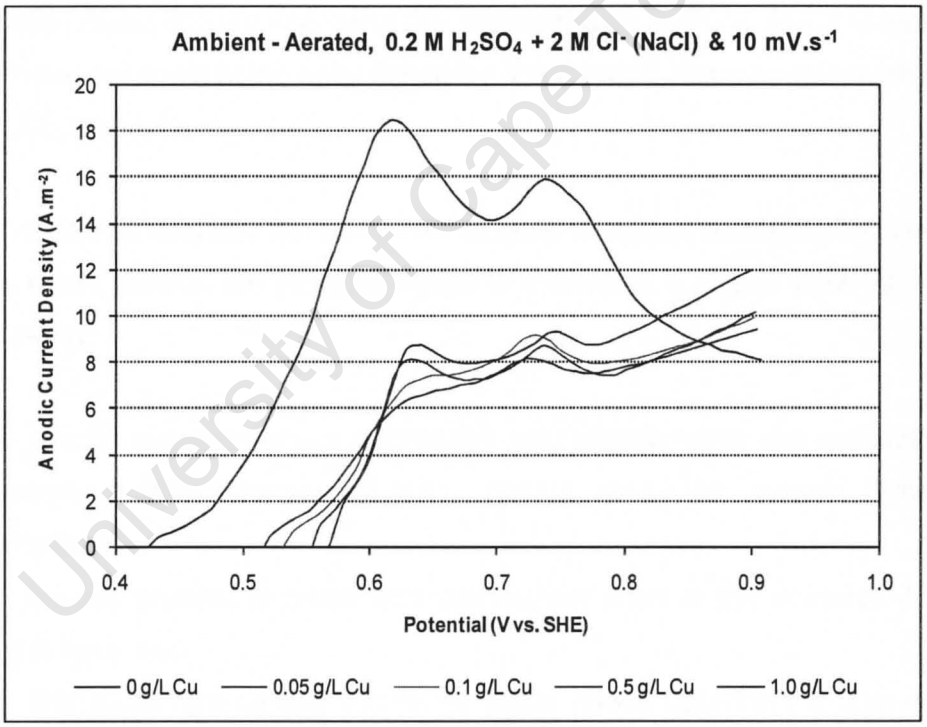

Figure 4.17 : The Effect of Copper Concentration on the Anodic Current Density at High Chloride Concentration

At high chloride concentration, the addition of copper (as $CuSO_4$) to the solution has a striking effect on the anodic response of the mineral electrode. Although the general shape of the voltammograms remains more or less the same as in the case of 0 g/L Cu, the current density is markedly smaller for copper concentrations ranging from 0.05 g/L to 1 g/L.

Both anodic peaks are still apparent and occur more or less at the same peak potentials as for 0 g/L Cu. However, the OCP shows a marked shift to more positive potentials (from 0.427 V to 0.568 V) as the copper concentration increases from 0.05 g/L to 1 g/L. Furthermore, it can also be seen that the slope of the current-potential curve increases with increased copper concentration (0.05 g/L to 1 g/L) over the range 0.5 V to 0.6 V.

Again, the anodic current intersects the potential-axis sharply, which is indicative of the mixed potential being established by a reversible redox couple such as the Cu(II) / Cu(I) couple.

Other notable differences for measureable concentrations of copper ions present initially, albeit outside the potential range of interest (i.e. above 0.62 V), include the following:

- The anodic current density decreases only slightly after the second peak, whereas in the absence of initial copper ions, the current decreases dramatically;
- The second plateau is much less pronounced than in the absence of initial copper ions, and
- The anodic current density increases again above potentials of about 0.8 V (i.e. after the second plateau), whereas the current in the absence of initial copper ions still decreases.

Low *versus* High Chloride Concentration

The effect of chloride concentration, in the presence of initial copper ions, is highlighted in Figure 4.18. This shows a comparison of the anodic current behaviour at low (0.2 M Cl^-) and high chloride concentration (2 M Cl^-) for a 0.2 M H_2SO_4 solution containing 1 g/L Cu (as $CuSO_4$).

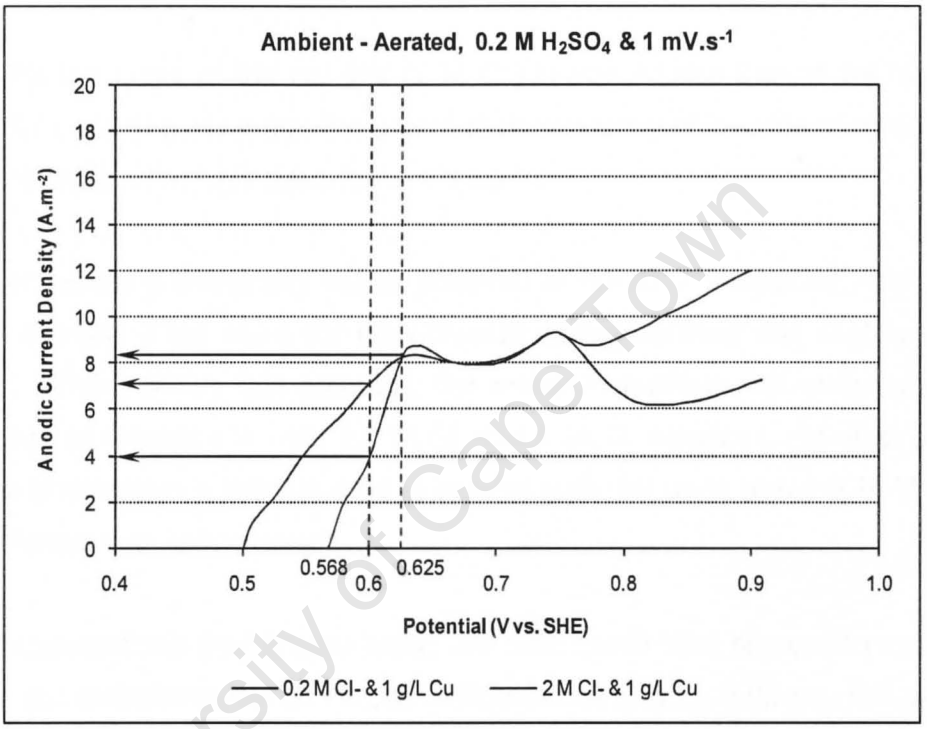

Figure 4.18 : A Comparison of the Anodic Current Density for Low and High Chloride Concentration in the Presence of Initial Copper Ions

A look at the potential range from the OCP to 0.625 V reveals some interesting findings. Firstly, it can be seen that the OCP of 0.5 V for the 0.2 M Cl^- solution is smaller than the value of 0.568 V at 2 M Cl^-. This implies that anodic oxidation of the mineral electrode will commence at lower potentials within low-chloride than high-chloride concentration solutions, in the presence of 1 g/L Cu.

In addition, at potentials where the mineral electrode can be oxidized in both low- and high chloride concentration solutions, the rate of oxidation will be faster in the low-chloride concentration solution if it is assumed that the contribution of other oxidation processes such as the oxidation of Cu(I) to Cu(II) ions is negligible. For example, when a potential of 0.6 V is applied to the mineral electrode's surface, the corresponding anodic current is 7 $A.m^{-2}$ for 0.2 M Cl^-, but only 4 $A.m^{-2}$ for 2 M Cl^-.

Secondly, the slope of the red line (2 M Cl^-) is about twice that of the blue line (0.2 M Cl^-), which means that the potential-dependency of the rate of oxidation is more pronounced at high chloride concentration.

However, when a marginally larger potential of 0.625 V is applied, the anodic current density is the same for both chloride concentrations and slightly above 8 $A.m^{-2}$. Thus, above this potential, the mineral electrode will experience the same rate of oxidation in both 0.2 M Cl^- and 2 M Cl^- solutions. In other words, the rate of oxidation is independent of applied potential up to about 0.75 V, when copper ions are initially present.

These observations (not shown here) are also made with respect to the other copper concentrations, which include: infinite small (0 g/L), 0.05 g/L, 0.1 g/L and 0.5 g/L. For the sake of brevity, only the effect of initial copper concentration on the OCP at low- and high chloride concentration is demonstrated in Figure 4.19.

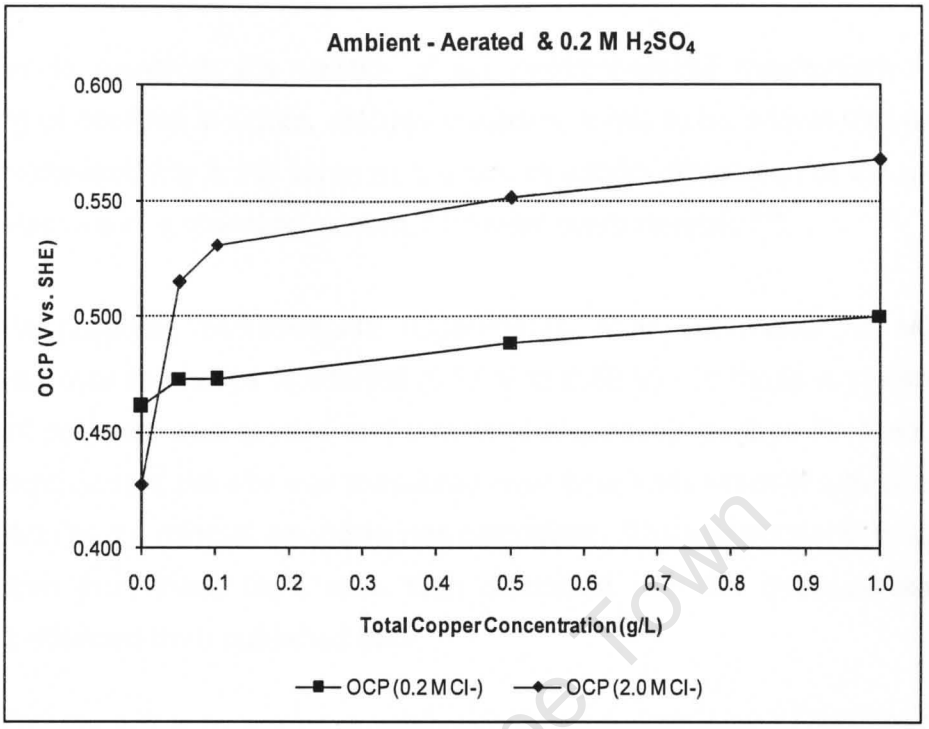

Figure 4.19 : The Effect of Initial Copper Concentration on the OCP at Low and High Chloride Concentration

4.3 Current Transient Measurements

In order to establish the validity of an electrochemical mechanism for the leaching of covellite in acidic, chloride solutions, it has to be shown that the rate of chemical leaching is the same as the rate of anodic dissolution of the mineral, in the absence of a chemical oxidant, at similar overpotentials [103].

For this purpose, potentiostatic experiments were conducted at selected potentials over the range of interest (0.55 V to 0.62 V). In these experiments a constant potential was applied to the mineral electrode's surface for 1 hour and the anodic current density was measured over time from which a rate of anodic dissolution of the mineral electrode was calculated. The electrochemical rates of dissolution from these tests were then compared with the chemical leaching kinetics obtained from published data.

4.3.1 The Effect of Potential on the Anodic Current Density

Figure 4.20 presents current transients for a stationary, Φ 1 mm covellite electrode in 0.2 M HCl at 25°C by applying a range of constant potentials to the mineral electrode's surface. These include: 0.540 V, 0.560 V, 0.580 V, 0.600 V, 0.620 V and 0.650 V.

It can be seen that when a potential is applied to the mineral electrode's surface, the anodic current increases quickly to a form a peak after 1 second. Thereafter, the current decreases rapidly over time and already reaches a very low value relative to that of the peak current after only 1 minute. For example, these constitute: 24% (0.540 V), 21% (0.560 V), 7% (0.580 V), 7% (0.600 V), 4% (0.620 V) and 4% (0.650 V) of the peak current. Surprisingly, these observations are very similar to those made by Lázaro-Báez in potentiostatic experiments on a pure chalcopyrite electrode in both acidic, sulphate (H_2SO_4) and acidic, chloride (HCl) solutions [10].

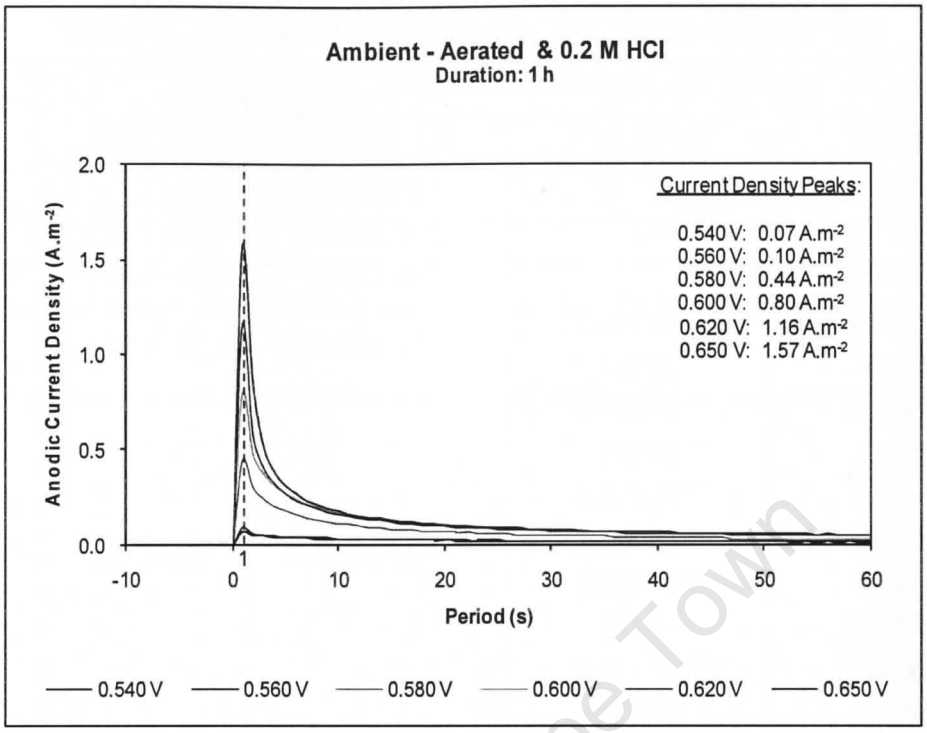

Figure 4.20 : Current Transients for Covellite in 0.2 M HCl at 25°C

Since negligible changes in the measured current density were observed after about 1 hour of operation, the 1-hour value was used to calculate a rate of anodic dissolution of the mineral electrode by assuming a two-electron process (Equation 4.4).

The measured anodic current densities and calculated rates of dissolution are listed in Table 4.5. These show a potential-dependency by increasing over the range 0.540 V to 0.650 V. Also included in this table are rates of chemical leaching of covellite obtained from the literature. Unfortunately, most of these studies were conducted at temperatures well above 25°C, which did not allow for a direct comparison to be made. Therefore, the measured rates of anodic dissolution (obtained in this study) were adjusted to the same temperature by application of the well-known Arrhenius equation [33,39,100] and using a reported value for the apparent activation energy of 77 kJ / mol [50].

Table 4.5 : Anodic Current Densities and Rates of Dissolution

E_m (V)	i_a ($A.m^{-2}$)	Rate of Dissolution (mol Cu $cm^{-2}.s^{-1}$)		
		This Study (25°C)	This Study (T°C)	Literature (T°C)
0.540	1.04×10^{-3}	5.38×10^{-13}	-	-
0.560	1.35×10^{-3}	7.00×10^{-13}	-	-
0.580	1.38×10^{-3}	7.13×10^{-13}	1.95×10^{-12} (35°C)	4.86×10^{-12} (35°C) [19]
0.600	3.21×10^{-3}	1.66×10^{-12}	2.10×10^{-10} (80°C) 3.02×10^{-10} (85°C) 4.32×10^{-10} (90°C) 6.10×10^{-10} (95°C)	5.35×10^{-10} (80°C) [50] 8.39×10^{-10} (85°C) [50] 1.13×10^{-9} (90°C) [50] 1.48×10^{-9} (95°C) [50]
0.620	3.27×10^{-3}	1.69×10^{-12}	-	-
0.636	-	-	-	6.61×10^{-12} (35°C) [19]
0.650	4.91×10^{-3}	2.55×10^{-12}	1.15×10^{-9} (98°C) 6.98×10^{-12} (35°C) 1.15×10^{-9} (98°C)	B: 1.65×10^{-9} (98°C) [49] K: 8.11×10^{-12} (35°C) [49] K: 3.71×10^{-9} (98°C) [49]
0.700	7.67×10^{-3}	3.97×10^{-12}	1.79×10^{-9} (98°C) 1.09×10^{-11} (35°C) 1.79×10^{-9} (98°C)	B: 1.65×10^{-9} (98°C) [49] K: 8.11×10^{-12} (35°C) [49] K: 3.71×10^{-9} (98°C) [49]

1) Detailed experimental conditions can be found in 2.4.3 Kinetics of Dissolution, Table 2.4.6, p. 53; B = Butte sample, K = Kennecott N° 2 sample.
2) The mixed potentials for [49,50] were estimated from solution conditions with a minimum (0.650 V) and a maximum (0.700 V) for [49].

Velásquez conducted a leaching test on fine-milled, synthetic covellite in a 0.2 M HCl + 0.5 g/L Cu (as $CuSO_4$) solution at 35°C, where the solution potential was controlled at about 0.580 V. A rate of dissolution of covellite of 4.86×10^{-12} mol Cu $cm^{-2}.s^{-1}$ was calculated from her data [19]. Although the solution potential as measured by a platinum electrode is not the mixed potential, it had been found (by measurement) that the latter was very similar to this value (0.580 V) under these conditions.

Although Cheng and Lawson did not report any potentials in their study on the leaching of fine-milled, synthetic covellite in 0.5 M H_2SO_4 + 0.5 M Cl^- (as NaCl), it is not unreasonable to expect that the mixed potential was in the vicinity of 0.6 V under their conditions [50]. Rates of dissolution of covellite, which ranged from 5.35×10^{-10} mol Cu $cm^{-2}.s^{-1}$ (80°C) to 1.48×10^{-9} mol Cu $cm^{-2}.s^{-1}$ (95°C), were calculated from their data.

In one of the earliest studies on the leaching behaviour of covellite in acidic, sulphate solutions, Sullivan also reported leaching results obtained in 0.18 M $FeCl_3$ + 0.14 M HCl (35°C) and 0.36 M $FeCl_3$ + 0.14 M HCl (98°C) with respect to two natural covellite samples, namely the Butte (B) and Kennecott N° 2 (K) samples [49]. The leaching kinetics calculated for these two samples are compared with the electrochemical kinetics at potentials of both 0.650 V and 0.700 V since it is likely that the mixed potential may have fallen in this region.

Thus, from Table 4.5, it can be seen that the rates of anodic dissolution (obtained in this study) are in fair agreement with the rates of chemical leaching of covellite (from the literature) at corresponding mixed potentials and temperatures. This presents evidence that the leaching of covellite in acidic, chloride solutions occur indeed according to an electrochemical mechanism in the presence of an oxidant.

An experiment was conducted to investigate whether the behaviour of the mineral electrode shown in Figure 4.20 was reversible. In other words, it was investigated whether the same peak response would be achieved on a subsequent potential application. The results of this experiment are shown in Figure 4.21.

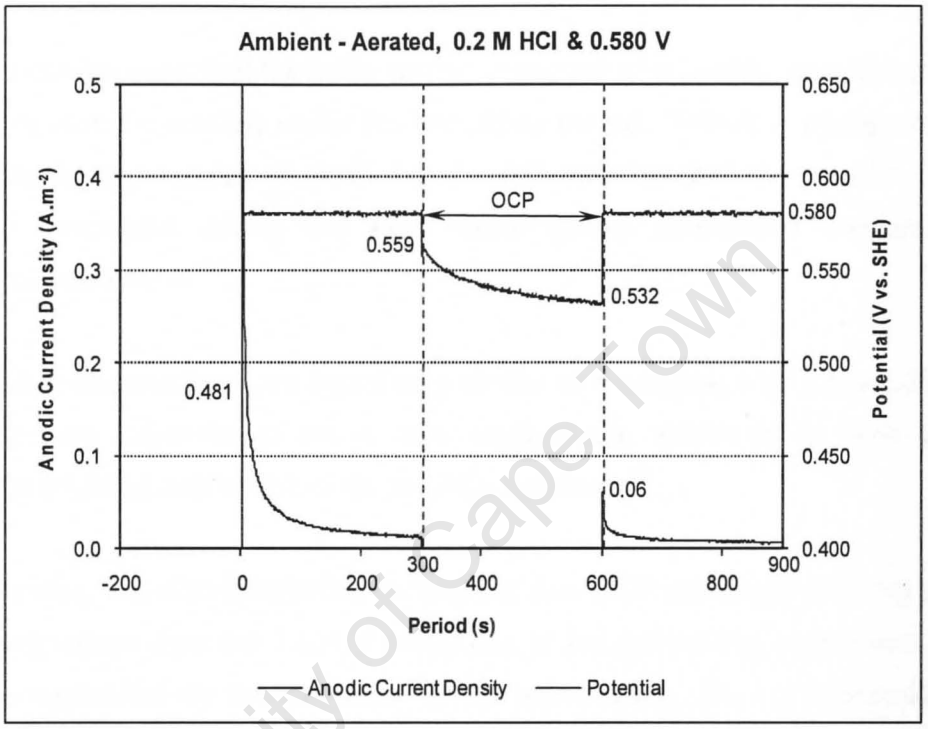

Figure 4.21 : Consecutive Current Transients for Covellite in 0.2 M HCl at 25°C

Initially, the mineral electrode was maintained under open circuit conditions for 3 minutes before a potential was applied to its surface. On application of 0.580 V, the anodic current density peaked at 0.495 $A.m^{-2}$ after 1 second with rapid current-decay thereafter. For example, a value of only 0.013 $A.m^{-2}$ was measured after 5 minutes. Immediately thereafter, the mineral electrode was maintained under open circuit conditions for a period of 5 minutes before a second application of 0.580 V was made. Once again the anodic current density peaked after only 1 second, but at a much smaller value of 0.060 $A.m^{-2}$.

Not shown (in Figure 4.21) is a third application of 0.580 V, which resulted in more or less the same peak current density of 0.051 $A.m^{-2}$ as was obtained for the second application; however, the mineral electrode was maintained at 15 minutes on OCP. Even when the mineral electrode was left under open circuit for 30 minutes, a fourth application of 0.580 V yielded a peak current density of only 0.038 $A.m^{-2}$.

Thus, it can be seen that the initial anodic response of a freshly, polished mineral electrode is not reversible under the conditions tested. This is in agreement with the voltammetry results of Ghali *et al.*, who showed that the anodic current density measured during the first linear sweep decreased markedly for subsequent sweeps [105].

The above observations are again very similar to those made by Lázaro-Báez in potentiostatic experiments on a pure chalcopyrite electrode in both acidic, sulphate (H_2SO_4) and acidic, chloride (HCl) solutions [10].

Furthermore, it is also interesting to note that the OCP increases to more anodic (positive) values than the 0.481 V measured at the start of the experiment. This can be explained by the presence of an infinitesimal, small concentration of copper ions, which raises the OCP (mixed potential) due to the interaction of the Cu(II) / Cu(I) couple with the mineral electrode's surface.

4.3.2 The Effect of Chloride Concentration on the Anodic Current Density

Cyclic voltammetry showed that chloride concentration had the most pronounced effect on the anodic current density of the mineral electrode. Therefore, it was decided to investigate this parameter also in potentiostatic experiments over a longer period (1 h).

The anodic current transients for 0.2 M HCl and 0.2 M HCl + 1.8 M Cl^- (as NaCl), which were generated at an applied potential of 0.600 V and 25°C, are compared in Figure 4.22 over the first minute of operation.

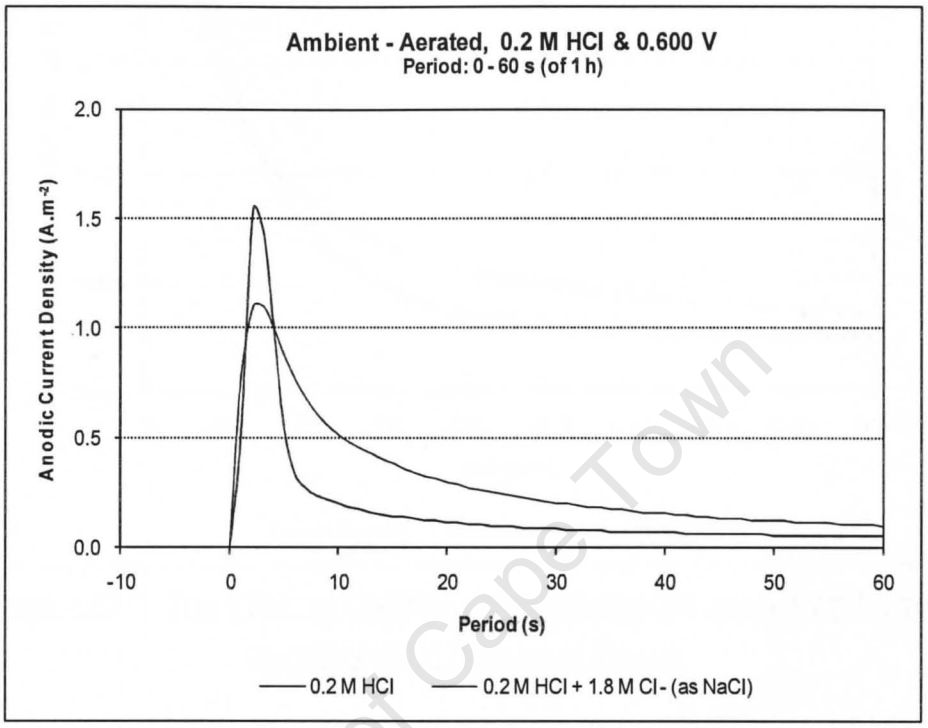

Figure 4.22 : The Effect of Chloride Concentration on the Anodic Current Density over a Short Period

These show anodic peak current densities of 1.55 $A.m^{-2}$ and 1.10 $A.m^{-2}$ for the 0.2 M Cl^- and 2 M Cl^- solutions, respectively. Thereafter, the current decays rapidly for both solutions, but somewhat more so in the case of the 0.2 M Cl^- solution. For example, the respective current densities after 1 minute of operation are: 0.051 $A.m^{-2}$ (0.2 M Cl^-) and 0.10 $A.m^{-2}$ (2 M Cl^-).

Another view of the anodic current densities for the two solutions up to a period of 1 h is portrayed in Figure 4.23.

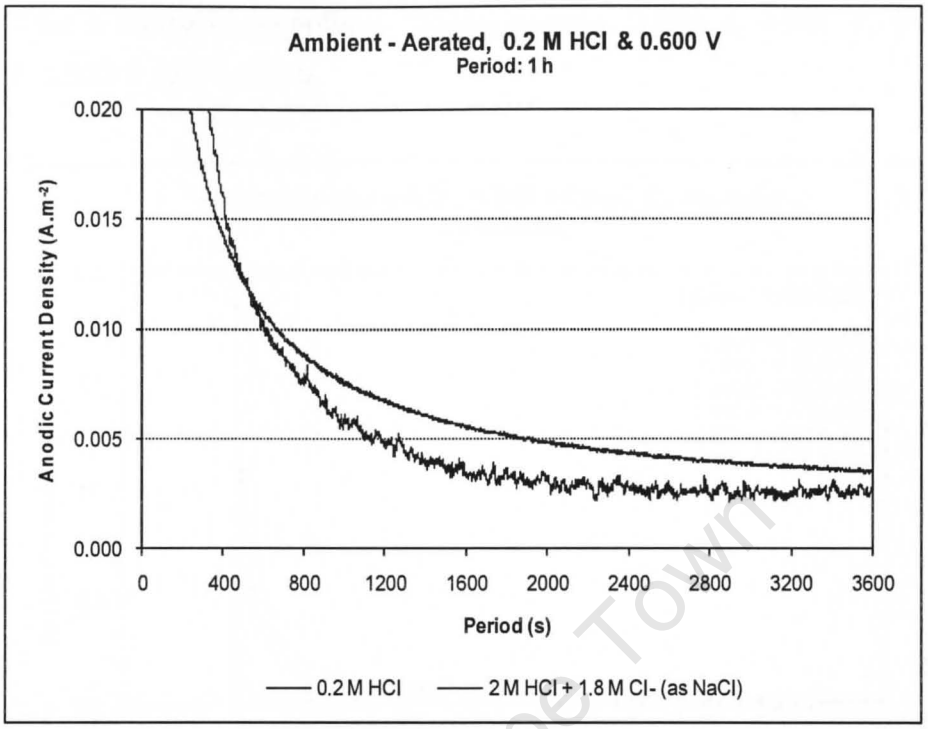

Figure 4.23 : The Effect of Chloride Concentration on the Anodic Current Density over a Prolonged Period

It can be seen that the positive effect of increased chloride ion concentration on the measured current density appears to be restricted to the initial stages of operation only.

4.3.3 The Effect of Copper Concentration on the Anodic Current Density

Cyclic voltammetry tests have shown that the presence of copper ions also affect the anodic current density. Therefore, potentiostatic experiments were executed in which this effect was investigated over a longer duration (1 h).

Figure 4.24 presents the results achieved in 0.2 M HCl + 0.5 g/L Cu (as $CuSO_4$) at 25°C for a range of potentials. These include: 0.540 V, 0.560 V, 0.580 V, 0.600 V, 0.620 V and 0.650 V.

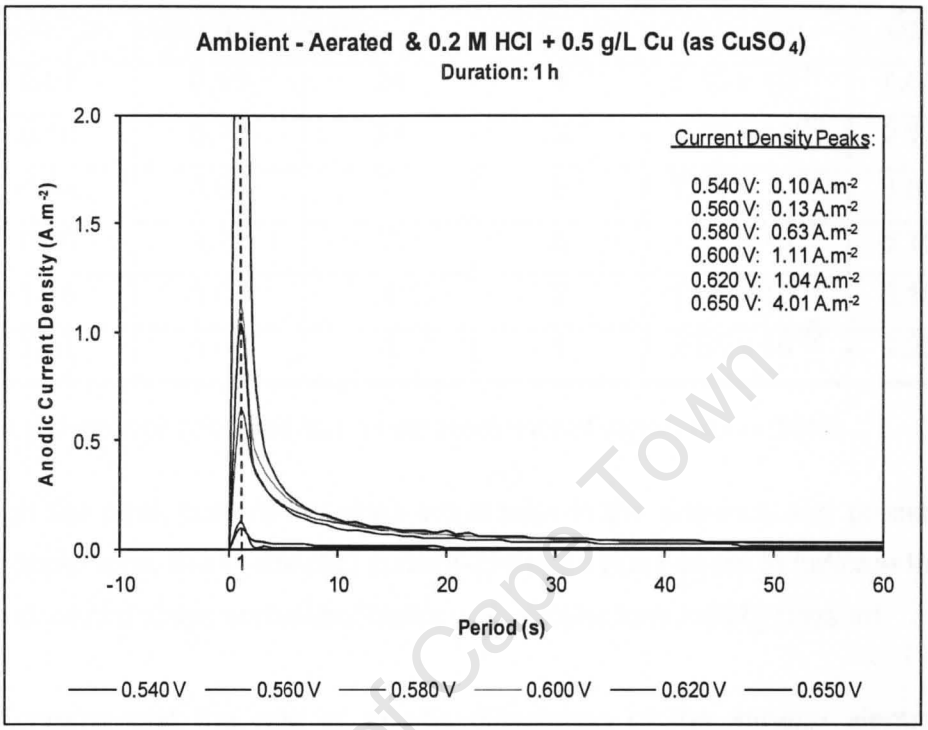

Figure 4.24 : Current Transients for Covellite in 0.2 M HCl + 0.5 g/L Cu (as $CuSO_4$) at 25°C

Again, the anodic current density increases quickly to form a peak after 1 second with rapid current-decay thereafter. For example, the current relative to the peak value after only 1 minute of operation constitutes: 9% (0.540 V), 3% (0.560 V), 5% (0.580 V), 3% (0.600 V), 2% (0.620 V) and 1% (0.650 V), respectively.

A comparison of the peak current densities, (1-minute) current-to-peak values and rates of anodic dissolution is made in Table 4.6 for a 0.2 M HCl solution, in the absence and presence of initial copper ions.

Table 4.6 : Anodic Peak Current Densities, Current-to-Peak Percentages and Rates of Dissolution

E_m (V)	i_p ($A.m^{-2}$)		$i_{a\ (1\ min)} / i_p$ (%)		Rate of Dissolution (mol Cu $cm^{-2}.s^{-1}$) [1]	
	0 g/L Cu	0.5 g/L Cu	0 g/L Cu	0.5 g/L Cu	0 g/L Cu	0.5 g/L Cu
0.540	0.07	0.10	24	9	5.38×10^{-13}	7.53×10^{-14}
0.560	0.10	0.13	21	3	7.00×10^{-13}	2.12×10^{-13}
0.580	0.44	0.63	7	5	7.13×10^{-13}	3.51×10^{-13}
0.600	0.80	1.11	7	3	1.66×10^{-12}	5.75×10^{-13}
0.620	1.16	1.04	4	2	1.69×10^{-12}	8.19×10^{-13}
0.650	1.57	4.01	4	1	2.55×10^{-12}	9.23×10^{-13}

1) Rate of dissolution calculated from 1-hour anodic current density values (25°C)

Although the peak current densities are similar in the absence and presence of initial copper ions, the (1-minute) current-to-peak values seem to indicate that the anodic current decays somewhat faster with copper ions initially present.

It also seems that the rate of anodic dissolution of the mineral electrode is somewhat lower in the presence of initial copper ions. Although this is not clear from the voltammetry results at low chloride concentration (Figure 4.16), the above observation is consistent with the voltammetry results at high chloride concentration, which indicated a marked decrease in the measured current with the addition of initial copper ions (Figure 4.17).

4.4 A Summary of the Experimental Results

A summary of the more general observations and findings are presented in this section, which will be used in aid to propose a mechanism for the leaching of covellite in acidic, chloride media (in the absence of ferric ions). These include the following:

Cyclic Voltammetry

- The anodic current density increases when an increasing potential is applied to a stationary covellite surface from the OCP of the mineral electrode to a potential corresponding to the first anodic peak. For example, in a pre-aerated, 0.2 M HCl solution (without initial copper ions present) this range spans 0.461 V to 0.625 V at 25°C.

- The covellite electrode shows typical active-passive behaviour in acidic, chloride solutions. In other words, over some ranges the anodic current density is potential-dependent (active), whereas over other ranges it is potential-independent (passive). For example, within a pre-aerated, 0.2 M HCl solution (without initial copper ions present) evidence of passive behaviour is observed at potentials above 0.625 V.

- The processes reigning at the first and second anodic peaks are irreversible and not mass transport controlled. Therefore, these have to be chemically (or electrochemically) controlled.

- In the absence of initial copper ions and at constant chloride concentration, an increase in acidity by means of sulphuric acid concentration seems to increase the anodic current density.

- The source of acidity has no significant effect on the anodic current density.

- The addition of sodium sulphate has no effect on the anodic current density.

- In the absence of initial copper ions, the addition of chloride as sodium chloride has a marked effect on the anodic current density, which increases with increased chloride ion concentration up to 1 M in a pre-aerated, 0.2 M H_2SO_4 solution. However, above this concentration no further increase in anodic current density is achieved.

- In the absence of initial copper ions, an increase in hydrochloric acid concentration also results in an increase in the anodic current density. At high chloride concentration (1 M and above), the first anodic peak becomes less pronounced than the second as the acidity is increased over the range 0.2 M to 2 M.

- Only one anodic peak is observed in the absence of chloride ions, which occurs in the vicinity of 0.6 V for a pre-aerated, 0.2 M H_2SO_4 solution.

- At low chloride concentration (0.2 M), an increase in initial copper concentration increases the OCP. Also, the anodic current densities measured in the presence of copper ions seem larger than in absence thereof. For example, with copper ions initially present, both anodic peaks are higher and the slopes of the anodic current density curves are all steeper over the same potential range (0.5 V to 0.550 V).

- At high chloride concentration (2 M), an increase in initial copper concentration increases the OCP. However, copper ions initially present result in markedly lower anodic current densities, which seem to indicate a negative effect on the rate of oxidation of the mineral electrode.

- The OCP increases with increased chloride concentration at the same initial copper concentration.

- Over the potential range up to the first anodic peak (0.625 V), the rate of oxidation of the mineral electrode, as indicated by the anodic current density, is greater in a low-chloride solution (0.2 M) than in a high-chloride solution (2 M), at the same potential. However, the potential-dependency of the rate of oxidation is more pronounced at the higher chloride concentration and, at potentials in excess of the first anodic peak (0.625 V), the rates of oxidation for both chloride concentrations are more or less the same.

Potentiostatic Tests

- Rates of anodic dissolution of the mineral electrode, which were obtained from potentiostatic experiments (in this study), are in fair agreement with the rates of chemical leaching of covellite (from literature) at corresponding mixed potentials and temperatures. This presents evidence that the leaching of covellite in acidic, chloride solutions occur according to an electrochemical mechanism in the presence of a chemical oxidant.

- The initial anodic response of a freshly, polished mineral electrode to an applied potential is not reversible under the conditions tested.

- The positive effect that an increased chloride concentration has on the anodic current density when the mineral electrode is subjected to a constant potential of 0.6 V (in the absence of initial copper ions) seems to be restricted to the initial stages of operation only. In other words, over prolonged times, the measured anodic current density is more or less the same at low (0.2 M) and high chloride concentration (2 M).

- The presence of initial copper ions seems to have a negative effect on the anodic current density over the potential range 0.540 V to 0.650 V.

4.5 The Mechanisms of Leaching of Covellite in Acidic, Chloride Media

4.5.1 Dissolution of Covellite by Direct Oxidation

It has been shown in this study that the oxidative dissolution of covellite in acidic, chloride solutions is an electrochemical process. Also, that the anodic dissolution of the mineral may proceed (from a thermodynamic point of view) according to either one of the half-cell reactions presented in Equations 4.3 and 4.4. This would entail a direct oxidative mechanism via either a one-electron (Equation 4.3) or a two-electron anodic process (Equation 4.4).

In both these reaction mechanisms, the cupric ion (as primary oxidant) has to diffuse through a growing, elemental sulphur layer to the mineral's surface where electron transfer takes place involving the reduction of cupric to cuprous ions. Also, in both cases, elemental sulphur is a product of the anodic dissolution of the mineral and could well be termed "anodic sulphur", which is formed directly on the surface of the mineral.

Cuprous ions, which are produced by either the anodic dissolution of the mineral itself (one-electron process) or by the reduction of cupric ions at the mineral surface (one- and two-electron processes), are oxidized back to cupric ions by dissolved oxygen in the so-called back-oxidation reaction. In order for this to occur, cuprous ions, dissolved oxygen and protons need to be in contact with each other.

It is proposed that the rate-controlling step, at least during the initial stages of leaching, is the anodic dissolution of the mineral (Equations 4.3 or 4.4). This is supported by the fact that published values for the apparent activation energy well exceed 40 $kJ.mol^{-1}$ (see 2.4.3 Kinetics of Dissolution), which indicates that the rate of dissolution of covellite shows a relatively strong temperature-dependency [33]. Of course, the growing or thickening sulphur layer may eventually affect diffusional transport of aqueous species to and from the mineral surface. In addition, it may also decrease the available surface area for leaching, which may, in part, explain the levelling-off of the copper dissolution profile observed during the latter stages of leaching.

Finally, it will be shown that both these mechanistic schemes render the same overall reaction (Equation 4.6) for the direct oxidative dissolution of covellite in acidic, chloride solutions.

One-Electron Process

Anodic:

$$CuS = Cu(I) + S^\circ + e^- \quad (4.3)$$

Cathodic:

$$Cu(II) + e^- = Cu(I) \quad (4.5)$$

$$\Sigma \; CuS + Cu(II) \rightarrow 2Cu(I) + S^\circ \quad (4.1)$$

Back-Oxidation:

$$2Cu(I) + 2H^+ + \tfrac{1}{2}O_2 \rightarrow 2Cu(II) + H_2O \quad (4.2)$$

Overall:

$$CuS + 2H^+ + \tfrac{1}{2}O_2 \rightarrow Cu(II) + S^\circ + H_2O \quad (4.6)$$

Figure 4.25 illustrates the above reaction mechanism schematically.

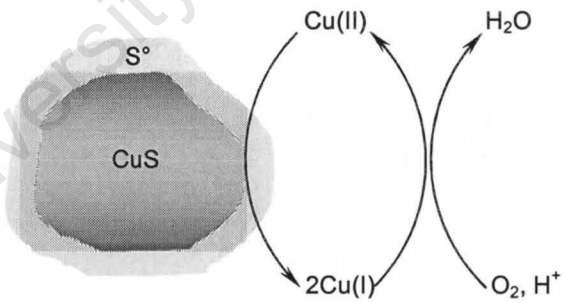

Figure 4.25 : A Schematic Diagram of the Direct Oxidation of Covellite via a One-Electron Anodic Process

For this reaction mechanism, the Butler-Volmer relationships for the mixed potential (E_m) and the rate of dissolution of the mineral (r_{CuS}) are shown below. A detailed derivation is presented in Appendix III.

$$E_m = \left(\frac{RT}{F}\right) \ln \left\{ \frac{k_{Cu(II)}[Cu(II)]}{k_{CuS} + k_{Cu(I)}[Cu(I)]} \right\} \tag{4.7}$$

$$r_{CuS} = \frac{i_{CuS}}{F} \tag{4.8}$$

$$= k_{CuS} \left\{ \frac{k_{Cu(II)}[Cu(II)]}{k_{CuS} + k_{Cu(I)}[Cu(I)]} \right\}^{1/2}$$

Case I

In the case of a large cuprous ion concentration and / or a very slow rate of mineral dissolution, it follows that $k_{CuS} << k_{Cu(I)}[Cu(I)]$; therefore,

$$E_m = \left(\frac{RT}{F}\right) \ln \left(\frac{k_{Cu(II)}[Cu(II)]}{k_{Cu(I)}[Cu(I)]} \right) \tag{4.9}$$

$$r_{CuS} = \frac{i_{CuS}}{F} \tag{4.10}$$

$$= k_{CuS} \left(\frac{k_{Cu(II)}[Cu(II)]}{k_{Cu(I)}[Cu(I)]} \right)^{1/2}$$

$$= k \left(\frac{[Cu(II)]}{[Cu(I)]} \right)^{1/2}$$

With:

$$k = k_{CuS} \left(\frac{k_{Cu(II)}}{k_{Cu(I)}} \right)^{1/2} \tag{4.11}$$

[Cu(II)] Cupric ion concentration at the mineral surface

[Cu(I)] Cuprous ion concentration at the mineral surface

E_m Mixed potential

i_{CuS} Anodic current density for covellite dissolution

k_{CuS} Electrochemical rate constant for the anodic dissolution of the mineral by a one-electron process (Equation 4.3)

$k_{Cu(I)}$ Electrochemical rate constant for the anodic half-cell reaction (Equation 4.5)

$k_{Cu(II)}$ Electrochemical rate constant for the cathodic half-cell reaction (Equation 4.5)

k Proportionality constant

r_{CuS} Rate of dissolution of covellite

Equation 4.10 predicts the rate of mineral dissolution to show a half-order dependency with respect to the cupric-to-cuprous ion ratio. Therefore, a plot of $\ln(r_{CuS})$ against $\ln([Cu(II)]/[Cu(I)])$ should render a straight line with a positive slope of 0.5 and y-intercept of ln(k) according to:

$$\ln(r_{CuS}) = \ln k + {}^1/_2 \ln\left(\frac{[Cu(II)]}{[Cu(I)]}\right) \qquad (4.12)$$

Table 4.7 : Electrochemical Data for the 0.2 M HCl + 0.5 g/L Cu Solution

E_m (V)	E_h [1] (V)	[Cu(II)] (x 10^{-3} M)	[Cu(I)] (x 10^{-5} M)	i_a ($A.m^{-2}$)	r_{CuS} [2] (mol Cu $cm^{-2}.s^{-1}$)
0.560	0.568	7.845	2.282	0.00041	2.12×10^{-13}
0.580	0.591	7.859	0.9442	0.00068	3.51×10^{-13}
0.600	0.614	7.864	0.3934	0.00111	5.75×10^{-13}
0.620	0.637	7.867	0.1553	0.00158	8.19×10^{-13}

1) Capillary solution potential values from which cupric and cuprous ion concentrations were calculated with the aid of the NIST database [40]
2) Rate of dissolution calculated from 1-hour anodic current density values (25°C)

The data of Table 4.7 were used to generate such a plot, which is presented in Figure 4.26.

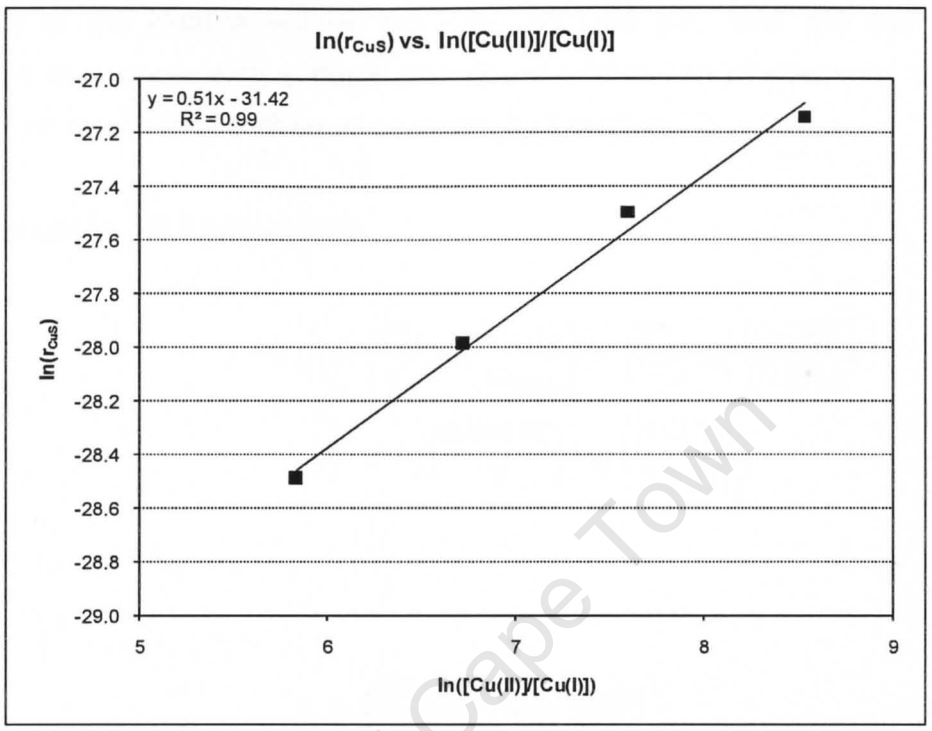

Figure 4.26 : The Effect of Cupric-to-Cuprous Ion Ratio on the Rate of Dissolution of Covellite

The experimental data depict a straight line with a slope of 0.51, which suggests a 0.51'th order rate-dependency on the cupric-to-cuprous ion ratio. This is in excellent agreement with the theoretical value of 0.5.

From Figure 4.26 it can be seen that the y-intercept is -31.42. Then, from Equation 4.11 it follows that:

$$k = k_{CuS}\left(\frac{k_{Cu(II)}}{k_{Cu(I)}}\right)^{1/2} \qquad (4.11)$$

$$= 2.26 \times 10^{-14} \text{ mol Cu cm}^{-2}.\text{s}^{-1}$$

Equation 4.10 also predicts that for a constant cupric-to-cuprous ion ratio (in other words solution potential) the mineral will show, at least during the initial stages of leaching, linear kinetics of dissolution. However, it is expected that the linearity of the kinetics will be adversely affected (i.e. level off) over time, because of a decreasing surface area due the formation of elemental sulphur directly on the mineral surface as predicted by Equation 4.3.

From Equation 4.9 it follows that:

$$E_m = \left(\frac{RT}{F}\right)\ln\left(\frac{k_{Cu(II)}}{k_{Cu(I)}}\right) + \left(\frac{RT}{F}\right)\ln\left(\frac{[Cu(II)]}{[Cu(I)]}\right) \qquad (4.13)$$

$$= k' + \left(\frac{2.303RT}{F}\right)\log\left(\frac{[Cu(II)]}{[Cu(I)]}\right)$$

With:

$$k' = \left(\frac{2.303RT}{F}\right)\log\left(\frac{k_{Cu(II)}}{k_{Cu(I)}}\right) \qquad (4.14)$$

k' Proportionality constant

R Universal gas constant, 8.31441 $J.mol^{-1}.K^{-1}$

T Temperature, 298.15 K

A plot of the mixed potential (E_m) against log([Cu(II)]/[Cu(I)] should render a straight line with:

$$\text{slope} = \left(\frac{2.303RT}{F}\right) \qquad (4.15)$$

$$= 0.059\ \text{V.decade}^{-1}$$

Equation 4.15 predicts that the mixed potential (E_m) should vary by 0.059 $V.decade^{-1}$ change of the cupric-to-cuprous ion ratio at the mineral surface.

A plot of E_m against log([Cu(II)]/[Cu(I)] for the experimental data listed in Table 4.7 is presented in Figure 4.27.

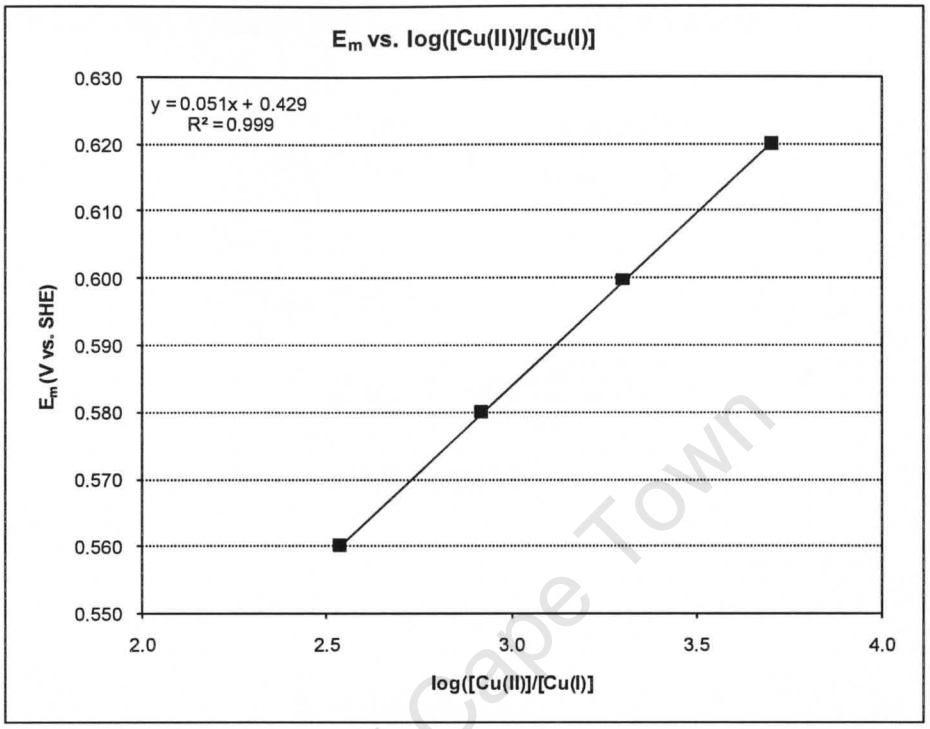

Figure 4.27 : The Effect of Cupric-to-Cuprous Ion Ratio on the Mixed Potential

The results show that the dependence of the cupric-to-cuprous ion ratio on the mixed potential (E_m) is 0.051 V.decade^{-1}. This is in very good agreement with the theoretical value of 0.059 V.decade^{-1}.

Substitution of the y-intercept of 0.429 into Equation 4.11 yields:

$$\frac{k_{Cu(II)}}{k_{Cu(I)}} = 1.83 \times 10^{7} \qquad (4.16)$$

$$k_{CuS} = 5.28 \times 10^{-18} \text{ mol Cu cm}^{-2}.\text{s}^{-1} \qquad (4.17)$$

Case II

In the case of a very small cuprous ion concentration and / or a very fast rate of mineral dissolution, it follows that $k_{CuS} >> k_{Cu(I)}[Cu(I)]$; therefore,

$$E_m = \left(\frac{RT}{F}\right) \ln\left\{\frac{k_{Cu(II)}[Cu(II)]}{k_{CuS}}\right\} \quad (4.18)$$

$$r_{CuS} = \frac{i_{CuS}}{F} \quad (4.19)$$

$$= k_{CuS}\left\{\frac{k_{Cu(II)}[Cu(II)]}{k_{CuS}}\right\}^{1/2}$$

$$= k'[Cu(II)]^{1/2}$$

With:

$$k' = \left(k_{CuS}k_{Cu(II)}\right)^{1/2} \quad (4.20)$$

k' Proportionality constant

Unfortunately, no steady state data were generated by potentiostatic tests that would allow this to be tested. Only cyclic voltammetry data are available, but these are not steady; therefore, considered unsuitable to use.

In contrast to the linear kinetics of dissolution expected for Case I, the mineral is expected to show parabolic kinetics from the onset of leaching for Case II, even at constant solution potential (see Equation 4.19). Elemental sulphur is also expected to form directly on the surface of the mineral as predicted by Equation 4.3.

Two-Electron Process

Anodic:

$$CuS = Cu(II) + S^\circ + 2e^- \quad (4.4)$$

Cathodic:

$$2Cu(II) + 2e^- = 2Cu(I) \quad (4.5)$$

$$\Sigma \; CuS + Cu(II) \rightarrow 2Cu(I) + S^\circ \quad (4.1)$$

Back-Oxidation:

$$2Cu(I) + 2H^+ + \tfrac{1}{2}O_2 \rightarrow 2Cu(II) + H_2O \quad (4.2)$$

Overall:

$$CuS + 2H^+ + \tfrac{1}{2}O_2 \rightarrow Cu(II) + S^\circ + H_2O \quad (4.6)$$

Figure 4.28 presents a schematic diagram of this reaction mechanism.

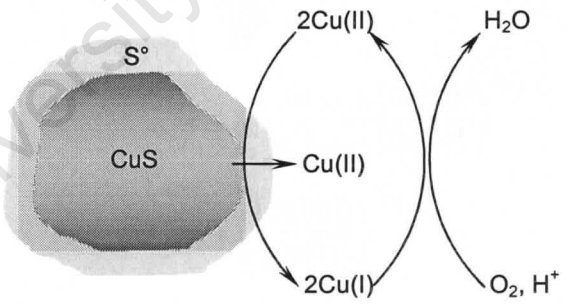

Figure 4.28 : A Schematic Diagram of the Direct Oxidation of Covellite via a Two-Electron Anodic Process

The Butler-Volmer relationships for the mixed potential (E_m) and the rate of dissolution of the mineral (r_{CuS}) for the two-electron anodic process are shown below. A detailed derivation can be found in Appendix IV.

$$E_m = \left(\frac{RT}{F}\right) \ln\left\{\frac{k_{Cu(II)}[Cu(II)]}{2k_{CuS} + k_{Cu(I)}[Cu(I)]}\right\} \tag{4.21}$$

$$r_{CuS} = \frac{i_{CuS}}{2F} \tag{4.22}$$

$$= k_{CuS}\left\{\frac{k_{Cu(II)}[Cu(II)]}{2k_{CuS} + k_{Cu(I)}[Cu(I)]}\right\}^{1/2}$$

Case I

In the case of large cuprous ion concentrations and / or very slow rates of mineral dissolution, it follows that $2k_{CuS} << k_{Cu(I)}[Cu(I)]$; therefore,

$$E_m = \left(\frac{RT}{F}\right) \ln\left(\frac{k_{Cu(II)}[Cu(II)]}{k_{Cu(I)}[Cu(I)]}\right) \tag{4.23}$$

$$r_{CuS} = \frac{i_{CuS}}{2F} \tag{4.24}$$

$$= k_{CuS}\left(\frac{k_{Cu(II)}[Cu(II)]}{k_{Cu(I)}[Cu(I)]}\right)^{1/2}$$

$$= k\left(\frac{[Cu(II)]}{[Cu(I)]}\right)^{1/2}$$

With:

$$k = k_{CuS}\left(\frac{k_{Cu(II)}}{k_{Cu(I)}}\right)^{1/2} \tag{4.25}$$

Case II

In the case of a very small cuprous ion concentrations and / or very fast rates of mineral dissolution, it follows that $k_{CuS} >> k_{Cu(I)}[Cu(I)]$; therefore,

$$E_m = \left(\frac{RT}{F}\right) \ln\left\{\frac{k_{Cu(II)}[Cu(II)]}{2k_{CuS}}\right\} \tag{4.26}$$

$$\begin{aligned} r_{CuS} &= \frac{i_{CuS}}{2F} \\ &= k_{CuS}\left\{\frac{k_{Cu(II)}[Cu(II)]}{2k_{CuS}}\right\}^{1/2} \\ &= k''[Cu(II)]^{1/2} \end{aligned} \tag{4.27}$$

With:

$$k'' = \left(1/2\, k_{CuS} k_{Cu(II)}\right)^{1/2} \tag{4.28}$$

k'' Proportionality constant

From the Butler-Volmer relationships for these two cases it is evident that the same conclusions as for the one-electron anodic process can be drawn with respect to the kinetic profiles of dissolution.

In order to determine whether the rate-determining step (rds) is governed by a one- or a two-electron process, Tafel plots were generated from the data presented in Tables 4.8 and 4.9. This entails a plot of the anodic overpotential (η_a) against the logarithm of the anodic current density (i_a) according to the "high-field" approximation of the Butler-Volmer or so-called Tafel equation [33]:

$$\eta_a = a + b\log_{10}(i_a) \quad (4.29)$$

Where:

$$\eta_a = E_m - E_e \quad (4.30)$$

$$a = -b\log_{10}(i_o) \quad (4.31)$$

$$b = 2.303RT / (1 - \beta_a)nF \quad (4.32)$$

With:

η_a Anodic overpotential, in V
b Tafel slope, in V.decade^{-1}
β_a Anodic transfer coefficient
E_m Electrode potential (mixed potential), in V
E_e Equilibrium potential of the anodic reaction, in V
i_a Anodic current density, in A.m^{-2}
i_o Exchange current density, in A.m^{-2}
R Universal gas constant, 8.31441 J.mol^{-1}.K^{-1}
T Temperature, in K
F Faraday's constant, 96487 C.mol^{-1} e$^-$
n Number of electrons, mol e$^-$

Such a plot should render a straight line with slope, b, and y-intercept, a.

From Tables 4.8 and 4.9 it can be seen that the anodic overpotential (η_a) values for the selected data are all well above 20 mV. This means that the mixed potential (E_m) is sufficiently far away from the equilibrium potential (E_e) for the mineral dissolution reaction (Equation 4.3 or 4.4). Therefore, the cathodic contribution to the anodic reaction (for mineral dissolution) can be neglected and the use of the "high-field" approximation of the Butler-Volmer or Tafel equation (Equation 4.29) is justified. In general, the latter approximation is true for the cathodic behaviour of most copper sulphide minerals, which exhibit highly irreversible electrochemical behaviour (see 2.5 Electrochemistry) [33].

Table 4.8 : Measurements for the 0.2 M HCl Solution

E_m (V)	E_e [1] (V)	η_a (V)	i_a [2] ($A.m^{-2}$)	$\log_{10}(i_a)$
0.560	0.466	0.094	0.00135	-2.869
0.580	0.466	0.114	0.00138	-2.861
0.600	0.466	0.134	0.00321	-2.494
0.620	0.466	0.154	0.00327	-2.486

1) Obtained from 3 min OCP values
2) Steady state current densities (1 h)

Table 4.9 : Measurements for the 0.2 M HCl + 0.5 g/L Cu Solution

E_m (V)	E_e [1] (V)	η_a (V)	i_a [2] ($A.m^{-2}$)	$\log_{10}(i_a)$
0.560	0.500	0.060	0.00041	-3.389
0.580	0.500	0.080	0.00068	-3.169
0.600	0.500	0.100	0.00111	-2.955
0.620	0.500	0.120	0.00158	-2.801

1) Obtained from 3 min OCP values
2) Steady state current densities (1 h)

Figures 4.29 and 4.30 portray the data graphically according to Equation 4.29.

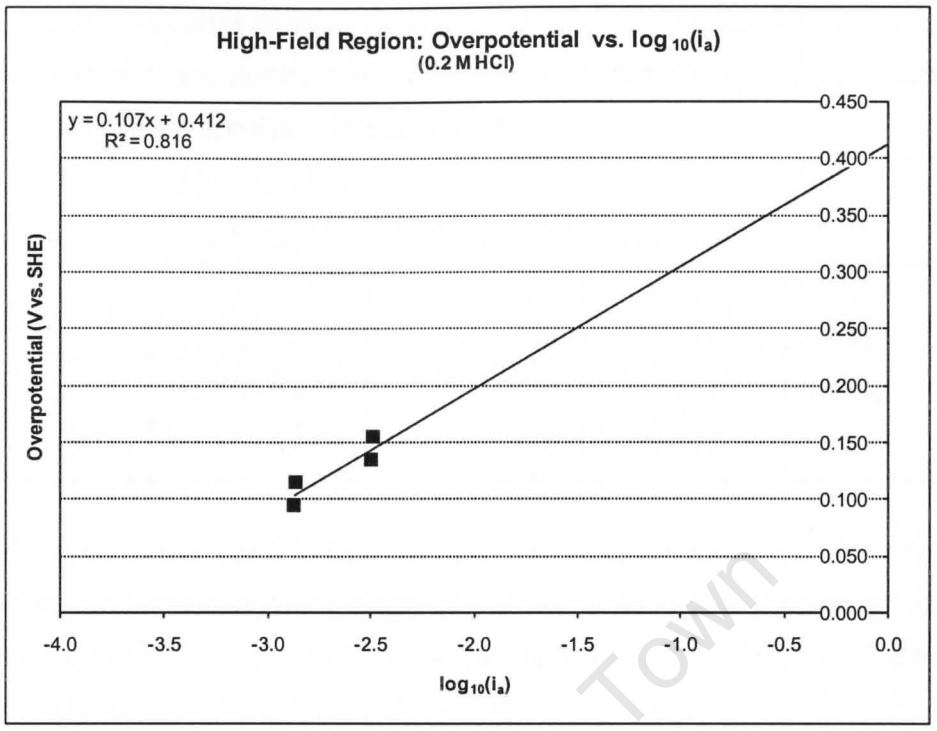

Figure 4.29 : A Tafel Plot for Current / Potential Data at 0.2 M HCl

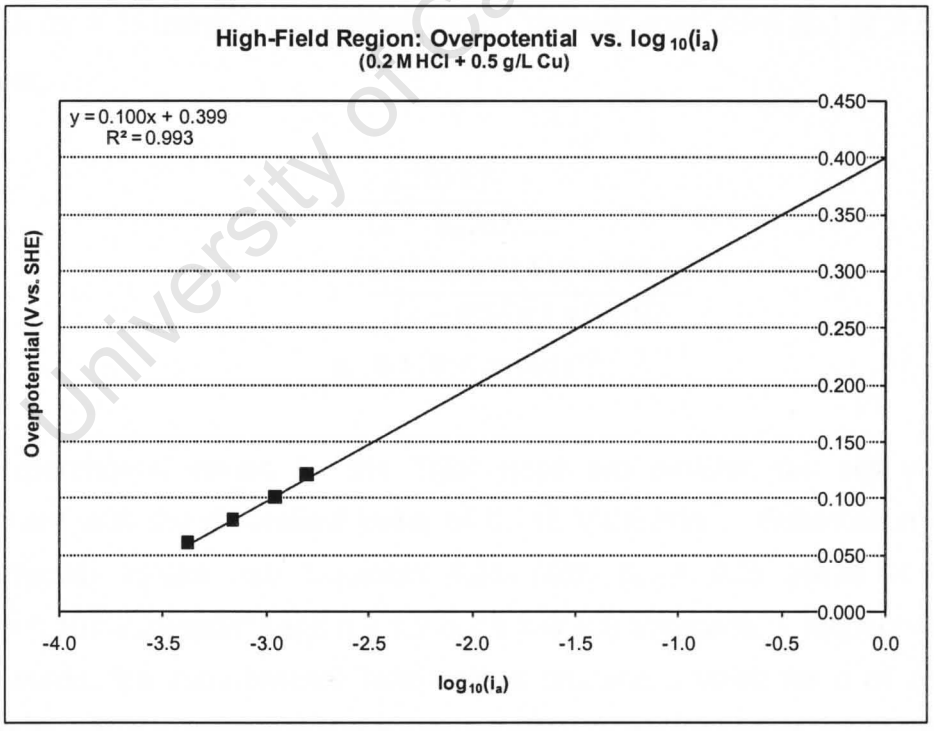

Figure 4.30 : A Tafel Plot for Current / Potential Data at 0.2 M HCl + 0.5 g/L Cu

The plots show straight lines of which the slopes and y-intercepts were used to calculate the relevant electrochemical parameters with the aid of Equations 4.30 to 4.32. The results are listed in Table 4.10.

Table 4.10 : Electrochemical Parameters

Solution	E_m (V)	η_a (V)	b (V.decade^{-1})	i_o (A.m^{-2})	β_a
0.2 M HCl	0.560 - 0.620	0.094 - 0.154	0.107	1.41 x 10^{-4}	0.5
0.2 M HCl + 0.5 Cu	0.560 - 0.620	0.060 - 0.120	0.100	1.02 x 10^{-4}	0.5

The electrochemical parameters for the two sets of data are in very good agreement and show a Tafel slope (b) of 0.100 to 0.107 V.decade^{-1} and an exchange current density (i_o) of 1.02 x 10^{-4} to 1.41 x 10^{-4} A.m^{-2} for an assumed anodic transfer coefficient (β_a) of 0.5.

Equation 4.32 predicts a Tafel slope of 0.118 V.decade^{-1} for a one-electron process (n = 1) using an assumed anodic transfer coefficient (β_a) of 0.5. For example,

$$b = \frac{2.303RT}{(1-\beta_a)nF} \qquad (4.32)$$

$$= \frac{2.303 \text{ x } 8.31441 \text{ x } 298.15}{(1-0.5) \text{ x } 1 \text{ x } 96487}$$

$$= 0.118 \text{ V. decade}^{-1}$$

The experimental values for the Tafel slope are smaller, but still in good agreement with the theoretical value of 0.118 V.decade^{-1}. Substitution of the experimental values into Equation 4.32 (with β_a = 0.5) yields n = 1.1 (for b = 0.107 V.decade^{-1}) and n = 1.2 (for b = 0.100 V.decade^{-1}), respectively. In other words, the experimental Tafel slopes produce a value for n of about 1 (electron), which suggests that the rate-determining step involves a one-electron

process. This is somewhat expected since it is well accepted in electrochemistry to exclude paths which would involve multiple electron transfers in a single reaction step, because of the low probability of two electrons tunnelling simultaneously between an ion and a metal [111].

Finally, the validity of the assumed value of 0.5 for the anodic transfer coefficient (β_a) was tested by substitution of the experimental Tafel slopes into Equation 4.32 for n = 1 (electron). This produced respective values of 0.45 (for 0.107 V.decade^{-1}) and 0.41 (for 0.100 V.decade^{-1}). These fall within the range of 0.4 to 0.6, which are typical for electrochemical reactions [31,33]; thus, justifying the original selection of 0.5.

Therefore, for the dissolution of covellite in acidic, chloride solutions over the potential range OCP to 0.62 V, a direct oxidative mechanism involving a one-electron anodic process as the rate-determining or slow step is preferred as opposed to a direct oxidative mechanism involving a two-electron process.

Even if the anodic or mineral dissolution reaction were to occur as a two-electron process (Equation 4.4), it would most likely occur as a sequence of one-electron steps for reasons already discussed [111]. For example:

$$CuS \xrightarrow{rds} Cu(I) + S^\circ + e^- \qquad (4.3)$$

$$Cu(I) \xrightarrow{fast} Cu(II) + e^- \qquad (4.33)$$

$$\sum CuS \rightarrow Cu(II) + S^\circ + 2e^- \qquad (4.4)$$

From the above it can be seen that the first step in the overall process is merely the one-electron anodic process (Equation 4.3), which is the rate-determining step. The second step entails the rapid oxidation of cuprous to cupric ions (Equation 4.33), which could be achieved by dissolved oxygen (Equation 4.2).

4.5.2 Direct Oxidation Mechanism - Consistency with Experimental Observations

Before a direct oxidation process for the dissolution of covellite in acidic, chloride solutions (within the potential range of the OCP to 0.62 V) can be proposed as a probable mechanism, it should first be evaluated for consistency with the experimental findings and observations. In order to do this, a summary of the main characteristics of this mechanism follows:

- The dissolution of the mineral by a one-electron anodic process (Equation 4.3) has been shown to be thermodynamically feasible under the experimental conditions tested.
- Mineral dissolution has been shown to be electrochemical in nature with the electrochemical rates in fair agreement with the rates of chemical leaching at corresponding mixed potentials and temperatures.
- Experimental values for the anodic transfer coefficient (0.41 to 0.45) are typical of an electrochemical process and are reasonably close to 0.5.
- Experimental Tafel slope values (0.100 V.decade^{-1} to 0.107 V.decade^{-1}) are in good agreement with 0.118 V.decade^{-1}, which supports a one-electron transfer process as the rate-determining step (rds).
- The measured mixed potential (E_m) has a dependency on the cupric-to-cuprous ion ratio (at the mineral surface) of 0.051 V.decade^{-1}, which is in good agreement with the theoretical value of 0.059 V.decade^{-1} as predicted for conditions of Case I.
- The experimental results are consistent with a reaction that has a half-order rate-dependency on the cupric-to-cuprous ion ratio (at the mineral surface) as predicted by the Butler-Volmer equation (Equation 4.10) for conditions of Case I.
- The experimental rate of dissolution of covellite increases with increased applied potential over the range OCP to 0.62 V, which is consistent with the Butler-Volmer rate equation (Equation 4.10) for conditions of Case I.

- The Butler-Volmer rate equation (Equation 4.27) predicts a half-order dependency on the cupric ion concentration (at the mineral surface) for conditions of Case II.

In addition, for Case I, linear kinetics of dissolution of the mineral are predicted at constant solution potential (at the mineral surface) by Equation 4.10. For Case II, parabolic kinetics are predicted from the onset of leaching by Equation 4.27. However, in both cases it is expected that the kinetics should level off to some extent over time, due to the formation of elemental sulphur on the mineral surface by Equation 4.3. A good example of this can be found in the work of Cheng *et al.* [50] (see 2.4.2 Deportment of Reaction Products).

There are some observations from the electrochemistry though, that remain unexplained when a direct oxidative mechanism is considered. For example:

- The positive effect of increased chloride concentration on the initial rate of mineral dissolution (see Figures 4.13, 4.14, 4.22 and 4.23).
- The detrimental effect that increased copper concentration has on the rate of mineral dissolution, especially at levels of high chloride concentration (see Figures 4.17 and 4.18; Table 4.6).

These may be due to the effect of the said constituents on the electrochemical parameters such as $k_{Cu(I)}$ and $k_{Cu(II)}$. For example, an increase in chloride ion concentration will decrease the rate of oxidation of cuprous to cupric ions and thereby $k_{Cu(I)}$ [86]. And, for the conditions of Case I, it can be seen from Equations 4.10 and 4.11 that a decrease in the value of $k_{Cu(I)}$ can result in an increase in the rate of dissolution of covellite (r_{CuS}).

It is suggested that the highlighted effects of chloride and copper ions should be further investigated in potentiostatic tests.

4.5.3 Dissolution of Covellite by a Non-Oxidative / Oxidative Process

Apart from the two proposed schemes describing the dissolution of covellite by direct oxidation with cupric ions, one could also be tempted to consider the possibility that dissolution of the mineral may occur via a non-oxidative ("free dissolving") coupled with an oxidative mechanism, especially in the potential range from the OCP to the first anodic peak (0.62 V).

Such a reaction mechanism was recently proposed by Nicol *et al.* for the dissolution of chalcopyrite in acidic, chloride solutions in the potential range 0.560 V to 0.620 V [19,47,112]. It was found that chalcopyrite showed enhanced rates of dissolution in this potential range in the presence of chloride ions, copper ions and dissolved oxygen, which could not be explained by the conventional mechanism of direct oxidative dissolution of the mineral. It was also found that the mineral dissolved in a linear fashion until near-completion without the occurrence of "passivation". Furthermore, that elemental sulphur was formed away from the mineral surface and preferably on the surface of other minerals such as fine-milled pyrite, which seemed to catalyze the rate of dissolution of chalcopyrite, as well as the rate of oxidation of dissolved hydrogen sulphide, significantly when present.

Consider this reaction mechanism adapted for the dissolution of covellite in acidic, chloride solutions (in the presence of dissolved oxygen) with cupric ion as the primary oxidant.

Non-Oxidative Process

$$CuS + 2H^{+} \overset{K}{=} Cu(II) + H_2S_{(aq)} \qquad (4.34)$$

With:

K Equilibrium constant

Oxidative Process

$$Cu(II) + e^- = Cu(I) \quad (4.5)$$

$$H_2S_{(aq)} = 2H^+ + S° + 2e^- \quad (4.35)$$

$$\Sigma\ 2Cu(II) + H_2S_{(aq)} \rightarrow 2Cu(I) + 2H^+ + S° \quad (4.36)$$

Back-Oxidation of Cuprous Ion

$$2Cu(I) + 2H^+ + ½O_2 \rightarrow 2Cu(II) + H_2O \quad (4.2)$$

Overall Reaction

$$CuS + 2H^+ + ½O_2 \rightarrow Cu(II) + S° + H_2O \quad (4.6)$$

This reaction mechanism essentially entails a two-stage process where the first stage involves a non-oxidative process with the mineral in equilibrium with protons, free or uncomplexed cupric ions and dissolved hydrogen sulphide according to Equation 4.34.

The second stage entails a perturbation of the equilibrium by the homogenous oxidation of dissolved hydrogen sulphide by cupric ions (Equation 4.36), which will drive the equilibrium to the right. In contrast to the two direct oxidative mechanisms, where elemental sulphur is formed on the mineral surface via its anodic dissolution reactions (Equations 4.3 and 4.4), elemental sulphur should form away from the mineral surface unless the rate of oxidation of dissolved hydrogen sulphide (by Equation 4.36) exceeds the rate of diffusion of hydrogen sulphide (by Equation 4.34) away from the mineral surface. In the latter case,

the mineral dissolution reaction will by controlled by mass transport (i.e. diffusion of soluble species away from the mineral surface) whereas in the former case, the reaction will be chemically controlled.

Cuprous ions, as a result of the reduction of cupric ions by dissolved hydrogen sulphide (Equation 4.36), will be oxidized back to cupric ions by dissolved oxygen according to the reaction presented in Equation 4.2.

Thus, the overall reaction for the non-oxidative / oxidative dissolution of covellite in acidic, chloride solutions (in the presence of dissolved oxygen) can again be presented by Equation 4.6, which is exactly the same as for the two direct oxidative mechanisms of the mineral.

A schematic diagram of the above reaction mechanism is presented in Figure 4.31.

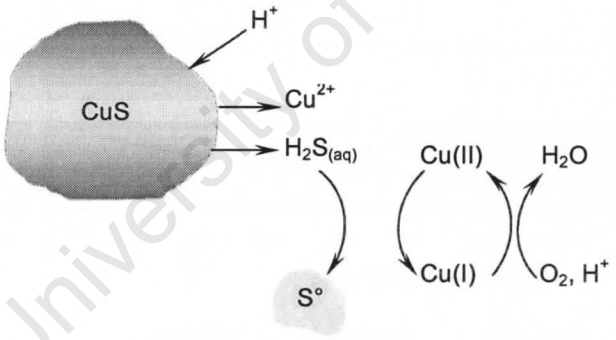

Figure 4.31 : A Schematic Diagram of the Dissolution of Covellite via a Coupled Non-Oxidative / Oxidative Process

4.5.4 Non-Oxidative / Oxidative Process - Thermodynamic Considerations

Consider a system where a covellite electrode is in equilibrium with a 0.2 M H^+ solution, with K = 3.38 x 10^{-17} at 25°C [40,114] as presented by Equation 4.34.

$$CuS + 2H^+ \overset{K}{=} Cu^{2+} + H_2S_{(aq)} \qquad (4.34)$$

The concentrations of the aqueous species in equilibrium with the mineral electrode as a function of increasing chloride concentration are presented in Figure 4.32.

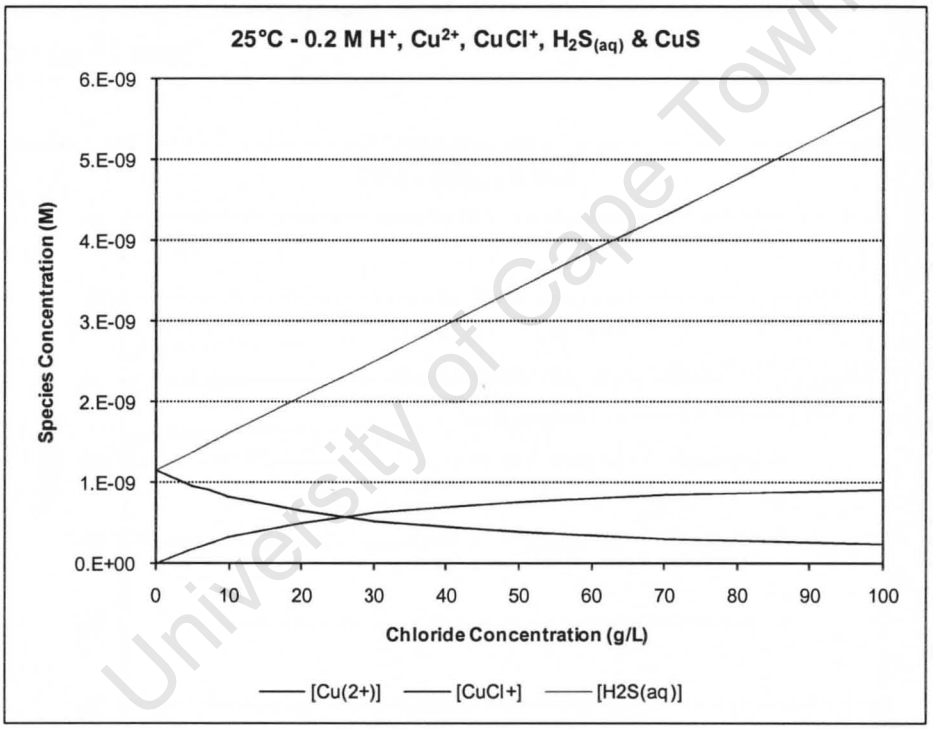

Figure 4.32 : A Species Distribution Diagram for Covellite in Equilibrium with 0.2 M H^+ at 25°C

It can be seen that the free or uncomplexed cupric ion (Cu^{2+}) concentration decreases with increased chloride concentration. This is due to the formation of cupric-chloro complexes such as the $CuCl^+$ ion amongst others. In contrast to

this, the hydrogen sulphide (H_2S) concentration increases with increased chloride concentration as is expected from the following relationship for the equilibrium constant (K).

$$K = \frac{[Cu^{2+}][H_2S_{(aq)}]}{[H^+]^2} \tag{4.37}$$

$$\therefore [H_2S_{(aq)}] = \frac{K[H^+]^2}{[Cu^{2+}]}$$

It is also evident that an increase in acidity, i.e. the proton concentration, will shift the equilibrium (in Equation 4. 34) to the right. This is illustrated in Figure 4.33, which depicts a plot of $\ln[H_2S_{(aq)}]$ against chloride concentration for 0.01 M H^+, 0.2 M H^+ and 2 M H^+.

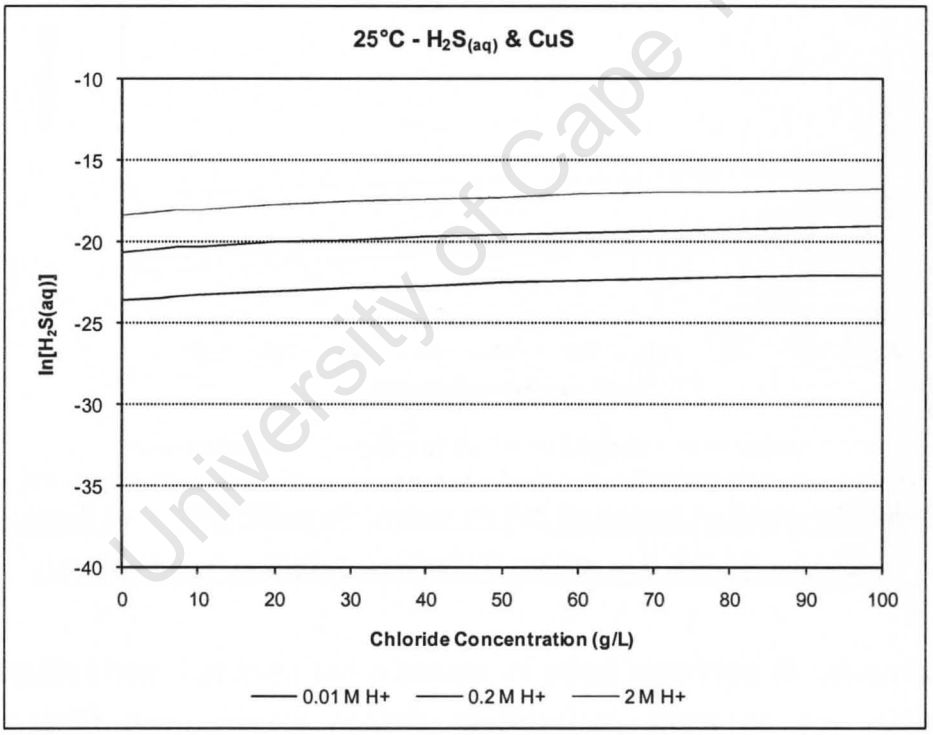

Figure 4.33 : The Effect of Acidity on the Dissolved Hydrogen Sulphide Concentration in Equilibrium with Covellite at 25°C

The results show that as the acidity is increased from 0.01 M H^+ to 2 M H^+, the dissolved hydrogen sulphide concentration also increases.

In contrast to this, an increase in copper concentration will shift the equilibrium to the left. In other words, the equilibrium concentration of hydrogen sulphide will decrease with increased free or uncomplexed cupric ion concentration. Figure 4.34, which presents a plot of $\ln[H_2S_{(aq)}]$ against chloride concentration for different copper concentrations, is illustrative of this effect.

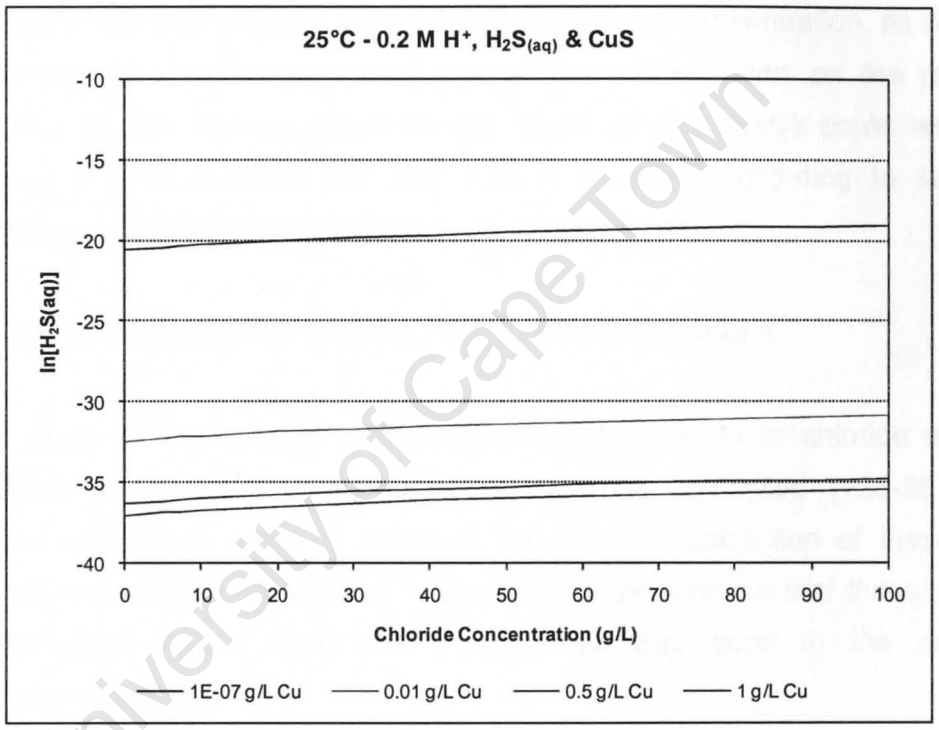

Figure 4.34 : The Effect of Copper on the Dissolved Hydrogen Sulphide Concentration in Equilibrium with Covellite at 0.2 M H^+ and 25°C

The results show that even the presence of small quantities of soluble copper (as low as 10 ppm) has a marked (decreasing) effect on the equilibrium concentration of dissolved hydrogen sulphide.

Thus, it follows from the thermodynamics that an increase in acidity (low pH) and chloride concentration will favour the non-oxidative process (Equation 4.34), whereas increased copper concentration will make it less favourable.

A mineral dissolution process according to the non-oxidative / oxidative process would render increased rates of dissolution of covellite by increasing the favourability of the non-oxidative process or by faster displacement of the equilibrium to the right.

The positive effect of increased acidity and chloride ion concentration, as well as the detrimental effect of increased copper ion concentration on the rate of dissolution of the mineral electrode (as found in this study) could well be explained if it is assumed that the mineral dissolves according to such a mechanism, which is under mass transport control.

4.5.5 Non-Oxidative / Oxidative Process - Kinetic Considerations

In her study of the kinetics of dissolution of chalcopyrite in chloride media, Velásquez also conducted two leaching tests on fine-milled (+25-38 μm), synthetic covellite in order to compare the rates of dissolution of these two minerals, under similar conditions [19]. *It should be pointed out that the synthetic covellite used in her study is the same as was used in the present electrochemical study.*

Both these tests were executed in a solution of 0.2 M HCl + 0.5 g/L Cu (as $CuSO_4$) at 35°C, where the bulk solution potential was controlled between 0.57 V and 0.58 V in one test and between 0.65 V and 0.66 V in the other. The results of the covellite leaching tests are presented in Figure 4.35, together with that of a chalcopyrite leaching test, which was also conducted in a solution of 0.2 M HCl + 0.5 g/L Cu (as $CuSO_4$) at 0.58 V and 35°C.

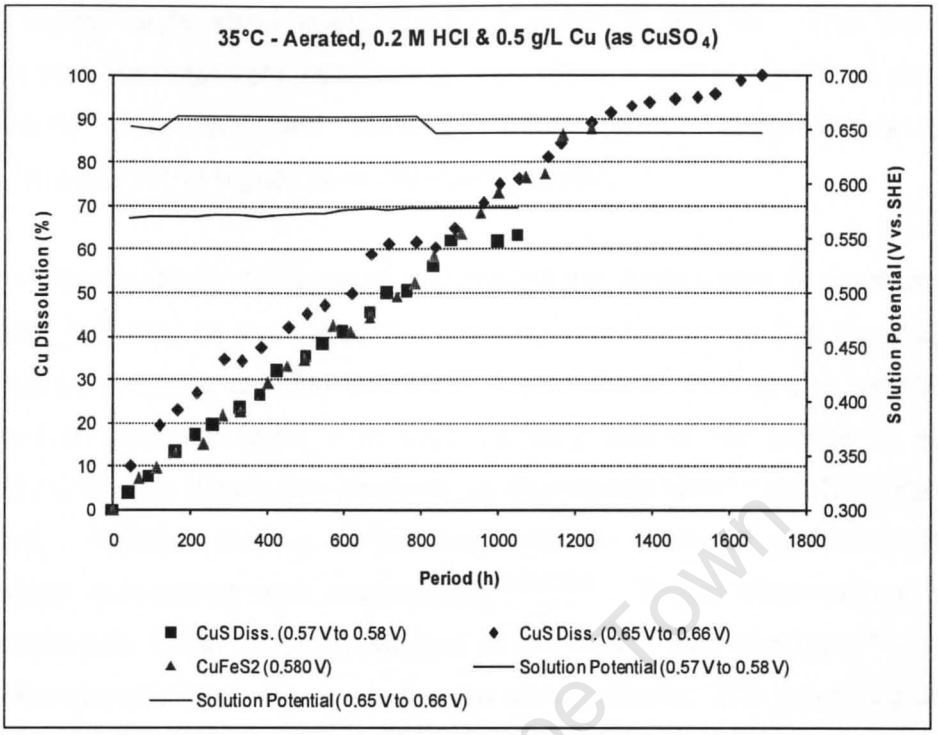

Figure 4.35 : A Comparison of the Copper Dissolution Transients of Chalcopyrite and Covellite

The blue and red data points represent copper dissolution from covellite at respective solution potentials of 0.57 V to 0.58 V (blue line) and 0.65 V to 0.66 V (red line). The lower potential test shows 63% copper dissolution after 1049 h of operation, whereas the higher potential test achieves about 75% copper dissolution in more or less the same time. Thus, the rate of dissolution of covellite is slightly faster at the higher solution potential of 0.65 V to 0.66 V.

The green data points represent copper dissolution from a +25-38 µm, high-grade (83%), chalcopyrite-bearing concentrate. It can be seen that the rates of dissolution of chalcopyrite and covellite are remarkably similar and it is tempting to suggest that the two minerals share, at least partially, a commonality in leaching mechanism.

Furthermore, it is also interesting to note that not only the chalcopyrite test, but both covellite tests show linear copper dissolution kinetics. This seems to indicate that both minerals' available surface areas for leaching do not decrease significantly over the test duration, even up to complete dissolution (as in the case of the higher potential covellite test).

In recent publications, Nicol *et al.* highlighted the deportment of sulphur as an important indicator of the prevailing leaching mechanism in the dissolution of chalcopyrite in acidic, chloride solutions. It was shown that, under conditions of low solution potential (0.56 V to 0.62 V), very little of the elemental sulphur formed during the dissolution process, is associated with residual chalcopyrite particles. Instead, sulphur occurs as isolated, spherical globules with an occasional association with chalcopyrite [19,47,112]. These observations are in agreement with those made by Majima *et al.* [113] and also Dutrizac [54] in acidic, ferric chloride solutions with respect to the same mineral. The latter author even suggested that the development of large, well-formed (euhedral) sulphur crystals is the result of sulphur being deposited from the leaching medium. Also, that the reaction must involve, at least in part, the presence of various dissolved hydrogen sulphide species. Such species, which are formed at the mineral surface, diffuse from the reaction interface and are oxidized by ferric ions [54].

A mineralogical examination by mineral liberation analysis (MLA) of the solids residue for the lower potential covellite test showed that a significant amount of sulphur is formed on the mineral's surface after 63% copper dissolution. However, it occurs as isolated islands with more than 95% of the mineral's surface free of sulphur [19,112]. Also, as in the case with chalcopyrite under the same leaching conditions (0.2 M HCl + 0.5 g/L Cu, 0.580 V at 35°C), the addition of fine-milled pyrite (d_{80} = 12 µm) in a mass ratio of 1 : 5 (covellite : pyrite) showed enhanced copper dissolution from covellite (in one test), albeit at a much lesser extent compared to chalcopyrite [19].

Apart from the rate of dissolution of covellite being marginally faster at higher solution potentials in the leaching tests, which is consistent with the electrochemical findings of this study, some of the other observations may not, at this stage, seem supportive of a mechanism that involves the direct oxidation of the mineral. These include:

- The linearity of the kinetics of mineral dissolution up to near-completion, and
- Enhanced mineral dissolution with the addition of fine-milled pyrite.

For the case where the non-oxidative / oxidative process is under chemical control, the rate of dissolution of covellite will be controlled by the homogenous oxidation of aqueous hydrogen sulphide as the slow step (Equation 4.36). In this case, the mineral dissolution process will be characterized by an apparent activation energy, which indicates a relatively strong temperature-dependency. Reported values from the literature for the atmospheric leaching of covellite in acidic, chloride solutions (in the absence of ferric ions) are all well-above 40 kJ.mol^{-1} (see 2.4.3 Kinetics of Dissolution), which is in support of a process controlled by a chemical (or electrochemical) reaction [33]. In conjunction, this requires the non-oxidative reaction (Equation 4.34) to be a faster step, which is somewhat expected due to the fast kinetics of equilibrium reactions in general [41].

Thus, the maximum rate of covellite dissolution that could theoretically be achieved by such a reaction mechanism would be where the equilibrium reaction (Equation 4.34) is rate-controlling. For this reaction under mass transport control, the maximum rate of dissolution of covellite can then be estimated (at least during the initial stages of leaching) by the following application of Fick's first law [33]:

$$r_{CuS} = k_L(C_{H_2S} - C_o) \qquad (4.38)$$

$$r_{CuS} = k_L C_{H_2S}$$

With:

r_{CuS} Maximum rate of dissolution of covellite, in mol Cu $cm^{-2}.s^{-1}$

k_L Liquid phase mass transfer coefficient, 10^{-3} $cm.s^{-1}$ [33]

C_{H_2S} Concentration of aqueous hydrogen sulphide at the mineral surface, in $mol.cm^{-3}$

C_o Concentration of aqueous hydrogen sulphide in the bulk solution, 0 $mol.cm^{-3}$

Substitution of Equation 4.37 into Equation 4.38, under the above conditions, renders:

$$r_{CuS} = \frac{k_L K[H^+]^2}{[Cu^{2+}]} \tag{4.39}$$

With:

$[Cu^{2+}]$ Concentration of free or uncomplexed cupric ions at the mineral surface, in $mol.cm^{-3}$

$[H^+]$ Concentration of protons at the mineral surface, in $mol.cm^{-3}$

Then, for E_m = 0.580 V, $E_{h,\ capillary}$ = 0.591 V and 0.2 M HCl + 0.5 g/L Cu (as $CuSO_4$), maximum rates of dissolution of covellite under conditions of mass transport control were calculated with Equation 4.39.

The results are presented in Table 4.11 together with experimental rates of dissolution obtained in this study and from the literature [19].

Table 4.11 : Mass Transport Rates of Covellite Dissolution

T (°C)	k_L [a] ($cm.s^{-1}$)	K [40,114] ($\times 10^{-17}$)	$[H^+]$ [b] ($mol.cm^{-3}$)	$[Cu^{2+}]$ [c] ($mol.cm^{-3}$)	r_{CuS} (mol Cu $cm^{-2}.s^{-1}$)		
					Eq. 4.39	This study	Literature [19]
25	10^{-3}	3.38	0.0002	6.18×10^{-6}	2.19×10^{-22}	7.13×10^{-13}	-
35	10^{-3}	10	0.0002	6.18×10^{-6}	6.47×10^{-22}	-	4.86×10^{-12}

a) Strictly speaking this value also increases with increased temperature; however, since the temperature-dependency is expected to be relatively small (for mass transport control), the same value has been used at both 25°C and 35°C.

b) Assumed

c) The free or uncomplexed cupric ion concentration has been estimated for a capillary solution potential of 0.591 V (at a mixed potential of 0.580 V) by means of the NIST database [40].

It is evident that the rate of dissolution of covellite under mass transport control is many orders of magnitude smaller than the experimental rates. The reason for this is that the equilibrium (Equation 4.34) is very unfavourable under the reigning conditions. Therefore, since this rate of dissolution of the mineral is so much smaller than the experimental rates, the non-oxidative / oxidative reaction mechanism cannot be accepted for the dissolution of covellite in acidic, chloride solutions under these conditions.

CHAPTER 5

CONCLUSIONS AND RECOMMENDATIONS

This thesis summarizes the results of an electrochemical study on the anodic dissolution of a stationary covellite electrode in acidic, chloride solutions at ambient conditions, with particular interest to the mineral surface potential range from the open circuit potential (OCP) to about 0.62 V.

It has been demonstrated by measurement of the solution potential close to the mineral surface (capillary solution potential) that cupric ions can oxidize covellite in acidic, chloride solutions by means of the Cu(II) / Cu(I) couple. This is in agreement with thermodynamic calculations, which show that the anodic dissolution of the mineral can occur by either a one- or two-electron process under these conditions, with the former being more favourable from a thermodynamic point of view.

The rates of anodic dissolution of the mineral obtained by electrochemical method (in the absence of a chemical oxidant) were found to be in fair agreement with published rates of chemical leaching at similar mixed potentials and temperatures. This suggests that the leaching of covellite, by a chemical oxidant in acidic, chloride solutions, occurs according to an electrochemical process.

By application of mixed potential theory to the following anodic and cathodic half-cell reactions,

Anodic:

$$CuS = Cu(I) + S^{\circ} + e^{-} \qquad (5.1)$$

Cathodic:

$$Cu(II) + e^{-} = Cu(I) \qquad (5.2)$$

It was found that:

- The measured mixed potential (E_m) showed a 0.051 V.decade^{-1} dependency on the cupric-to-cuprous ion ratio at the mineral surface. This is in excellent agreement with the theoretically calculated value of 0.059 V.decade^{-1}.

- Experimental Tafel slope values of 0.100 V.decade^{-1} to 0.107 V.decade^{-1} were in good agreement with the theoretically calculated value of 0.118 V.decade^{-1} for a one-electron reaction as the rate-determining step (rds).

- Experimental values for the anodic transfer coefficient (β_a) of 0.41 to 0.45 fell well within the range of 0.4 to 0.6, which is typical of electrochemical reactions.

- The rate of anodic dissolution of the mineral by electrochemical method showed a 0.51th order rate-dependency on the cupric-to-cuprous ion ratio at the mineral surface. This is in excellent agreement with the theoretical value of 0.5 as predicted by the Butler-Volmer equation.

Therefore, it can be concluded that the oxidative dissolution of covellite in acidic, chloride solutions, over the potential range of interest, occurs according to the reaction,

$$CuS + Cu(II) = 2Cu(I) + S^\circ \qquad (5.3)$$

with the anodic dissolution of the mineral, according to a one-electron process (Equation 5.1), as the rate-determining step (rds).

Furthermore, it is proposed that the resultant cuprous ions are oxidized back to cupric ions, by dissolved oxygen according to:

$$2Cu(I) + 2H^+ + \tfrac{1}{2}O_2 \rightarrow 2Cu(II) + H_2O \qquad (5.4)$$

With the overall reaction as:

$$CuS + 2H^+ + \tfrac{1}{2}O_2 \rightarrow Cu(II) + S^\circ + H_2O \qquad (5.5)$$

Thus, describing the leaching of covellite in acidic, chloride solutions, in the presence of dissolved oxygen, by a direct oxidative mechanism.

Cyclic voltammetry showed that the anodic dissolution of the mineral is potential-dependent with an increase in measured current density with increased applied potential over the range of interest.

This electrochemical method also revealed the presence of two, distinct (anodic) peaks at corresponding peak potentials of 0.625 V and 0.744 V in a 0.2 M HCl solution. The mineral was found to show active behaviour up to the first peak; thereafter, both active and passive behaviour. The processes reigning at both peaks were found to be irreversible and not mass transport controlled. Therefore, these have to be chemically or electrochemically controlled.

Cyclic voltammetry showed to be an excellent scanning method by which the effect of constituents, such as acidity (pH), chloride ions, copper ions and sulphate ions, on the rate of anodic dissolution of the mineral could be identified in a short period of time. Of these constituents, only chloride ions and copper ions showed a significant influence on the measured current density with an increase in current density with increased chloride concentration and an unexpected decrease in current density, especially at high chloride concentration, with increased copper concentration.

The detrimental effect of increased copper concentration and the positive effect of increased chloride concentration on the rate of anodic dissolution of the mineral were further investigated in constant-potential, potentiostatic tests over prolonged periods. These effects were confirmed; however, it was found that the positive effect of increased chloride concentration on the measured current density only pertains to the initial stages of leaching and that similar rates of mineral dissolution are achieved at high (2 M Cl^-) and low chloride concentration (0.2 M Cl^-) over prolonged periods. This may be due to the increase in copper concentration with time by leaching of the mineral.

Capillary potential measurements showed that the solution potential close to the mineral surface decreased with increased capillary length. This phenomenon will be relevant to the application of heap leaching of whole ores, where the mineral may occur in cracks or pores in the gangue matrix or be covered (or partially covered) by precipitates and / or reaction products such as elemental sulphur. In this context, a decreased solution potential close to the mineral surface could effect a decrease in the mixed potential and thereby also a decrease in the rate of leaching of the mineral.

It is recommended that the following be considered for further or more detailed investigation:

- The effect of chloride ion concentration on the electrochemical rate parameters, $k_{Cu(II)}$ and $k_{Cu(I)}$.
- The effect of copper ion concentration on the electrochemical rate parameters.
- Extension of the present study to higher temperatures.
- An extensive chemical leaching study on a high-purity, covellite sample in acidic, chloride solutions (in the absence of ferric ions) under conditions of controlled solution potential and where corresponding measurements of the reigning mixed potential is made with a covellite electrode.

REFERENCES

1. Anon., **Metal of Civilisation (copper supplement)**, Mining Journal, **325**, 1995, p. 23.

2. Sullivan, J.D., **Chemistry and Physical Features of Copper Leaching**, Trans. RIME, **106**, 1933, p. 515 - 546.

3. Biegler, T. and Swift, D.A., **Anodic Electrochemistry of Chalcopyrite**, J. Appl. Electrochem., **9**, 1979, p. 545 - 554.

4. Burkin, A.R., **Solid-State Transformations During Leaching**, Min. Sci. Eng., **4**, 1969, p. 4 - 14.

5. Dutrizac, J.E., MacDonald, R.J.C. and Ingraham, T.R., **Kinetics of Dissolution of Synthetic Chalcopyrite in Aqueous Acidic Ferric Sulphate Solutions**, Trans. Met. Soc. AIME, **245**, 1969, p. 955 - 959.

6. Ferreira, R.C.H., **Leaching of Chalcopyrite**, Ph.D. Thesis, University of London, 1972.

7. Hiroyoshi, N., Miki, H., Hirajima, T. and Tsunekawa, M., **A Model for Ferrous Promoted Chalcopyrite Leaching**, Hydrometallurgy, **57**, 2000, p. 31 - 38.

8. Kametani, H. and Aoki, A., **Effect of Suspension Potential on the Oxidation Rate of Copper Concentrate in a Sulphuric Acid Solution**, Metall. Trans. B., **16B**, 1985, p. 695 - 705.

9. Nicol, M.J. and Miki, H., Personal Communication, 2004.

10. Lázaro-Báez, M.I., **Electrochemistry of the Leaching of Chalcopyrite**, Ph.D. Thesis, Murdoch University, 2001.

11. Warren, G.W., Wadsworth, M.E. and El-Raghy, S.M., **Passive and Transpassive Anodic Behaviour of Chalcopyrite in Acid Solutions**, Metall. Trans., B, **13B**, 1982, p. 571 - 579.

12. Muller, E.L., Basson, P. and Nicol, M.J., **Chloride Heap Leaching**, WO 2007/134343, 2007.

13. Muller, E.L., Basson, P. and Nicol, M.J., **Chloride Tank Leaching**, WO 2007/134344, 2007.

14. Velásquez-Yévenes, L., Nicol, M.J. and Miki, H., **The Dissolution of Chalcopyrite in Chloride Solutions Part 1: The Effect of Solution Potential**, Hydrometallurgy, **103**, 2010, p. 108 - 113.

15. Du Plessis, C.A., Batty, J.D. and Dew, D.W., **Commercial Applications of Thermophile Bioleaching**. In: Rawlings, D.E. and Johnson, D.B. (eds.), **Biomining**, Springer, 2007, p. 57 - 80.

16. Dew, D.W., Personal Communication, 2003.

17. Photograph taken by P. Basson, Murdoch University, 2006.

18. Nicol, M.J., Personal Communication, 2007 - 2008.

19. Velásquez-Yévenes, L., **The Kinetics of the Dissolution of Chalcopyrite in Chloride Media**, Ph.D. Thesis, Murdoch University, 2008.

20. Biegler, T. and Swift, D.A., **Anodic Behaviour of Pyrite in Acid Solutions**, Electrochimica Acta, **24**, 1979, p. 415 - 420.

21. Masuko, N. and Hisamatsu, Y., **On the Electrochemical Behaviour of Pyrite**, Denki-Kayaku, **31**, 1963, p. 907 - 912.

22. Boon, M., **Theoretical and Experimental Methods in the Modelling of Bio-Oxidation Kinetics of Sulphide Minerals**, Ph.D. Thesis, Technical University of Delft, 1996.

23. Holmes, P.R., **An Electrochemical Study of the Anodic, Oxidative and Bacterial Dissolution of Pyrite**, Ph.D. Thesis, University of the Witwatersrand, 1998.

24. Holmes P.R. and Crundwell, F.K., **The Kinetics of the Oxidation of Pyrite by Ferric Ions and Dissolved Oxygen: An Electrochemical Study**, Geochimica et Cosmochimica Acta, **64**, 2, 2000, p. 263 - 274.

25. Preece, R., Personal Communication, 2004.

26. Muller, E.L., Personal Communication, 2006.

27. Mellor, J.W., **A Comprehensive Treatise on Inorganic and Theoretical Chemistry**, Volume III, Longmans, Green and Co., London, 1952 (New Impression).

28. Hurlbut, C.S., **Dana's Manual of Mineralogy**, 18th Edition, John Wiley and Sons Inc., New York, 1971.

29. Ďuda, R. and Rejl, L., **Minerals of the World**, published by Spring Books (an imprint of the Hamlyn Publishing Group Ltd.), 1986.

30. **The MacDonald Encyclopaedia of Rocks and Minerals**, MacDonald and Co. (Publishers) Ltd. (a member of the Maxwell Macmillan Pergamon Publishing Corporation), 1990.

31. Wadsworth, M.E., **Electrochemical Reactions in Hydrometallurgy**. In: Tien, J.K. and Elliott, J.F. (eds.), **Metallurgical Treatises**, A Publication of the Metallurgical Society of AIME, 1981, p. 1 - 22.

32. Walsh, C.A. and Rimstidt, J.D., **Rates of Reaction of Covellite and Blaubleibender Covellite with Ferric Ion at pH 2.0**, Canadian Mineralogist, **24**, 1986, p. 35 - 44.

33. Nicol, M.J., **Hydrometallurgy - Theory and Practise - Study Guide 2008**, University of Cape Town, 2008.

34. Burkin, A.R., **Chemical Hydrometallurgy - Theory and Principles**, Imperial College Press, 2001.

35. Duby, P., **The Thermodynamic Properties of Aqueous Inorganic Copper Systems**, International Copper Research Association Inc., 1977.

36. Nicol, M.J., Personal Communication, 2004.

37. Nicol, M.J., Personal Communication, 2003.

38. Latimer, W.M., **The Oxidation of the Elements and their Potentials in Aqueous Solutions**, First Edition, Prentice-Hall Inc., New York, 1938.

39. Cruywagen, J.J., Heyns, J.B.B., Raubenheimer, H.G. and Van Berge, P.C., **Inleiding tot die Anorganiese en Fisiese Chemie**, Second Edition, Butterworth, 1986.

40. National Institute of Standards and Technology (NIST) Database

41. Nicol, M.J., Personal Communication, 2003 - 2010.

42. McDonald, G.W. and Langer, S.H., **Cupric Chloride Leaching of Model Sulfur Compounds for Simple Copper One Concentrates**, Metall. Trans. B, **14B**, 1983, p. 559 - 570.

43. Senanayake, G., **A Review of Chloride Assisted Copper Sulfide Leaching by Oxygenated Sulfuric Acid and Mechanistic Considerations**, Hydrometallurgy, **98**, 2009, p. 21 - 32.

44. Winand, R., **Chloride Hydrometallurgy**, Hydrometallurgy, **27**, 1991, p. 285 - 316.

45. Nicol, M.J., Personal Communication, 2007.

46. Basson, P., Miki, H., Nicol, M.J. and Velásquez-Yévenes, L., **Enhanced Leaching of Chalcopyrite at Low Potentials in Chloride Solutions 1. Concentrates**. In: Harre, J. (ed.), **Proceedings of Copper 2010**, **5**, Hamburg, 2010, p. 1737 - 1752.

47. Basson, P., Miki, H., Nicol, M.J. and Velásquez-Yévenes, L., **Enhanced Leaching of Chalcopyrite at Low Potentials in Chloride Solutions 2. Mechanisms**. In: Harre, J. (ed.), **Proceedings of Copper 2010**, **5**, Hamburg, 2010, p. 1753 - 1770.

48. Basson, P., Muller, E.L., Nicol, M.J., **Enhanced Leaching of Chalcopyrite at Low Potentials in Chloride Solutions 3. Ores**. In: Harre, J. (ed.), **Proceedings of Copper 2010, 5**, Hamburg, 2010, p. 1771 - 1782.

49. Sullivan, J.D., **Chemistry of Leaching of Covellite**, Technical Paper, **487**, US Bureau of Mines, 1930, p. 1 - 18.

50. Cheng, C.Y. and Lawson, F., **The Kinetics of Leaching Covellite in Acidic, Oxygenated Sulphate-Chloride Solutions**, Hydrometallurgy, **27**, 1991, p. 269 - 284.

51. Parker, A.J., Paul, R.L. and Power, G.P., **Electrochemical Aspects of the Leaching of Copper from Chalcopyrite in Ferric and Cupric Salt**, Aust. J. Chem., **34**, 1981, p. 13 - 34.

52. Lázaro-Báez, M.I. and Nicol, M.J., **The Mechanism of the Dissolution and Passivation of Chalcopyrite - An Electrochemical Study**. In: **Hydrometallurgy 2003**, Proceedings of the Fifth International Symposium, Vancouver, 2003, p. 405 - 417.

53. Miki, H. and Nicol, M.J., **Synergism in the Oxidation of Covellite and Pyrite by Iron(III) and Copper(II) Ions in Chloride Solutions**. In: Young, C., Anderson, C.G and Choi, Y. (eds.), **Hydrometallurgy 2008**, Proceedings of the Sixth International Symposium, Phoenix, 2008, p. 646 - 652.

54. Dutrizac, J.E., **The Leaching of Sulphide Minerals in Chloride Media**, Hydrometallurgy, **29**, 1992, p. 1 - 45.

55. Langer, S.H., Nametz, M.A., Kaun, T.D. and Anderson, J.H., **The Application of the Cupric Chloride Process to Copper Recovery from Scrap and Ore**. In: **Chloride Hydrometallurgy Proceedings**, Benelux Metallurgie, Brussels, 1977, p. 134 - 153.

56. Peacy, J., Guo, X.J. and Robbs, E., **Copper Hydrometallurgy - Current Status, Preliminary Economics, Future Direction and Positioning versus Smelting**. In: Riveros, P.A., Dixon, D.G., Dreisinger, D.B. and Menacho, J.H. (eds.), **Proceedings of Copper 2003**, Book 1, **VI**, Santiago, 2003, p. 205 - 222.

57. Ramachandran, V., Lakshmanan, V.I. and Kondos, P.D., **Hydrometallurgy of Copper Sulfide Concentrates: An Update**. In: Riveros, P.A., Dixon, D.G., Dreisinger, D.B. and Collins, M.J. (eds.), **Proceedings of Copper 2007**, Book 1, **IV**, Toronto, 2007, p. 101 - 128.

58. Leimala, R., Hyvärinen, O., Hämäläinen, M. and Jyrälä, M., **The Outokumpu HydroCopper™ Process - Design, Implementation and Operation of a Demonstration Plant**. In: Riveros, P.A., Dixon, D.G., Dreisinger, D.B. and Menacho, J.H. (eds.), **Proceedings of Copper 2003**, Book 1, **VI**, Santiago, 2003, p. 281 - 288.

59. Chilean patent N° 40891, 2001.

60. Van Buuren, C., Personal Communication, 2008.

61. Fischer, W.W., Flores, F.A. and Henderson, J.A., **Comparison of Chalcocite Dissolution in the Oxygenated, Aqueous Sulfate and Chloride Systems**, Minerals Engineering, Vol. 5, **7**, 1992, p. 817 - 834.

62. Thomas, G. and Ingraham, T.R., **Kinetics of Dissolution of Synthetic Covellite in Aqueous Acidic Ferric Sulphate Solutions**, Can. Metall. Q., **6**, 1967, p. 153 - 165.

63. Lowe, D.F., **The Kinetics of the Dissolution Reaction of Copper and Copper-Iron Sulphide Minerals Using Ferric Sulphate Solutions**, Ph.D. Thesis, University of Arizona, 1970.

64. Mulak, W., **Kinetics of Dissolving Polydispersed Covellite in Acidic Solutions of Ferric Sulphate**, Roczn. Chem., **45**, 1971, p. 1417 - 1424.

65. Dutrizac, J.E. and MacDonald, R.J.C., **The Kinetics of Dissolution of Covellite in Acidified Ferric Sulphate Solutions**, Can. Metall. Q., **13**, 1974, p. 423 - 433.

66. Fischer, W.W., **Technical Note: Comparison of Chalcocite Dissolution in the Sulfate, Perchlorate, Nitrate, Chloride, Ammonia and Cyanide Systems**, Minerals Engineering, Vol. 7, **1**, 1994, p. 99 - 103.

67. Cheng, C.Y. and Lawson, F., **The Kinetics of Leaching Chalcocite in Acidic Oxygenated Sulphate-Chloride Solutions**, Hydrometallurgy, **27**, 1991, p. 249 - 268.

68. Deng, T. and Muir, D., **Selective Leaching of Copper from Telfer Copper-Gold-Pyrite Concentrate Using Copper(II) or Oxygen in Acidic Chloride Media**, Proceedings of Sixth AusIMM Extractive Metallurgy Conference, 1994, p. 155 - 159.

69. Ruiz, M.C., Honores, S. and Padilla, R., **Leaching Kinetics of Digenite Concentrate in Oxygenated Chloride Media at Ambient Pressure**, Metallurgical and Material Transactions B, **29B**, 1998, p. 961 - 969.

70. Vracăr, R.Ž., Parezanović, I.S. and Cerović, K.P., **Leaching of Copper(I) Sulfide in Calcium Chloride Solution**, Hydrometallurgy, **58**, 2000, p. 261 - 267.

71. Deng, T., Lu, Y., Wen, Z. and Liu, D., **Oxygenated Chloride-Assisted Leaching of Copper Residue**, Hydrometallurgy, **62**, 2001, p. 23 - 30.

72. Herreros, O., Quiroz, R., Longueira, H., Fuentes, G. and Viñals, J., **Leaching of Djurelite in Cu^{2+} / Cl^- Media**, Hydrometallurgy, **82**, 2006, p. 32 - 39.

73. Herreros, O. and Viñals, J., **Leaching of Sulfide Copper Ore in a NaCl - H_2SO_4 - O_2 Media with Acid Pre-Treatment**, Hydrometallurgy, **89**, 2007, p. 260 - 268.

74. Berger, J.M. and Winand, R., **Solubilities, Densities and Electrical Conductivities of Aqueous Copper(I) and Copper(II) Chlorides in Solutions Containing Other Chlorides such as Iron, Zinc, Sodium and Hydrogen Chlorides**, Hydrometallurgy, **12**, 1984, p. 61 - 81.

75. Albery, J., **Electrode Kinetics**, Oxford University Press, 1975.

76. Sullivan, J.D., **Chemistry of Leaching of Chalcocite**, Technical Paper **473**, US Bureau of Mines, 1930, p. 1 - 24.

77. Mulak, W., **Kinetics of Cuprous Sulphide Dissolution in Acidic Solutions of Ferric Sulphate**, Roczn. Chem., **43**, 1969, p. 1387 - 1394.

78. Kopylov, G.A. and Orlov, A.I., **Rates of Bornite and Chalcocite Dissolution in Ferric Sulphate**, Jr Irkutsh. Politckh. Inst., **41**, 1969, p. 127 - 132.

79. Thomas, G., Ingraham, T.R. and MacDonald, R.J., **Kinetics of Dissolution of Synthetic Digenite and Chalcocite in Aqueous Acidic Ferric Sulphate Solutions**, Can. Metall. Q., **6**, 1967, p. 281 - 291.

80. King, J.A., **Solid State Changes in the Leaching of Copper Sulphides**, Ph.D. Thesis, University of London, 1966.

81. King, J.A., Burkin, A.R. and Ferreira, R.C.H., **Leaching of Chalcocite by Acidic Chloride Solutions**. In: Burkin, A.R. (ed.), **Leaching and Reduction in Hydrometallurgy**, Inst. Min. Metall., London, 1975, p. 36 - 45.

82. Trachenko, O.B. and Tseft, A.L., **Kinetics of the Dissolution of Chalcocite in Ferric Chloride**, Trncly Inst. Metall. Obogashch., Alma Ata, **30**, 1969, p. 15 - 23.

83. Rossi, G., **Biohydrometallurgy**, McGraw-Hill Book Company Gmbh, 1989.

84. Dutrizac, J.E. and MacDonald, R.J.C., **Ferric Ion as a Leaching Medium**, Minerals Sci. Eng., Vol. 6, **2**, 1974, p. 59 - 100.

85. Tran, T. and Swinkels, D.A.J., **The Kinetics of Oxidation of Copper(I) Chloride by Oxygen in NaCl-HCl Solutions**, Hydrometallurgy, **15**, 1986, p. 281 - 295.

86. Nicol, M.J., **Kinetics of the Oxidation of Copper(I) by Oxygen in Acidic Chloride Solutions**, S. Afr. J. Chem., **37**, 1984, p. 77 - 80.

87. Burkin, A.R., **The Chemistry of Hydrometallurgical Processes**, E. & F.N. Spon Ltd., London, 1966.

88. Nicol, M.J. and Colborn, R.C., **Kinetics of the Oxidation of Iron(II) in Chloride Solutions**, J. S. Afr. Inst. Min. Metall., **73**, 1973.

89. Weast, R.C., **CRC Handbook of Chemistry and Physics**, 1st Student Edition, CRC Press Inc., 1988.

90. Brown, S.L., **Dissolution of Some Common Copper Minerals**, M.Sc. Thesis, University of Arizona, 1931.

91. Brown, S.L. and Sullivan, J.D., **Dissolution of Various Copper Minerals**, Report 1-3228, US Bureau of Mines, 1934.

92. Narita, E., Lawson, F. and Han, K.N., **Solubility of Oxygen in Aqueous Electrolyte Solutions**, Hydrometallurgy, **10**, 1983, p. 21 - 37.

93. Langer, S.H., Kaun, T.D. and Nametz, M.A., J. Met., Vol. 28, **7**, 1976, p. 9 - 14.

94. Bolorunduro, S.A., **Kinetics of Leaching Chalcocite in Acidic Ferric Sulfate Media: Chemical and Bacterial Leaching**, M.Sc. thesis, University of British Columbia, 1999.

95. Madsen, B.W. and Wadsworth, M.E., **A Mixed Kinetics Dump Leaching Model for Ores Containing a Variety of Copper Sulphide Minerals**, U.S. Bureau of Mines, R.I. N° 8547, 1981, p. 44.

96. Marcantonio, P., **Kinetics of Dissolution of Chalcocite in Ferric Sulphate Solutions**, Ph.D. thesis, University of Utah, 1976.

97. Nicol, M.J. and Lázaro-Báez, M.I., **The Role of E_H Measurements in the Interpretation of the Kinetics and Mechanisms of the Oxidation and Leaching of Sulphide Minerals**, Hydrometallurgy, **63**, 2002, p. 15 - 22.

98. Vetter, K.J., **Electrochemical Kinetics: Theoretical and Experimental Aspects**, Academic Press, New York, 1967.

99. Marsden, J. and House, I., **The Chemistry of Gold Extraction**, First Edition, Ellis Horwood, New York, 1993.

100. Kotz, J.C. and Purcell, K.F., **Chemistry and Chemical Reactivity**, Second Edition, Saunders College Publishing, 1991.

101. Power, G.P. and Richie, I.M., **Experimental Illustrations of an Important Concept in Practical Electrochemistry**, J. Chem. Educ., **60**, 1983, p. 1022 - 1025.

102. Li, J., Zhong, T.K. and Wadsworth, M.E., **Application of Mixed Potential Theory in Hydrometallurgy**, Hydrometallurgy, **29**, 1992, p. 47 - 60.

103. Nicol, M.J., Needes, C.S. and Finkelstein, N.P., **Electrochemical Model for the Leaching of Uranium Dioxide 1 - Acid Media**. In: Burkin, A.R., **Leaching and Reduction in Hydrometallurgy**, The Institution of Mining and Metallurgy, The Chameleon Press Limited, London, 1975, p. 1 - 11.

104. Nicol, M.J., Needes, C.S. and Finkelstein, N.P., **Electrochemical Model for the Leaching of Uranium Dioxide 2 - Alkaline Carbonate Media**. In: Burkin, A.R., **Leaching and Reduction in Hydrometallurgy**, The Institution of Mining and Metallurgy, The Chameleon Press Limited, London, 1975, p. 12 - 19.

105. Ghali, E., Dandapani, B. and Lewenstam, A., **Electrodissolution of Synthetic Covellite in Hydrochloric Acid**, J. Appl. Electrochem., **12**, 1982, p. 369 - 376.

106. Jones, D.A. and Paul, A.J.P., **Acid Leaching Behaviour of Sulphide and Oxide Minerals Determined by Electrochemical Polarization Measurements**, Min. Eng., Vol. 8, **4/5**, 1995, p. 511 - 521.

107. Bard, A.J. and Faulkner, L.R., **Electrochemical Methods: Fundamentals and Applications**, John Wiley and Sons, New York, 1980.

108. Macdonald, D.D., **Transient Techniques in Electrochemistry**, Plenum Press, New York, 1977.

109. Orchard, S.W., **Methods of Determining the Rates and Mechanisms of Electrochemical Reactions**, School of Pure and Applied Electrochemistry, South Africa, 1979.

110. Lee, M.S., Nicol, M.J. and Basson, P., **Cathodic Processes in the Leaching and Electrochemistry of Covellite in Mixed Sulfate - Chloride Media**, Journal of Applied Electrochemistry, Vol. 38, **3**, 2008, p. 363 - 369.

111. Bockris, J.O. and Reddy, A.K.N., **Modern Electrochemistry: An Introduction to An Interdisciplinary Area**, Vol. 2, Plenum Press, New York, 1970.

112. Nicol, M.J., Miki, H. and Velásquez-Yévenes, L., **The Dissolution of Chalcopyrite in Chloride Solutions Part 3: Mechanisms**, Hydrometallurgy, **103**, 2010, p. 86 - 95.

113. Hirato, T., Hiai, H., Awakura, Y. and Majima, H., **The Leaching of Sintered CuS Disks with Ferric Chlorides**. In Laughlin, D.E. (ed.), **Metallurgical Transactions B**, 20B, **4**, 1989, p. 485 - 491.

114. Outotec's HSC 6.1 Software

APPENDIX I

The data used to produce the graphs in Figures 4.7(a) to 4.7(f) were generated using the NIST database [40] and Outotec's HSC 6.1 software [114], in conjunction with the following equations:

$$E_{Cu(II)/Cu(I)} = 0.162 - 0.0591\log\frac{[Cu^{+}]}{[Cu^{2+}]} \quad \text{(A1)}$$

$$E_{Cu(I),S^{\circ}/CuS} = 1.106 - 0.0591\log\frac{1}{[Cu^{+}]} \quad \text{(A2)}$$

$$E_{Cu(II),S^{\circ}/CuS} = 0.631 - \frac{0.0591}{2}\log\frac{1}{[Cu^{2+}]} \quad \text{(A3)}$$

Table A1 : Data for Figure 4.7(a)

$[Cl^{-}]$ (g/L)	$E_{Cu(II)/Cu(I)}$ (V)	$E_{Cu^{+},S^{\circ}/CuS}$ (V)		$E_{Cu^{2+},S^{\circ}/CuS}$ (V)	
		10^{-8} g/L Cu	0.05 g/L Cu	10^{-8} g/L Cu	0.05 g/L Cu
0	0.476	-	-	0.353	0.538
3.55	0.476	0.266	0.636	0.351	0.536
7.09	0.476	0.229	0.600	0.350	0.535
14.2	0.476	0.191	0.562	0.347	0.532
21.3	0.476	0.169	0.539	0.345	0.530
28.4	0.476	0.152	0.522	0.343	0.528
35.5	0.476	0.139	0.509	0.342	0.527
42.5	0.476	0.127	0.498	0.341	0.525
49.6	0.476	0.118	0.488	0.339	0.524
56.7	0.476	0.110	0.480	0.338	0.523
63.8	0.476	0.102	0.472	0.337	0.522
70.9	0.476	0.095	0.466	0.336	0.521

Table A2 : Data for Figure 4.7(b)

$[Cl^-]$ (g/L)	$E_{Cu(II)/Cu(I)}$ (V)	$E_{Cu^+,S°/CuS}$ (V)		$E_{Cu^{2+},S°/CuS}$ (V)	
		10^{-8} g/L Cu	0.05 g/L Cu	10^{-8} g/L Cu	0.05 g/L Cu
0	0.496	-	-	0.368	0.539
3.55	0.496	0.277	0.618	0.367	0.537
7.09	0.496	0.240	0.581	0.365	0.536
14.2	0.496	0.203	0.543	0.363	0.533
21.3	0.496	0.180	0.520	0.361	0.531
28.4	0.496	0.163	0.503	0.359	0.529
35.5	0.496	0.150	0.490	0.357	0.528
42.5	0.496	0.139	0.479	0.356	0.526
49.6	0.496	0.129	0.469	0.355	0.525
56.7	0.496	0.121	0.461	0.353	0.524
63.8	0.496	0.113	0.454	0.352	0.523
70.9	0.496	0.106	0.447	0.351	0.522

Table A3 : Data for Figure 4.7(c)

$[Cl^-]$ (g/L)	$E_{Cu(II)/Cu(I)}$ (V)	$E_{Cu^+,S°/CuS}$ (V)		$E_{Cu^{2+},S°/CuS}$ (V)	
		10^{-8} g/L Cu	0.05 g/L Cu	10^{-8} g/L Cu	0.05 g/L Cu
0	0.554	-	-	0.391	0.539
3.55	0.554	0.364	0.561	0.389	0.538
7.09	0.554	0.328	0.524	0.388	0.536
14.2	0.554	0.290	0.486	0.385	0.534
21.3	0.554	0.267	0.463	0.383	0.531
28.4	0.554	0.250	0.446	0.382	0.530
35.5	0.554	0.237	0.433	0.380	0.528
42.5	0.554	0.226	0.422	0.379	0.527
49.6	0.554	0.216	0.412	0.377	0.525
56.7	0.554	0.208	0.404	0.376	0.524
63.8	0.554	0.200	0.397	0.375	0.523
70.9	0.554	0.194	0.390	0.374	0.522

Table A4 : Data for Figure 4.7(d)

$[Cl^-]$ (g/L)	$E_{Cu(II)/Cu(I)}$ (V)	$E_{Cu^+,S^\circ/CuS}$ (V)		$E_{Cu^{2+},S^\circ/CuS}$ (V)	
		10^{-8} g/L Cu	0.05 g/L Cu	10^{-8} g/L Cu	0.05 g/L Cu
0	0.575	-	-	0.400	0.539
3.55	0.575	0.262	0.540	0.398	0.538
7.09	0.575	0.225	0.503	0.397	0.536
14.2	0.575	0.187	0.465	0.394	0.534
21.3	0.575	0.164	0.442	0.392	0.532
28.4	0.575	0.148	0.425	0.390	0.530
35.5	0.575	0.134	0.412	0.389	0.528
42.5	0.575	0.123	0.401	0.387	0.527
49.6	0.575	0.114	0.392	0.386	0.525
56.7	0.575	0.105	0.383	0.385	0.524
63.8	0.575	0.098	0.376	0.384	0.523
70.9	0.575	0.091	0.369	0.383	0.522

Table A5 : Data for Figure 4.7(e)

$[Cl^-]$ (g/L)	$E_{Cu(II)/Cu(I)}$ (V)	$E_{Cu^+,S^\circ/CuS}$ (V)		$E_{Cu^{2+},S^\circ/CuS}$ (V)	
		10^{-8} g/L Cu	0.05 g/L Cu	10^{-8} g/L Cu	0.05 g/L Cu
0	0.605	-	-	0.408	0.539
3.55	0.605	0.247	0.510	0.406	0.538
7.09	0.605	0.210	0.473	0.405	0.536
14.2	0.605	0.172	0.436	0.402	0.534
21.3	0.605	0.149	0.413	0.400	0.532
28.4	0.605	0.133	0.396	0.398	0.530
35.5	0.605	0.119	0.383	0.397	0.528
42.5	0.605	0.108	0.372	0.395	0.527
49.6	0.605	0.099	0.362	0.394	0.525
56.7	0.605	0.090	0.354	0.393	0.524
63.8	0.605	0.083	0.346	0.392	0.523
70.9	0.605	0.076	0.339	0.391	0.522

Table A6 : Data for Figure 4.7(f)

$[Cl^-]$ (g/L)	$E_{Cu(II)/Cu(I)}$ (V)	$E_{Cu^+,S°/CuS}$ (V)		$E_{Cu^{2+},S°/CuS}$ (V)	
		10^{-8} g/L Cu	0.05 g/L Cu	10^{-8} g/L Cu	0.05 g/L Cu
0	0.625	-	-	0.412	0.539
3.55	0.625	0.235	0.490	0.410	0.538
7.09	0.625	0.199	0.453	0.409	0.536
14.2	0.625	0.161	0.415	0.406	0.534
21.3	0.625	0.138	0.392	0.404	0.532
28.4	0.625	0.121	0.376	0.402	0.530
35.5	0.625	0.108	0.362	0.401	0.528
42.5	0.625	0.097	0.351	0.399	0.527
49.6	0.625	0.087	0.342	0.398	0.525
56.7	0.625	0.079	0.334	0.397	0.524
63.8	0.625	0.072	0.326	0.396	0.523
70.9	0.625	0.065	0.319	0.395	0.522

APPENDIX II

Figure A.1 shows a voltammogram for a stationary, Φ 1 mm covellite electrode in a 1 M HCl solution. The mineral was swept from the open circuit potential (OCP) of 0.476 V in a positive direction up to about 0.967 V; thereafter, the sweep was reversed into a negative direction up to a value of 0.476 V.

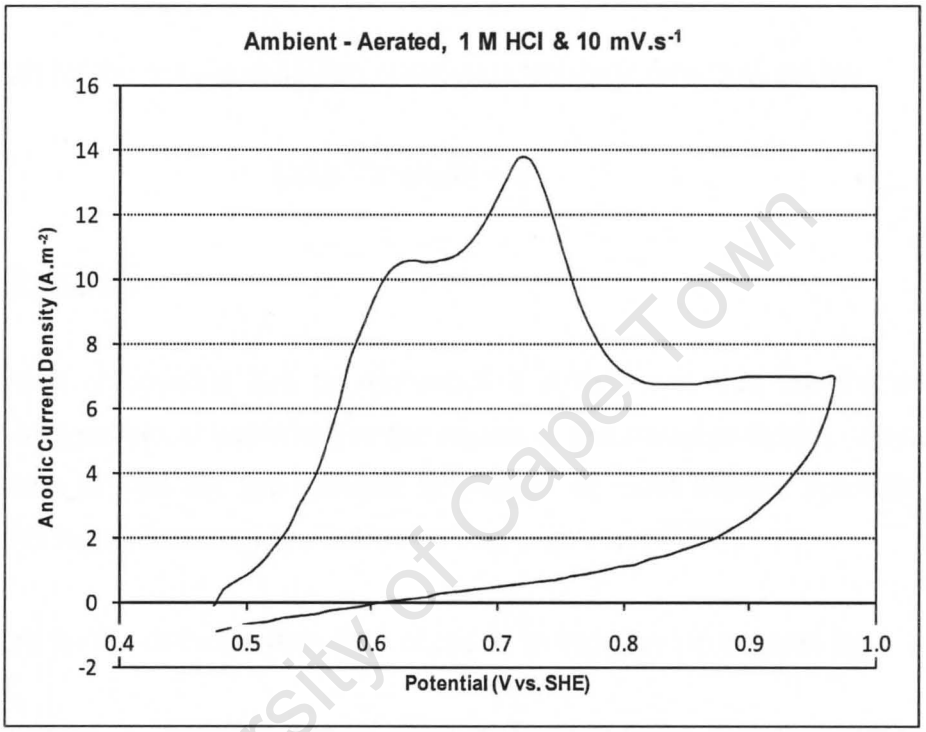

Figure A.1 : A Voltammogram for Covellite in a 1 M HCl Solution at 25°C

The reverse sweep shows no distinct cathodic peaks over the whole potential range. This is in agreement with the fact that the mineral shows highly, irreversible behaviour in the vicinity of the mixed potential [33].

APPENDIX III

Anodic Reactions

The reaction for the anodic dissolution of covellite by a one-electron process is given by:

$$CuS \overset{k_{CuS}}{\rightarrow} Cu(I) + S^{\circ} + e^{-} \quad (A4)$$

The reaction for the anodic oxidation of cuprous to cupric ions is given by:

$$Cu(I) \overset{k_{Cu(I)}}{\rightarrow} Cu(II) + e^{-} \quad (A5)$$

Cathodic Reactions

The reduction of covellite can be ignored if it is assumed that the oxidation of the mineral is irreversible at potentials in the region of the mixed potential. Generally, this approximation is true for the cathodic behaviour of most copper sulphide minerals, which exhibit highly irreversible electrochemical behaviour [31,33,97].

The reaction for the cathodic reduction of cupric to cuprous ion is given by:

$$Cu(II) + e^{-} \overset{k_{Cu(II)}}{\rightarrow} Cu(I) \quad (A6)$$

At the mixed potential (E_m):

$$i_{CuS} + i_{Cu(I)} = -i_{Cu(II)} \neq 0 \quad (A7)$$

With:

$$i_{CuS} = Fk_{CuS}e^{\left(\frac{\beta_{CuS}FE_m}{RT}\right)} \quad (A8)$$

$$i_{Cu(I)} = F[Cu(I)]k_{Cu(I)}e^{\left(\frac{\beta_{Cu(I)}FE_m}{RT}\right)} \quad (A9)$$

$$-i_{Cu(II)} = F[Cu(II)]k_{Cu(II)}e^{\left(\frac{-\beta_{Cu(II)}FE_m}{RT}\right)} \quad (A10)$$

Substitution of Equations A8 to A10 into Equation A7 together with,

$$\begin{aligned} \beta_{CuS} &= \beta_{Cu(I)} \\ &= \beta_{Cu(II)} \\ &= \beta \\ &= 0.5 \end{aligned} \quad (A11)$$

renders the following expression for the mixed potential (E_m):

$$E_m = \left(\frac{RT}{F}\right)\ln\left\{\frac{k_{Cu(II)}[Cu(II)]}{k_{CuS} + k_{Cu(I)}[Cu(I)]}\right\} \quad (A12)$$

The above approximation allows an analytical solution for Equation A7 and is reasonable given that the transfer coefficients (β) for electrochemical reactions are often close to 0.5 [31,33,97].

From Faraday's law [33,98] and substitution of Equation A12 into Equation A8, the following expression for the rate of dissolution of covellite (r_{CuS}) is obtained:

$$\begin{aligned} r_{CuS} &= \frac{i_{CuS}}{F} \\ &= k_{CuS}\left\{\frac{k_{Cu(II)}[Cu(II)]}{k_{CuS} + k_{Cu(I)}[Cu(I)]}\right\}^{1/2} \end{aligned} \quad (A13)$$

APPENDIX IV

Anodic Reactions

The reaction for the anodic dissolution of covellite by a two-electron process is given by:

$$CuS \xrightarrow{k_{CuS}} Cu(II) + S^{\circ} + 2e^{-} \quad (A14)$$

The reaction for the anodic oxidation of cuprous to cupric ions is given by:

$$Cu(I) \xrightarrow{k_{Cu(I)}} Cu(II) + e^{-} \quad (A15)$$

Cathodic Reactions

The reduction of covellite can be ignored if it is assumed that the oxidation of the mineral is irreversible at potentials in the region of the mixed potential. Generally, this approximation is true for the cathodic behaviour of most copper sulphide minerals, which exhibit highly irreversible electrochemical behaviour [31,33,97].

The reaction for the cathodic reduction of cupric to cuprous ion is given by:

$$Cu(II) + e^{-} \xrightarrow{k_{Cu(II)}} Cu(I) \quad (A16)$$

At the mixed potential (E_m):

$$i_{CuS} + i_{Cu(I)} = -i_{Cu(II)} \neq 0 \quad (A17)$$

With:

$$i_{CuS} = 2Fk_{CuS}e^{\left(\frac{\beta_{CuS}FE_m}{RT}\right)} \quad (A18)$$

$$i_{Cu(I)} = F[Cu(I)]k_{Cu(I)}e^{\left(\frac{\beta_{Cu(I)}FE_m}{RT}\right)} \quad (A19)$$

$$-i_{Cu(II)} = F[Cu(II)]k_{Cu(II)}e^{\left(\frac{-\beta_{Cu(II)}FE_m}{RT}\right)} \quad (A20)$$

Substitution of Equations A18 to A20 into Equation A17 together with,

$$\begin{aligned} \beta_{CuS} &= \beta_{Cu(I)} \\ &= \beta_{Cu(II)} \\ &= \beta \\ &= 0.5 \end{aligned} \quad (A21)$$

renders the following expression for the mixed potential (E_m):

$$E_m = \left(\frac{RT}{F}\right)\ln\left\{\frac{k_{Cu(II)}[Cu(II)]}{2k_{CuS} + k_{Cu(I)}[Cu(I)]}\right\} \quad (A22)$$

The above approximation allows an analytical solution for Equation A17 and is reasonable given that the transfer coefficients (β) for electrochemical reactions are often close to 0.5 [31,33,97].

From Faraday's law [33,98] and substitution of Equation A22 into Equation A18, the following expression for the rate of dissolution of covellite (r_{CuS}) is obtained:

$$\begin{aligned} r_{CuS} &= \frac{i_{CuS}}{2F} \\ &= k_{CuS}\left\{\frac{k_{Cu(II)}[Cu(II)]}{2k_{CuS} + k_{Cu(I)}[Cu(I)]}\right\}^{1/2} \end{aligned} \quad (A23)$$

APPENDIX V

This section contains some examples of typical calculations for the rate of dissolution of covellite (r_{CuS}).

Rate of Dissolution of Covellite from Electrochemical Test Data

Measured: $i_a = 1.38 \times 10^{-3}$ A.m^{-2} (25°C and 0.580 V; see Table 4.5)

From the reaction,

$$CuS \rightarrow Cu(II) + S^{\circ} + 2e^{-} \qquad (A24)$$

and Faraday's law [33,98] follows:

$$r_{CuS} = \frac{i_a}{nF} \qquad (A25)$$

$$= \frac{1.38 \times 10^{-3} \times 10^{-4}}{2 \times 96487}$$

$$= 7.15 \times 10^{-13} \text{ mol Cu cm}^{-2}.\text{s}^{-1}$$

Then, if an apparent activation energy of 77 kJ.mol^{-1} is assumed (see p. 118), it follows from the Arrhenius relationship [33,39,100] that (see Table 4.5):

$$r_{CuS}(T) = r_{CuS}(T_o)e^{\left[\frac{E_a}{R}\left(\frac{1}{T_o}-\frac{1}{T}\right)\right]} \qquad (A26)$$

$$r_{CuS}(35°C) = r_{CuS}(25°C)e^{\left[\frac{77000}{8.31441}\left(\frac{1}{298.15}-\frac{1}{308.15}\right)\right]}$$

$$= 7.15 \times 10^{-13} \times e^{\left[\frac{77000}{8.31441}\left(\frac{1}{298.15}-\frac{1}{308.15}\right)\right]}$$

$$= 1.96 \times 10^{-12} \text{ mol Cu cm}^{-2}.\text{s}^{-1}$$

Rate of Dissolution of Covellite from Leach Test Data

For a concentrate (wet) screened at +25-38 μm, the (geometric) average diameter (d_p) for a spherical particle is given by:

$$d_p = (25 \times 38)^{1/2}$$
$$= 31\ \mu m$$

The specific surface area (SSA) for a spherical, covellite particle is given by:

$$SSA = \frac{6}{d_p SG}$$
$$= \frac{6}{\left(\frac{31}{10000}\right) \times 4.675}$$
$$= 416\ cm^2.g^{-1}$$

The total surface area (SA) for all the covellite particles is given by:

$$SA = SSA \times \sum m_p \times \frac{C_p}{100}$$
$$= 416 \times 9 \times \frac{98.5}{100}$$
$$= 3691\ cm^2$$

For an experimentally determined dissolution of 40% copper after 575 h, the rate of dissolution of covellite (CuS) is given by (see Tables 2.4.6 and 4.5):

$$r_{CuS} = \frac{\sum m_p C_p X}{Mr_{CuS} SAt}$$
$$= \frac{9 \times \left(\frac{98.5}{100}\right) \times \left(\frac{40}{100}\right)}{95.6 \times 3691 \times 575 \times 3600}$$

$$= 4.86 \times 10^{-12} \text{ mol Cu cm}^{-2}.\text{s}^{-1}$$

With:

C_p	Purity of covellite, in % w/w
d_p	Particle diameter for a spherical particle, in µm
E_a	Apparent activation energy, in $J.mol^{-1}$
F	Faraday's constant, 96487 $C.mol^{-1}$ e^-
i_a	Anodic current density, in $A.m^{-2}$
Mr_{CuS}	Molar mass of covellite, 95.6 $g.mol^{-1}$
$\sum m_p$	Total mass of particles, in g
n	Number of electrons, in mol e^-
R	Universal gas constant, 8.31441 $J.mol^{-1}.K^{-1}$
r_{CuS}	Rate of dissolution of covellite, in mol Cu $cm^{-2}.s^{-1}$
SA	Total surface area of particles, in cm^2
SG_{CuS}	Specific gravity for covellite, 4.675
SSA	Specific surface area of a spherical particle, in $cm^2.g^{-1}$
t	Reaction time for the dissolution of covellite, in s
T	Temperature, in K
X	Fraction of copper dissolved from covellite

APPENDIX VI

Experimental data included on CD